Geological history and fracture network characterization in unconventional reservoirs of the McArthur Basin (NT Australia)

A. N. Pragt

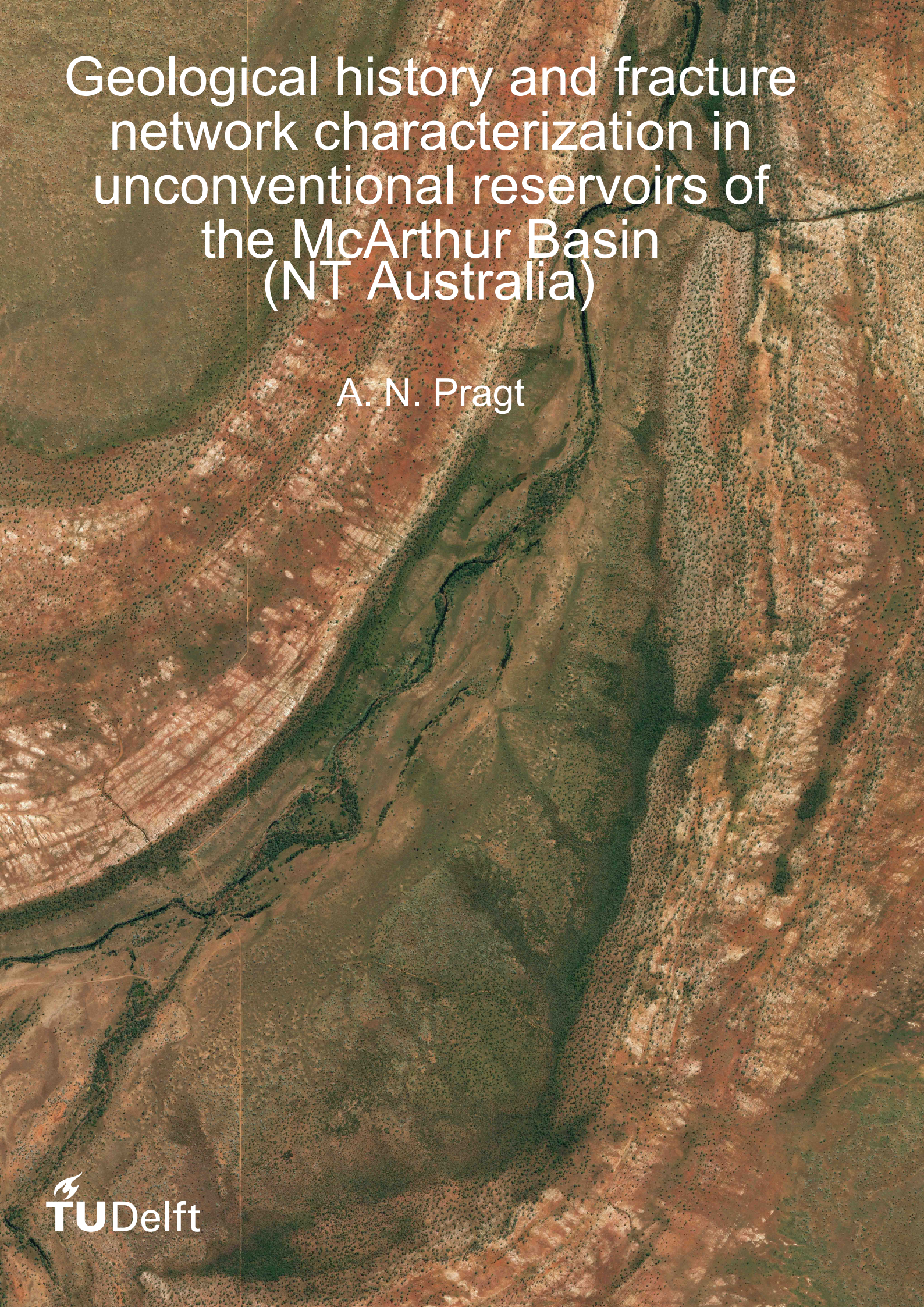

TU Delft

Geological history and fracture network characterization in unconventional reservoirs of the McArthur Basin (NT Australia)

by

A. N. Pragt

to obtain the degree of Master of Science
at the Delft University of Technology.
to be defended publicly on Thursday August 30th, 2018 at 10:00 AM.

Project duration:	October 24, 2017 – August 15, 2018	
Supervisors:	Prof. Dr. G. Bertotti,	TU Delft
	Drs J. K. Blom,	TU Delft
	Dr. P. B. R. Bruna,	TU Delft
Thesis committee:	Prof. Dr. G. Bertotti,	TU Delft
	Drs J. K. Blom,	TU Delft
	Dr. P. B. R. Bruna,	TU Delft
	Dr. A. Barnhoorn,	TU Delft

TU Delft

Preface

For me this was a very interesting and challenging topic. It consisted of different phases that asked a lot of literature study and problem solving. Of course many of the topics and skills that I learned in my academic career were used and improved. During the fieldwork Professor Giovanni Bertotti said something that really inspired during the writing of this report:

"It is easy to make a concept more difficult, but it is difficult to make it easier."

Although this is a personal achievement, it could not be done without the support of others. This thesis is part of the larger NT-Works project which is funded by the Dr. Schürmann Foundation. The majority of the costs of the fieldwork was covered by them. I was personally also funded for this fieldwork by the Molengraaff Fund. Without their funds the fieldwork would not have taken place, I therefore thank them both for their support. The majority of data comes from the NTGS (Northern Territory Geological Survey). Their open data sharing policy is not common. Most of it could be accessed and downloaded from their website. Large datafiles were even sent by post from Australia to the Netherlands. This thesis benefited from this a lot. The hospitality of the Australian people and the NTGS during my stay in Australia left me with a positive impression of the country.

I would also like to thank my three supervisors who guided me during the meetings we had. I know Professor Giovanni Bertotti and Drs Jan Kees Blom from other courses during my bachelor and master. I would like to thank them and other lecturers and staff for providing me with a successful, challenging and enjoyable academic education. I would like to thank my 'daily' supervisor Dr. Pierre-Olivier Bruna. Our discussions led to better and new insights which benefited this study. His enthusiasm always motivated me to improve my work. Even when he was very busy with his own research he always would make time to help me out with the questions I had. I would also thank Ir. Quinten Boersma with his support with the Techlog software and Dr. Auke Barhoorn for reviewing this report. Lastly I would like to thank my mother and my sister for their unconditional support. Throughout my academic education their support helped and motivated me to achieve this degree.

A.N. Pragt

Delft, August 2018

Abstract

The geological history of the McArthur Basin (NT Australia) is poorly understood. It consists of five onshore Paleo- to Mesoproterozoic packages with mainly siliciclastic and carbonate rocks, with cumulative thicknesses up to 15km. The basin contains the world's oldest hydrocarbons, principally hosted in unconventional reservoirs in the Wilton Package. Fluid flow in these reservoirs is related to natural, reactivated or induced fractures. Characterizing the fracture network is an important part of predicting fluid flow. This study tries to link the geological history to the generation of fractures.

The geological history needs to be better understood to characterize the fracture network. In this study seismic, well, outcrop and geophysical data are integrated to construct a cross section that links outcrops (Batten Fault Zone and Broadmere Complex) with the subsurface (Beetaloo Sub-basin). The literature in combination with the cross section is used to revise the geological history.

A fieldwork is conducted to study fracture geometries on outcrops of the Wilton Package that are analogues to subsurface fracture networks. A drone is used to image fracture pavements at an order ($10^2 m$) that is normally missed by geologists ($10^1 m$) and satellite images ($10^3 m$). The Tanumbirini-1 well, located in the sub-basin, provides a FMI log for interpreting fractures in the subsurface. A key objective is to differentiate fractures associated with fracture drivers like regional stress, folds and faults.

This study identified two unconformities in the seismic data, corresponding to two deformation events. The Carpenteria Event between the Wilton Package and the Inacumba Group is associated with a dominantly N-S oriented stress field and the Borroloola Event within the Inacumba Group corresponds to a mainly E-W oriented stress field. Both events created their own fracture sets and are observed on outcrops and in the subsurface. The tectonic stress is σ_1 at the surface but $\sigma_{H,max}$ in the Beetaloo Sub-basin. Fracture generation in the sub-basin happened at another stress regime than the surface outcrop analogues, making any direct comparison less reliable. Hence this study gives a prediction of the fracture density and permeability trends in the sub-basin. A conceptual model of the subsurface permeability is proposed where the permeability trend is mainly E-W oriented.

Contents

1

Introduction

The modern world has reached a conundrum. The global population is rising and so are its energy needs. Meanwhile the consumption of dirty fossil fuels is wreaking havoc on the Earth's climate. Renewable energy sources are increasingly being developed but are still far away from providing a significant share. The hydrocarbons that are extracted today are derived from more and more complex reservoirs. A new source of cleaner hydrocarbon energy is provided by the advent of profitable unconventional gas fields. With new technology, insights and concepts, known fields are revisited to study their potential.

The McArthur Basin is located in the Northern Territory of Australia. The detailed structure of the basin is poorly understood. The structural history is very incomplete as it did not receive much attention. Wells that were drilled over the years proved the presence of unconventional gas trapped in black shales. The gas is dated to 1.8 Ga, making it one of the world's oldest hydrocarbon occurrences. An estimated amount of up to 293 TCF is present in just one of the many formations (Revie, 2017). The famous Barnett shale in the USA, in comparison, is estimated to contain an average of about 53 TCF of gas (United States Geological Survey, 2015). The structural geology needs to be understood to successfully develop these hydrocarbons. A study of the McArthur Basin is thus driven by both scientific and economic interest.

A conventional reservoir derives the majority of its permeability from connected porosity between grains, e.g. like sandstones. The effective porosity in shales is extremely low resulting in non-existing permeabilities. If fractures are present they can act as permeability pathways. The fracture network geometry is characterized by its orientation, lengths, heights, abutments and densities. An preferred orientation of the fractures will lead to an increased permeability that is also oriented the same way. Understanding this geometry will impact the development of a potential unconvential gas field.

Fractures are the result of stresses that act on a rock. The stresses can be regional or influenced locally by folds and faults. These are called drivers, and each of them can influence the geometry. The local drivers themselves are caused by the regional stress field. The regional stress is generated by tectonic movements. A thorough understanding of the tectonic history is needed to understand fracture geometries. Although the geological history has been studied before (Ahmad et al., 2013, Rogers, 1996), the fracture geometries never have.

This thesis will focus on the McArthur Basin. The Basin consists of five onshore Paleo- to Mesoproterozoic packages with mainly siliciclastic and carbonate rocks, with cumulative thicknesses up to 15km. The packages were deposited between 1.8 and 1.3 Ga. The Beetaloo Sub-basin is one of several subbasins that have been identified. The basin lies within the North Australian Craton (NAC), which was part of the Nuna supercontinent (Betts et al., 2015).

The area of interest or research area roughly covers an area of $30.000km^2$. It is located 400km to the south west of the city of Katherine. It is bounded by the -15.7 and -17.0 latitudes and the 134.5 and 136.2 longitudes. This region is chosen because it contains the same rocks in outcrops (Broadmere Complex, Batten Fault Zone) and in the subsurface (Beetaloo Sub-basin). The Beetaloo Sub-basin in the area of interest is also known as the OT Downs Sub-basin. In this report it will be referred to as the Beetaloo Sub-basin. The investigated packages are from old to young the Redbank, Glyde, Favenc and Wilton Package. These are all part of the McArthur Basin in *sensu strictu*. The important hydrocarbon formations are within the Wilton Package and will be the focus of this study. However there are also formations that are not part of the basin, but overlie the packages. They play a crucial role in the understanding of the phase of the geological history after the deposition of the Wilton Package.

The Mallapunyah fault has been traditionally identified with a prominent fault at the surface. During this study it became evident that it was actually part of a fault zone. One of the faults plays an important role in the geological history but cannot be observed at the surface. In this report the latter fault will be referred to as the Mallapunyah Fault.

A fieldwork was conducted to study fracture networks from key outcrops of the Wilton Package. These outcrops were chosen such that they represent the geometries generated by different drivers (e.g. crest of a fold). The use of a drone allowed the geometries to be mapped at a scale that is traditionally missed by geologists. A geologist can observe fractures at a small scale ($10^0 m$) or interpret them on a satellite image ($10^3 m$). A drone acquires data at a scale in between ($10^{1-2} m$). The observations done in the field are integrated with the geological framework. The result will be a conceptual model of the fracture geometry in the subsurface.

The questions that this study tries to answer are:

- *What is the structural history of McArthur Basin?*
- *How to predict the subsurface fracture network geometries in the Beetaloo Sub-basin from outcrop analogues?*

1.1. Outline

The first objective is to understand the structural history of the area. This is done by both studying the literature and constructing a cross section based on seismic and well data. In chapter 2 a synthesis of the geology and stratigraphy is given based on the available literature. The data that is used is discussed in chapter 3. The cross section links the Beetaloo Sub-basin with the outcrops in the Batten Fault zone. The section and a revised geological history of the McArthur basin is given in chapter 4.

The acquired data from the fieldwork are discussed in chapter 5, in addition the interpretation of the borehole images is given. Chapter 6 discusses the concepts of stress, strain and driver superposition. It also explains how the outcrops are linked to the subsurface. Results of the fieldwork and well interpretation are discussed in chapter 7. In this chapter the results are used to make a prediction of the fracture network geometry in the subsurface. In chapter 8 the shortcomings of this study and recommendations for further research are discussed. The conclusion is given in chapter 9.

2

Geological Setting

This chapter will cover the existing literature on the geological setting of the McArthur Basin. The goal is to show the present-day situation, competing tectonic models and introduce the stratigraphy. Additionally the Inacumba Group is proposed for grouping formations overlying the Wilton Package.

2.1. Present day situation

The Paleo- Mesoproterozoic McArthur Basin is located in the Northern Territory of Australia and covers an area of 180 000 km^2. The rocks are largely undeformed and unmetamorphized. They are organized in four packages lying unconformably on a paleoproterozoic basement. The basement consists of the Pine Creek Orogen (West), the Murphy Province (South) and the Arnhem Province (North East) (Munson, 2014). The four onshore packages are the Redbank, Glyde, Favenc and Wilton packages with a total combined thickness of up to 15km. They are mainly composed of siliciclastic, carbonate and some minor volcanic rocks.

Three fault zones divide the McArthur Basin in four parts. The east-west trending Urapunga Fault Zone separates the northern from the southern McArthur Basin. The Batten and the Walker Fault zones divide the northern and southern basins in an eastern and western part (figure 2.1). The fault zones show a complex history of polyphased deformation. Multiple extensional and compressional phases acted on the basin, creating uplift and subsidence. They played a key role in the accumulation of sediments throughout the basin's history. In more recent times the fault zones were exhumed exposing significantly older rocks. This contrasts with adjacent areas like the Beetaloo Sub-basin where the same rocks are at a depth of more than 4km.

The area of interest consists of four distinct regions (figure 2.2): the Bukalara Range, the Batten Fault Zone (BFZ), the Broadmere Complex and the Beetaloo Sub-basin from east to west respectively. The Bukulara Range is bounded by the map in the east and by the Emu Fault in the west. It consists of formations of the Wilton Package and the overlying Bukulara Sandstone. There is little to no deformation of the units.

Most outcrops in the heavily faulted BFZ are of the Glyde Package. Smaller outcrops of the Wilton, Favenc and Redbank Packages are also present. The Broadmere Complex is a north-south oriented synclinorum with mainly Wilton Package outcrops. It is bounded to the west by the Mallapunyah fault system, where outcrops of the Redbank are located. The Beetaloo sub-basin is bounded to the east by the Mallapunyah fault system. Similar to the Bukalara Range, there is little deformation. All packages are in the subsurface and are covered by Phanerozoic rocks.

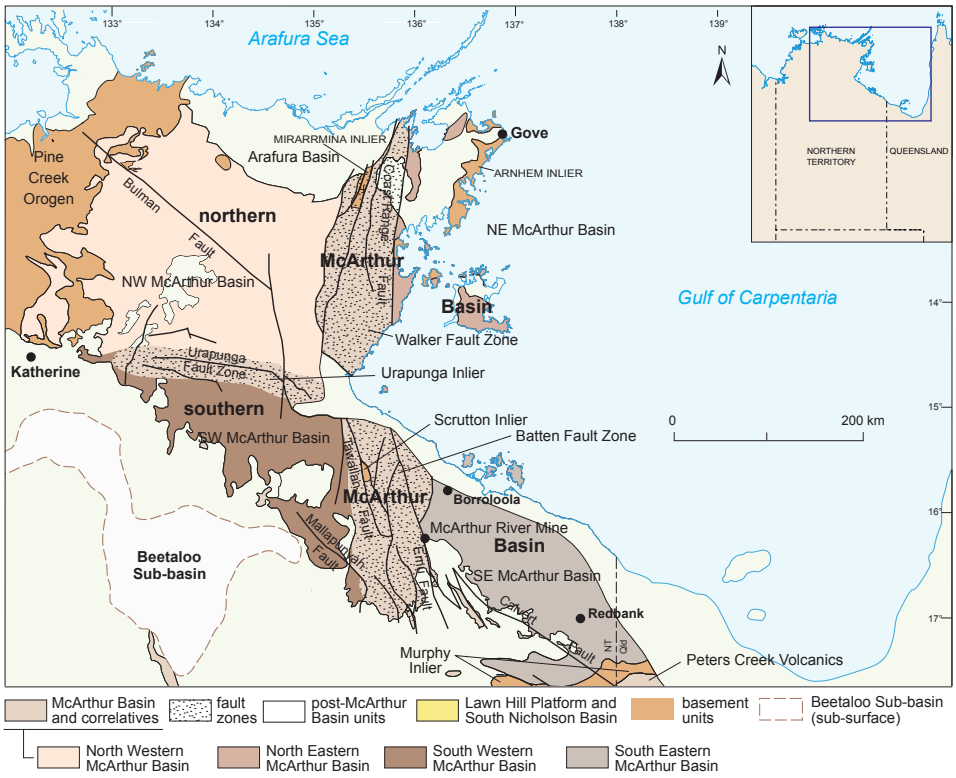

Figure 2.1: The major structural features of the McArthur Basin with sub divisions indicated by the different color, figure modified from (Munson, 2014).

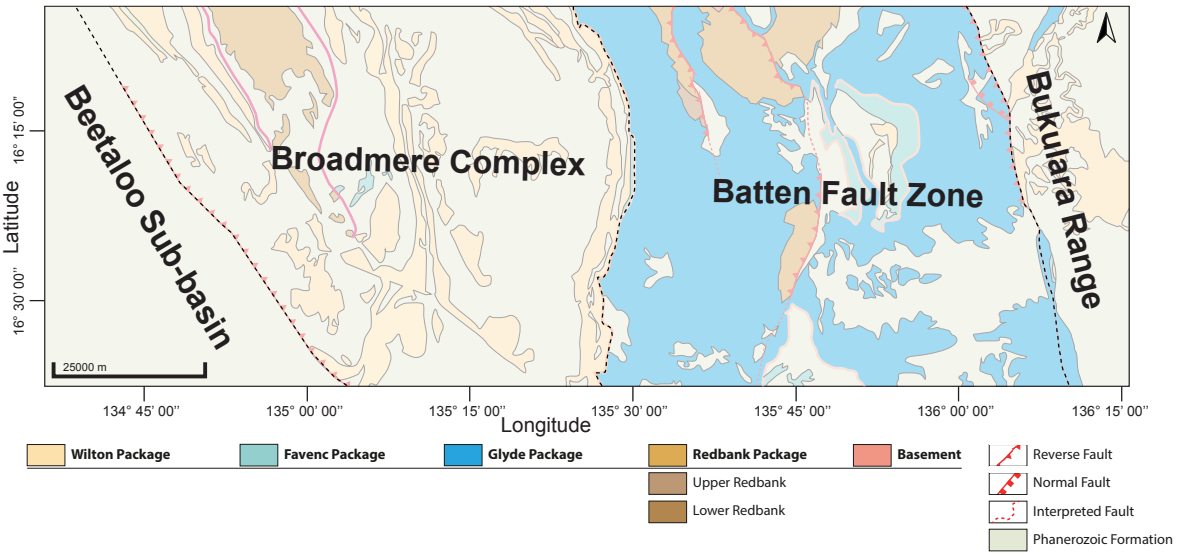

Figure 2.2: The outcrops of the four packages in the area of interest.

2.2. Tectonic Models

The basin has experienced multiple deformation events since the middle Proterozoic. Younger events obscure older ones, making it hard to observe and interpret structures generated early in the basin history. Tectonic mechanisms during the Proterozoic where possibly different. 'Paleomechanisms' are based on a lot of assumptions, with no modern analogues. Therefore there two competing theories based on whether or not present day tectonic processes also worked in the past. New insights are increasingly pointing towards uniconformatism up to the Paleoproterozoic (Darbyshire et al., 2017, Polat et al., 2016).

Intracontinental rift system

In the first model the basin was formed as an intracontinental rift system (Etheridge et al., 1987). The main idea is that plate tectonics would have behaved differently during the Proterozoic. The Earth was hotter as it had less time to cool since its formation. This impacts the heat flow from the core to the crust. Potentially this could lead to different mechanics when compared with the Phanerozoic, e.g. a higher rate of crustal recycling and a thinner lithosphere (Kröner, 1981). The evolution of such basin is exemplified in figure 2.3.

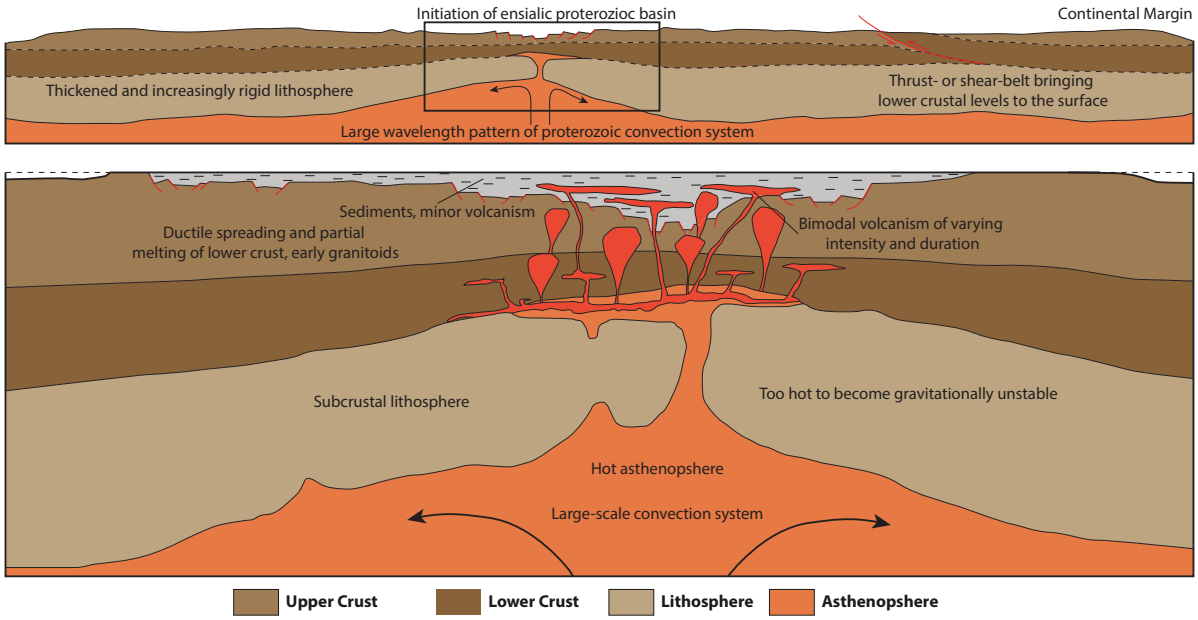

Figure 2.3: Upwelling of an asthenosphere plume initiates an ensialic basin (upper) and the subsequent filling of an ensialic basin and the creation of igneous intrusions (lower). Illustrations modified from (Kröner, 1981).

This model is marked by vertical instead of horizontal lithospherical accretion (Rutland, 1976). Basins and orogens are created by intermittent extensive crustal thinning and thickening, crustal restacking and lithospherical delamination, whereas sea floor spreading and subduction did not have a large impact during this time (Kröner, 1984).

Continental Back Arc Basin

The other model proposes a continental back arc setting (figure 2.4). Evidence supports the existence of subduction zones present at the southern margin of the North Australian Craton (Zhao, 1995). This margin is situated at the Arunta Inlier, a Paleoproterozoic terrain located in central Australia. Coinciding with this subduction are thermal events 1500km inland from the margin. The type of volcanic rocks that are found inland support the continental back arc setting. An analogue would be the East China rift system (Giles et al., 2002).

Despite different tectonic models, both of them result in the basin being formed by rifting and subsequent basin fill. During initial rifting volcanic activity deposited volcanic rich sediments and intrusive rocks. After this first phase many more followed. Basin subsidence and uplift kept influencing sedimentation style, resulting in distinct packages separated by unconformities.

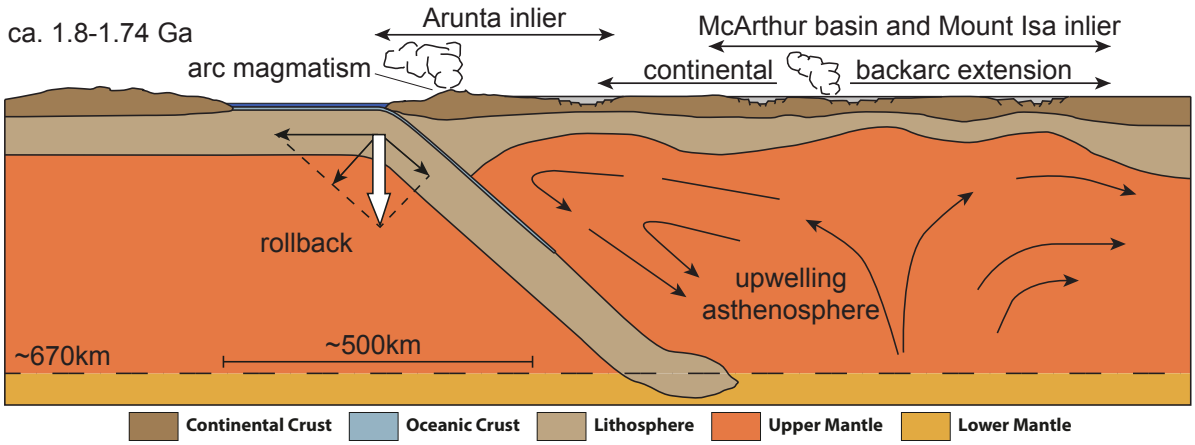

Figure 2.4: The model proposed by (Giles et al., 2002) for the McArthur basin. Figure is modified from (Giles et al., 2002)

2.3. Stratigraphy

The area of interest contains about 45 formations that are grouped in four packages (see figure 2.5). These are the Redbank, Glyde, Favenc and Wilton Packages.

The Redbank Packpage is dominated by fluvial and shallow marine sandstones. There are minor formations of siltstones, volcanics, intrusions and lacustrine carbonates (Rogers, 1996). The timing of initiation is poorly constrained, but happened after ±1800 (Blaikie et al., 2017) and before 1713±7 Ma (Page and Sweet, 1998). The package can reach thicknesses of 5km, and consist mainly of the Yiyinti and Sly Creek Sandstones. Together they account for more than 4km of sediments (Ahmad et al., 2013, Pietsch et al., 1991). The base is characterized by a transgressive sequence, changing from an alluvial braided plain to a shallow sub aqueous facies towards the upper Redbank Package. This report follows the division of the package in an upper and lower part, with the boundary between Settlement Creek Volcanics and Wanunmanyala Sandstone. This is discussed further in chapter 4.

The Glyde Package is dominated by stromatolitic dolostone and clastic sediments and was deposited between 1713±6 and 1614±4 Ma (Ahmad et al., 2013). In contrast with the previous package it does not contain proximal volcanics (Rogers, 1996). The outcrops are confined to the Batten Fault Zone, however seismic data suggests a larger extent in the subsurface.

The Favenc Package was deposited between ±1610 and 1589±3 (Ahmad et al., 2013). It contains a basal conglomerate unit with overlying stromalitic dolostones. The package lies unconformably above the Glyde Package, and can reach a thickness of 1600m in the Batten Fault Zone. Thickness variations are considered to be due to post depositional erosion (Pietsch et al., 1991). The facies change from a mainly fluvial setting to a shallow marine setting. The three formations that are present in the study area are the Smythe Sandstone, Balbirini Dolostone and the Dungaminnie Formation.

The Wilton Package contains mostly siliclastic sediments as opposed to the older dolostone rich groups. It was deposited between 1492±4 and 1324±4 Ma (Jackson et al., 1999), during a basin wide sag phase (Ahmad et al., 2013, Jackson et al., 1999, Kralik, 1982, Plumb and Wellman, 1987). It is characterized by asymmetric coarsening upward cycles dominated by regressive successions from storm dominated black shales up to tidal platform sandstone (Abbott and Sweet, 2000). In contrast to the previous packages, the centre of deposition moved away from the Batten Fault zone to the Beetaloo Sub-basin (Bruna et al., 2015, Rawlings, 1999).

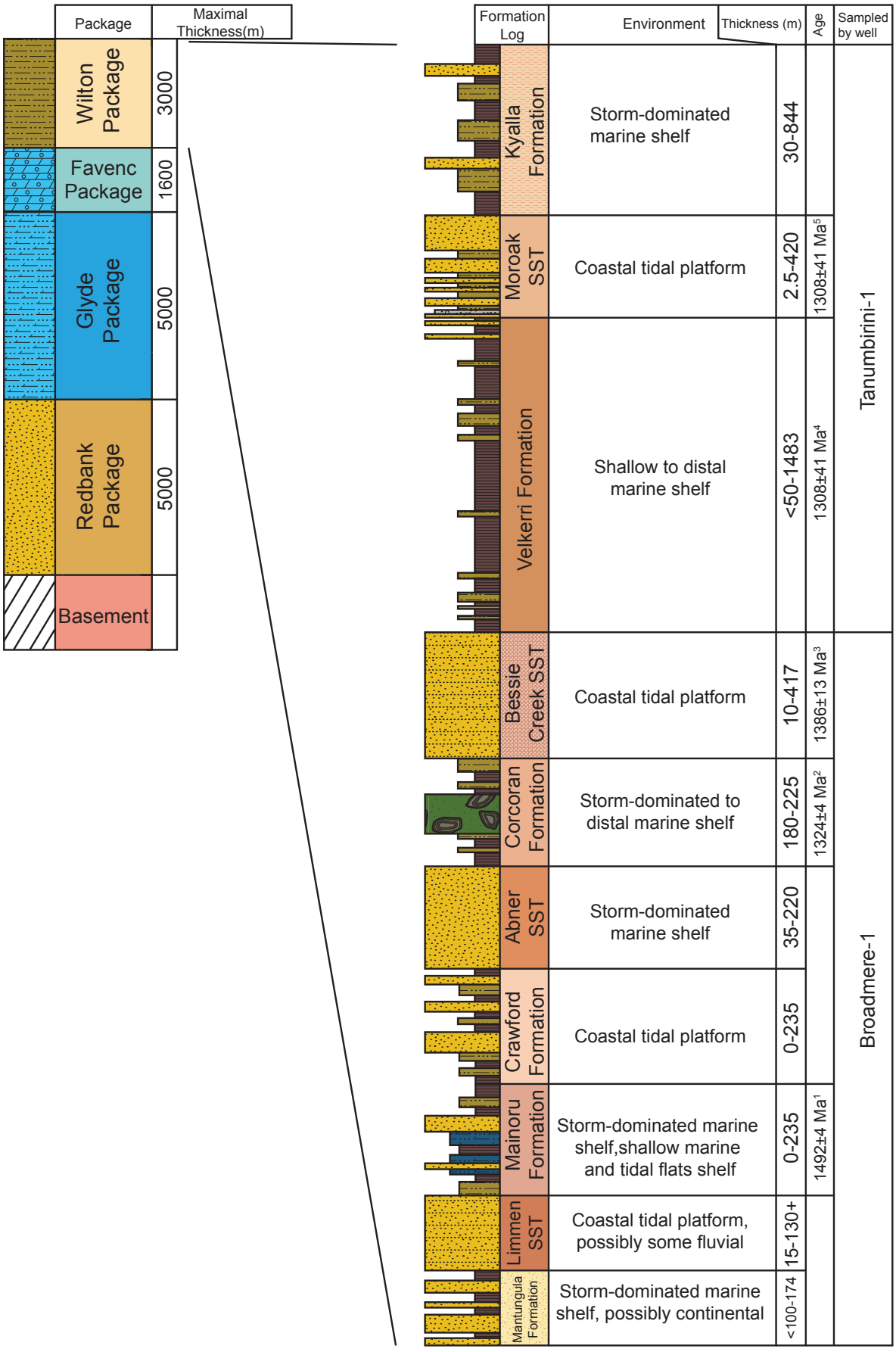

Figure 2.5: Stratigraphic column of the McArthur Basin packages and the formations of the Wilton Packages.

2.4. Potential Reservoir Formations

The potential reservoir formations of the Wilton Package are the Kyalla Formation, Moroak Sandstone, Velkerri Formation and the Bessie Creek Sandstone. The Barney Creek Formation is part of the Glyde Package and has reservoir potential too but will not be discussed. These formations have the right properties to act as a good reservoir (Revie, 2017). The most promising is the Velkerri Formation of the Wilton packages. This shale reaches a thickness of 1500m in the Tanumbirini-1 well. This Velkerri and the Kyalla Formations, also a shale, has gathered great interest for unconventional gas production and compare favourably with shale plays in the USA. (Revie, 2017). Table 2.1 gives an overview of the hydrocarbon volumes present in the discussed formations.

Formation	**Shale and Tight Gas** (Bscf)	**Shale Oil and Condensate** (mmbbl)
Barney Creek Fm	-	1123.4
lower Kyalla Fm	52260	70985
middle Velkerri Fm	104220	159658
Moroak Sst	8260	337982
Bessie Creek Sst	62310	568625

Table 2.1: Overview of the potential resources in the different formations, modified from Revie (2017). Data for the Barney Creek Formation is from Wal et al. (2012), the remaining is from RPS Group Plc (2013)

Bessie Creek Sandstone

The Bessie Creek Sandstone is conformably overlain by the Velkerri formation. It consists of thin bedded, fine to medium-grained, locally coarse and granule-rich quartz sandstone (Munson, 2014). It has been interpreted as a tide dominated shoreline (Abbott and Sweet, 2000). The thickness in wells ranges from 20m up to 442m. The Bessie Creek Sandstone has the potential as a conventional oil and gas reservoir. At shallow to moderate depths it could contain oil, while in deeper parts it would be filled with gas. The potential has been confirmed by oil shows in different wells. From the Amoco 82-8 well an average porosity of 9.6% and an average permeability of 111mD have been reported (Dorrins and Womer, 1983). However it has been suggested that in deeper parts diagenetic processes negatively impacted the porosity (Lanigan et al., 1994). There are numerous outcrops of this formation throughout the study area, especially at the Broadmere Complex. Many of the outcrops visited during the fieldwork were from this unit (figure 2.6).

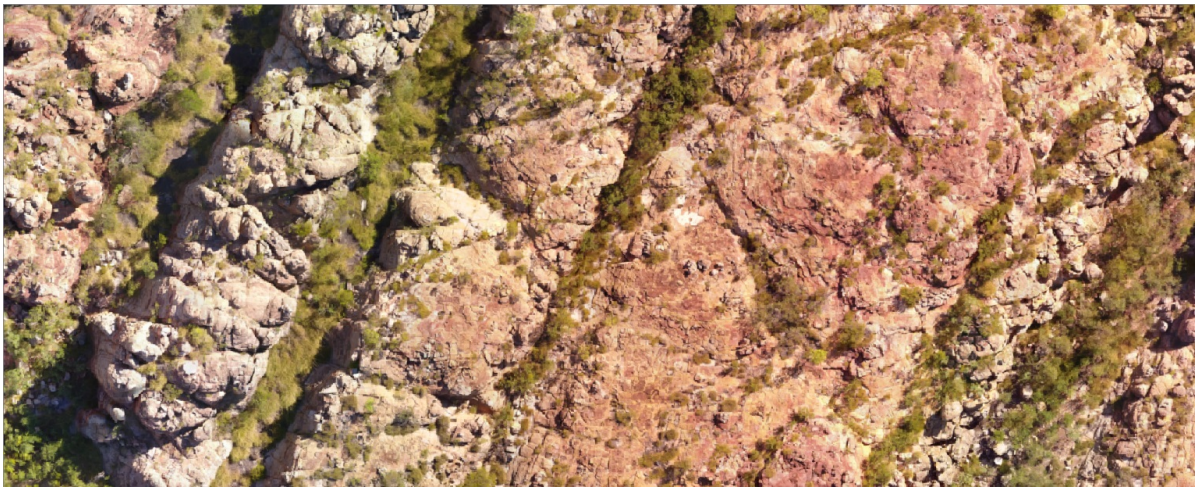

Figure 2.6: Fracture pavement on an outcrop of the Bessie Creek Sandstone. The image was acquired with a drone.

Velkerri Formation

The Velkerri Formation is mainly composed of claystones, mudstones, and siltstones. In addition, minor fine sandstone intervals are present (Munson, 2014). The formation is divided into a lower, middle and upper part. The lower interval consists of claystones and silty mudstones. Towards the base of the formation thin sandstone intervals become more common. The middle Velkerri contains dark grey to brown black claystones, mudstones and minor siltstones. The upper part consist of grey mudstones and siltstones, towards the top the number of intervals of thin sandstones increases (Munson, 2014).

The middle Velkerri has a high organic content in contrast to the relative organic poor upper and lower Velkerri (Lanigan et al., 1994). The total organic content (TOC) of the middle Velkerri ranges from 2-12% in the northern wells (Jackson et al., 1988, Warren et al., 1998). In the central part of the Beelaloo Sub-basin it is 2% (Hoyer et al., 2012).

It is believed that changes in organic content from organic lean intervals were caused by changing water conditions (e.g. becoming anoxic), instead of a change in water depth or depositional energy (Warren et al., 1998). The middle Velkerri was supposedly deposited in a distal deltaic and restricted marine basin. The lack of current structures among others indicates that the water depth was larger than the wave base. There are almost no outcrops of the Velkerri Formation, but cores do exist. Figure 3.2 shows a section of cores from the Marmbulligan-1 well.

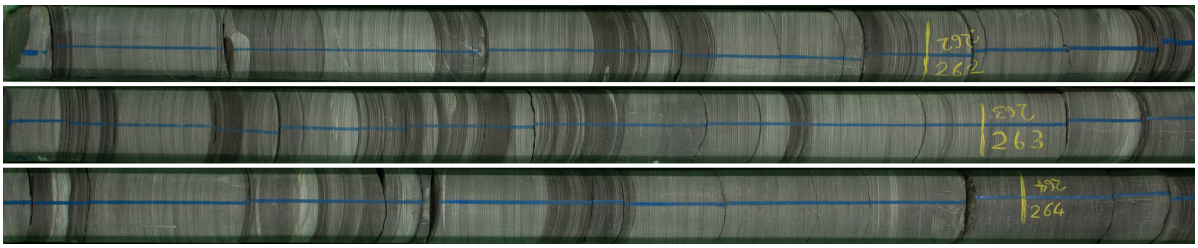

Figure 2.7: Cores of the Velkerri Formation from the Marmbulligan-1 well at the interval of 261.28 and 264.28m.

Moroak Sandstone

The Moroak Sandstone is a thinly to medium bedded and fine to medium grained quartz sandstone. Quartz granule rich and coarse grained intervals up to 1m occur at the base of the unit (Ahmad et al., 2013). The thickness ranges from just 2.5m up to 485m (Hoyer et al., 2012) in the Beetaloo Sub-basin. It has been interpreted as a tide-dominated shoreline deposit (Abbott and Sweet, 2000). Another theory is that the Moroak Sandstone is the lateral equivalent of the Velkerri Formation. In this setting the Moroak is part of a regional deltaic progradation (Silverman et al., 2008). The Broadmere Complex contains the only outcrops of the sandstone (figure 2.8), but these are often covered with vegetation.

Figure 2.8: Satellite image of the Moroak Sandstone.

As the Moroak Sandstone lies between two significant source units, it has the potential to act as a conventional oil or gas reservoir at the shallower depths of the sub-Basin. At larger depths, e.g. the centre of the Beetaloo Sub-basin, it can act as an unconventional gas reservoir. Porosities have been measured between 5-15% (Lanigan et al., 1994). However it is reduced at large depths, probably because of secondary pore filling cements (Munson, 2014).

Kyalla Formation

The Kyalla Formation is a regressive unit of interbedded grey to black silty mudstone, siltstone and fine sandstone (Abbott et al., 2001, Lanigan et al., 1994). It lies conformably on top of the Moroak Sandstone. The formation is identified as a high stand system tract within a sequence together with the Sherwin Formation and Bukalorkmi Sandstone. However these are not present in the study area (Abbott and Sweet, 2000). Thicknesses in the Beetaloo sub-basin range from 170-395m in the northern part (Hibbird, 1993, Menpes, n.d.) to 777m in the deeper part of the basin (Hoyer et al., 2012). The formation can be divided into a lower and upper member. The unit has great potential as an unconventional reservoir and also has limited conventional potential. Cumulative thicknesses of individual porous sandstone intervals can reach up to 70m (Lanigan et al., 1994). There are almost no outcrops of this formation.

2.5. Inacumba Group

An set of ungrouped formations unconformably overlie the Wilton Package. They are not part of the later Kalkarindji Province or the Georgina Basin. These formations are the Jamison Sandstone, the Hayfield Mudstone and the Bukalara Sandstone. Yang et al. (2018) found that the provenances of the first two units were different from the older Wilton Package formations. The provenance of the Bukalara Sandstone was found to be similar to the other two units (T.J. Munson, personal communication, May 18th, 2018). Therefore a new name is proposed for these three formations, the Inacumba Group after the Inacumba Creek in the OT Downs. An unconformity, which is observed in seismics, separates the Hayfield Mudstone and Bukalara Sandstone. This group will be important for understanding the geological history after deposition of the Wilton Package.

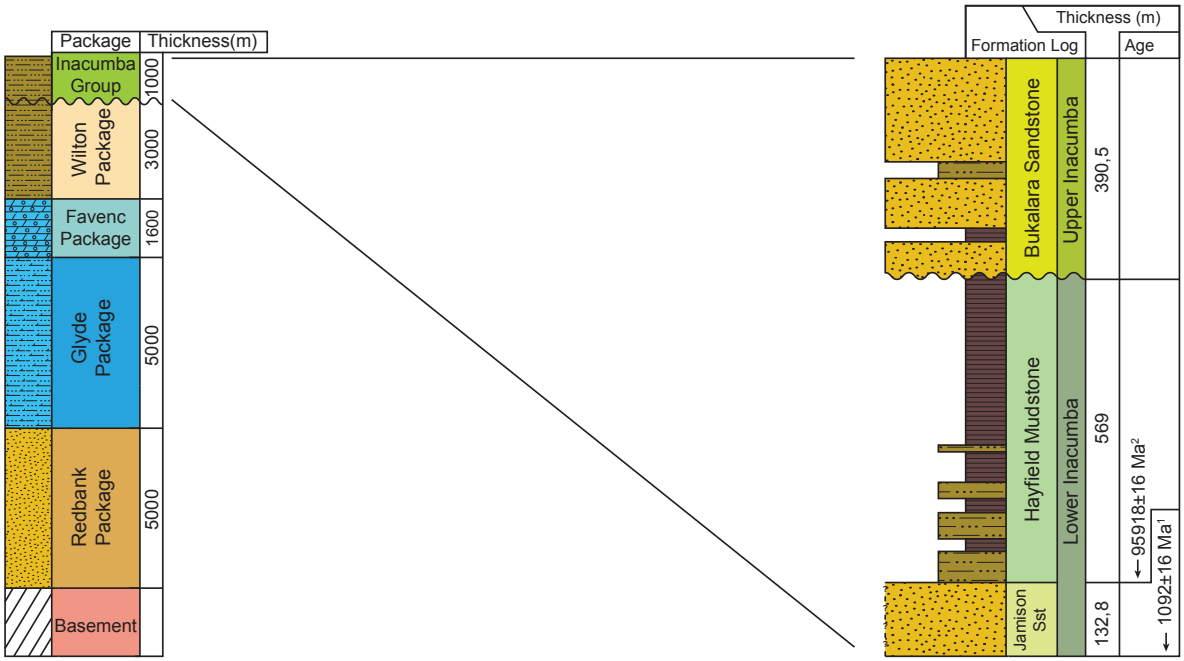

Figure 2.9: Stratigraphical column of the Inacumba Group based on the Tanumbirini-1 well.

3

Data Integration

The objective of this chapter is to link the Batten Fault Zone and the Broadmere Complex (outcrop areas) with the subsurface Beetaloo Sub-basin with a cross section. Different data sources can be used to create the cross section. These vary from georeferenced outcrop maps, seismic surveys, wells and other geophysical data e.g. gravity maps. Petrel software was used to import, view and interpret all the data. This resulted in a pseudo 3D model that was used to construct a cross section from the Bukalara Range in the east to the Beetaloo Sub-basin in the west. The Beetaloo-Broadmere area is modelled in 3D, as this required more focus. This helps visualize and identify large scale structures, unconformities and thickness differences. In this chapter the different data sources are discussed:

- Seismic surveys
- Well logs
- Georeferenced outcrop maps
- Magnetic surveys
- Gravity surveys
- AFTA based vertical movement curves

The wells are discussed in section 3.1. The seismic data is described in section 3.2 and the interpretation of the seismic composite line in section 3.3. The geophysical magnetic and gravity surveys are discussed in section 3.4. In section 3.5 two AFTA based subsidence curved are discussed. The main 'end product' of this chapter is a cross section and a 3D model (appendix B) of the Broadmere Complex and Beetaloo Sub-basin made in Petrel that contains all the relevant information.

3.1. Wells

There are four wells in the area of interest that intersect or are located nearby a seismic line. These wells are Tanumbirini-1, Marmbulligan-1, Broadmere-1 and Cow Lagoon-1 located from west to east respectively (figure 3.1). Although they give information about the depth of key formations they do not penetrate more than one package. This leaves the interpretation of deeper seismic horizons uncertain.

Tanumbirini-1
The Tanumbirini-1 is drilled at the location of the seismic line MCSAN13-05 reaching a depth of 3900 meters, going through the Wilton Package down to the Bessie Creek Formation. While matching the synthetic seismic signature to the seismic survey a bulk shift of 40ms was applied. Well tops were interpreted from the mud log report ((Santos Ltd, 2014)) and were used to constrain the interpretation in this study. Strong seismic reflectors align with the formation boundaries that have a sharp change in seismic impedance.

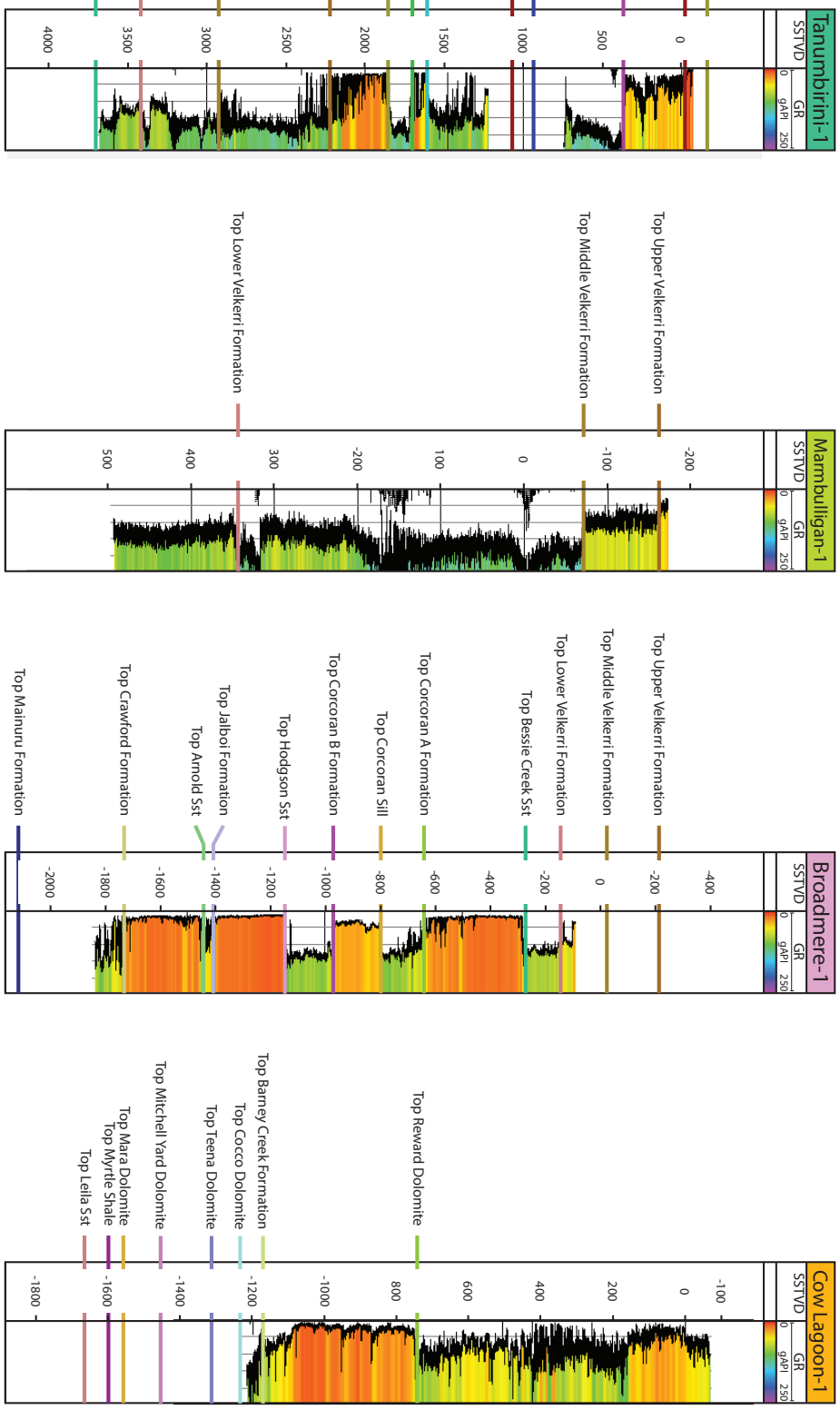

Figure 3.1: The four wells located in the area of interest.

The well can be used to trace most formations in the seismic lines because the layers are continuous. The Velkerri Formation reaches a thickness of almost 1500m. The well also gives detailed information on the Inacumba Group. Besides conventional logs, Formation Micro Image (FMI) and Ultrasonic Borehole Image (UBI) logs are also available. These will be used later on for the interpretation of fractures.

Marmbulligan-1
The Marmbulligan-1 is located on seismic line MCSAN13-04 and penetrates 674.8 meters of the Wilton Package (Velkerri Formation) at the western flank of an anticline structure (figure 3.2). This well had no checkshot data, so the sonic log was used and matched by tracing seismic horizons from the Tanumbirini-1 well. In addition it has an UBI log and cores over the whole interval. This is also used for fracture interpretation later on. It contrasts with the deeper and undeformed formations in the Tanumbirini-1 well.

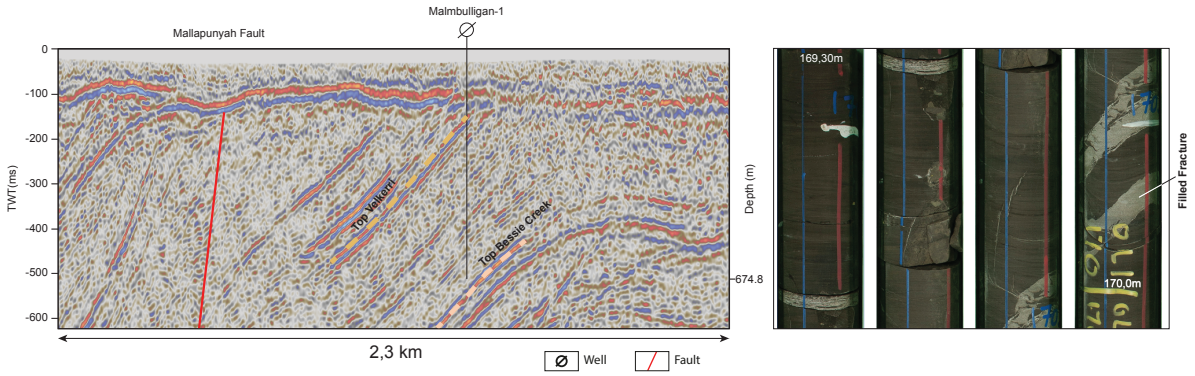

Figure 3.2: MSCAN13-04 seismic line with the Marmbulligan-1 well penetrating the Velkerri Formation (right). ±1m interval of core from the well (left).

Broadmere-1
The Broadmere-1 well is located at the crest of an anticline in the Broadmere Complex. It penetrates part of the lower Velkerri to the Mainuru Formation, but is only logged from the Bessie Creek Formation to midway in the Crawford Formation. Matching the synthetic with the actual seismic was successful.

Cow Lagoon-1
The last well is Cow Lagoon-1, which was difficult to match. Possibly because of issues with the checkshot data. In addition deviation data needed to be corrected before it could be used in Petrel. It penetrates the Reward Dolomite to the Leila Sandstone (both Glyde Package formations) and is logged down to the Barney Creek Formation (Glyde Package).

3.2. Seismic Data

Three seismic surveys are used in the study area (figure 3.3), from west to east these are:

- Green - MCSAN13 2D SS (2013)
- Blue - McArthur River 2D SS 1983 (1983)
- Red - 02-GA BT Survey (2002)

When seismic lines of different surveys intersect each other, horizons can be tracked from one survey to the other. The intersecting lines together form a composite line which is used to make a cross section that connects the outcrops with the subsurface. The composite line includes from east to west the 02GA-BT1, Broadmere 1983-120, Broadmere 1983-115, MCSAN13-08 and MCSAN13-02 lines.

There are different combinations possible of seismic lines to create the composite line. The 02GA-BT1 and the MCSAN13-08 lines ought to be used as they are the only lines connecting the three surveys. The criteria that were used are:

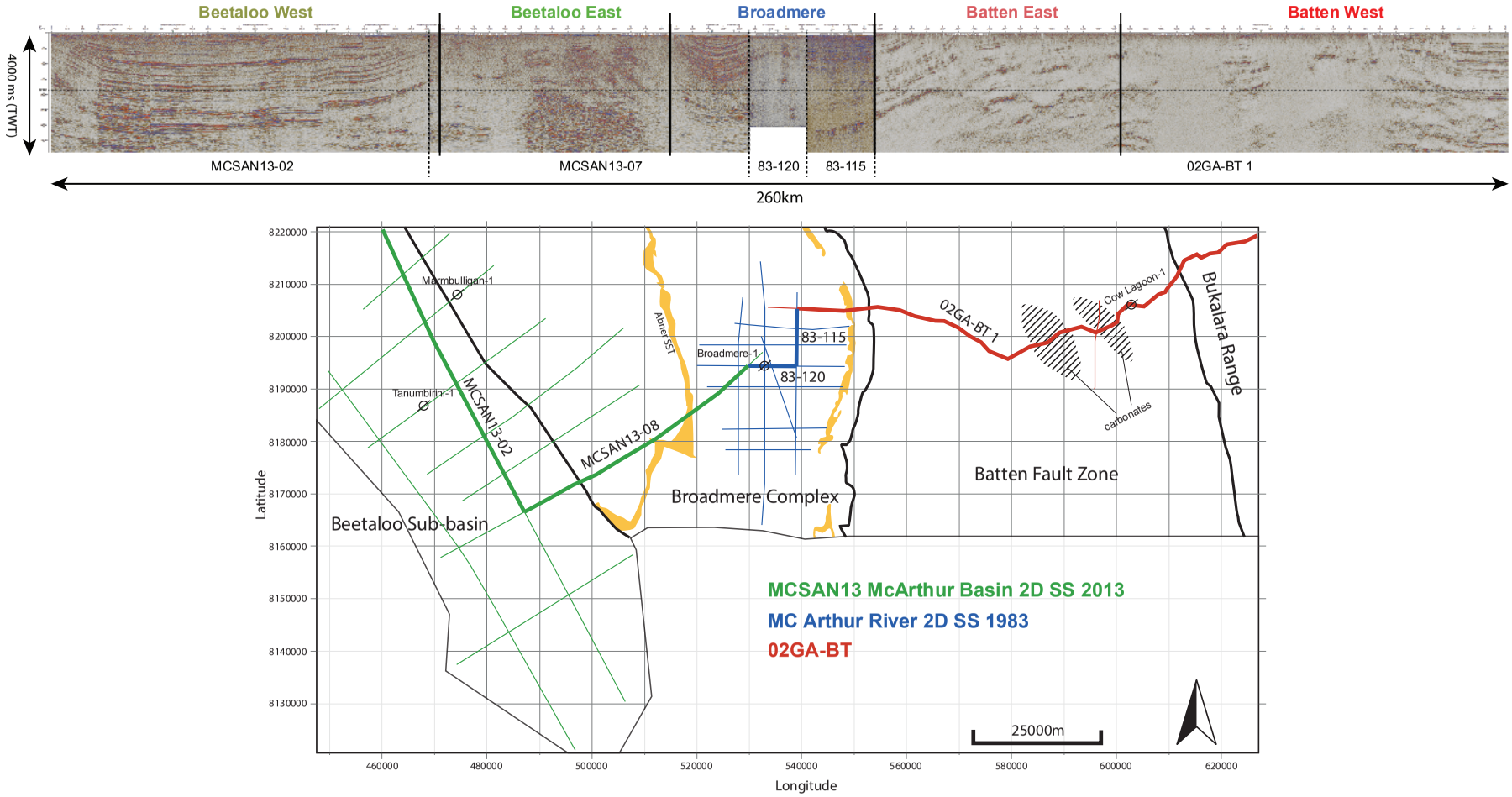

Figure 3.3: (Top) Seismic composite line connecting the outcrops with the subsurface. The line is divided in uninterpreted sections in appendix A. (bottom) The layout of the three seismic surveys. The yellow outline represents the Abner Sandstone outcrops in the Broadmere Complex.

- A lower number of different seismic lines is better. Interpreting on the same seismic line is easier.
- The quality of the seismic image (especially in the MC Arthur River 2D SS 1983 survey) is an important criteria. Some lines are very bad, making interpretation difficult.
- The lines should ideally be oriented perpendicular to the strike of important features.

The MCSAN13-02 and MCSAN13-08 intersect each other perpendicularly, this is unfavourable. In figure 3.4 the whole MCSAN13-02 line can be seen. A structure can be seen at the intersection with the MCSAN13-08 line. The southern part is similar to the continuation of the MCSAN13-08 line. The northern part of the MCSAN13-02 line is representable of the whole Beetaloo Sub-basin. Additionally the Tanumbirini-1 well can be used to interpret the formations in the seismic lines.

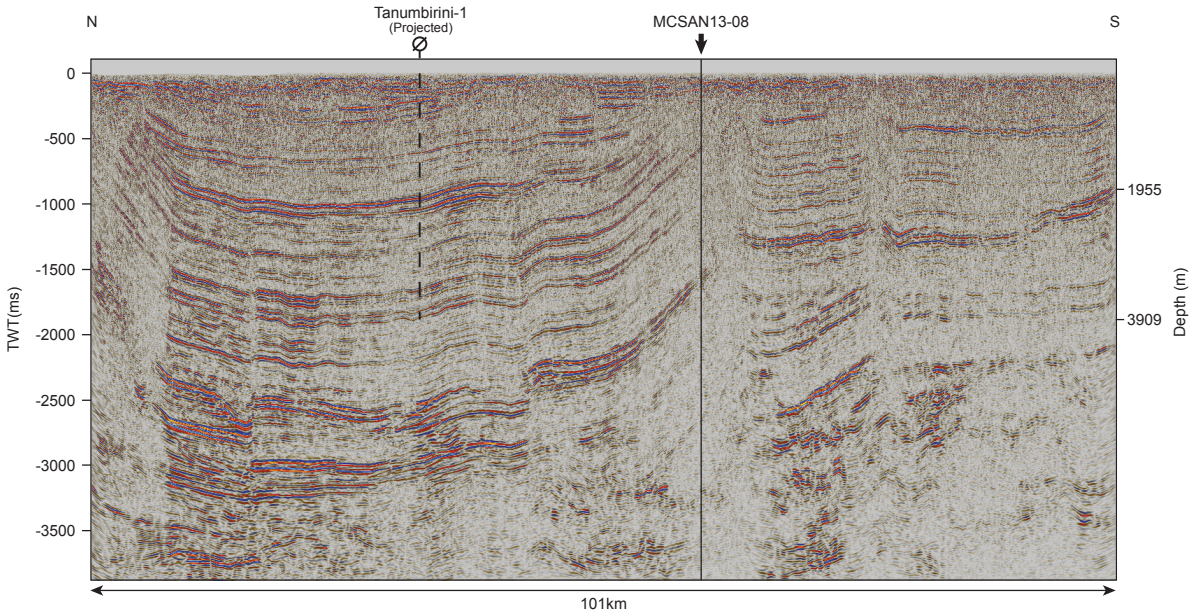

Figure 3.4: The MCSAN13-02 line, with the structural feature.

The MCSAN13 2D SS survey was shot over the Beetaloo Sub-basin. The seismic lines are organized in a grid pattern. This makes it easy to create a 3D model were horizon depths can be interpolated from surrounding seimsic lines. The Mesozoic and Cenozoic outcrops have a good acoustic conductivity, resulting in high quality seismic images. MCSAN13-08 extends into the Broadmere Complex. Here it intersects multiple lines of the next survey. This line captures both the western side of the Broadmere Complex (outcrops), a fault zone (structurally separating outcrop and subsurface) and the Beetaloo Sub-basin.

The McArthur River 2D SS 1983 is an old survey, hence the quality is not as good as the other two surveys. There is noise and especially the layers deeper than ±1000ms are not well imaged. Some of the lines are bad, while others are closer in quality to the previous survey. The grid pattern is denser than the MCSAN13 2D SS. Grid lines are oriented parallel and perpendicular to the main fold axes of the Broadmere Complex (N-S). With the exception of one line that is rotated 45 degrees counter clock wise with respect to the north.

The 02-GA BT survey was not shot in a grid pattern but along a road which is going from west to east. The quality is good in most places, but when the line encounters carbonates (figure 3.3) the quality of the image is degraded, resulting in a very low seismic response in some sections across the seismic line. Nevertheless the survey managed to image very deep in to the subsurface, even reaching the Moho (Rawlings et al., 2004).

3.3. Seismic Interpretation

In this section a description is given of the different sections of the seismic composite line. The sections have some overlap with each other to make it clearer to trace the interpreted horizons.

Batten East
In the eastern end of the composite section lies the Bukalara Range (see figure 3.5). The layers are flat and largely undeformed. The layers are dipping towards the east when nearing the Emu Fault. The deformation around the Emu Fault decreases the quality of the image. The fault has been described in literature as a positive flower structure (Rawlings et al., 2004).

The Cow Lagoon-1 well is situated between the Emu and the Crocodile Fault. The Glyde package outcrops consist of formations of the lower part of the package. A clear group of seismic horizons is visible just above 1000ms. The well has logged into the Barney Creek Formation reaching a depth of 1283m. However the Leila Sandstone (even further down the stratigraphic column) has been observed to be at a depth of 1739m and is still above the grouped horizons. The lack of other horizons below 1000ms except for the basement led to the interpretation that the grouped horizons are the boundary between the Glyde and lower Redbank Package.

Between the Crocodile and Tawallah Faults large gaps in the image occur, which have been caused by outcropping carbonates of the Favenc Package. This is likely caused by unsaturated porosity and karsts (Rawlings et al., 2004). Areas around faults also result in a poorer seismic response. Faults have been interpreted from the surface first and then into the seismic images. The area between the Crocodile and the Glass Faults contains no other major faults. However it is also shot above carbonates, decreasing image quality. This is exemplified by horizons popping up east of the Glass Fault, here the geophones are not in carbonates but in sandstones. The carbonates and a bad image quality occur again west of the fault. The Tawallah Fault brings sandstones to the surface again improving the image significantly.

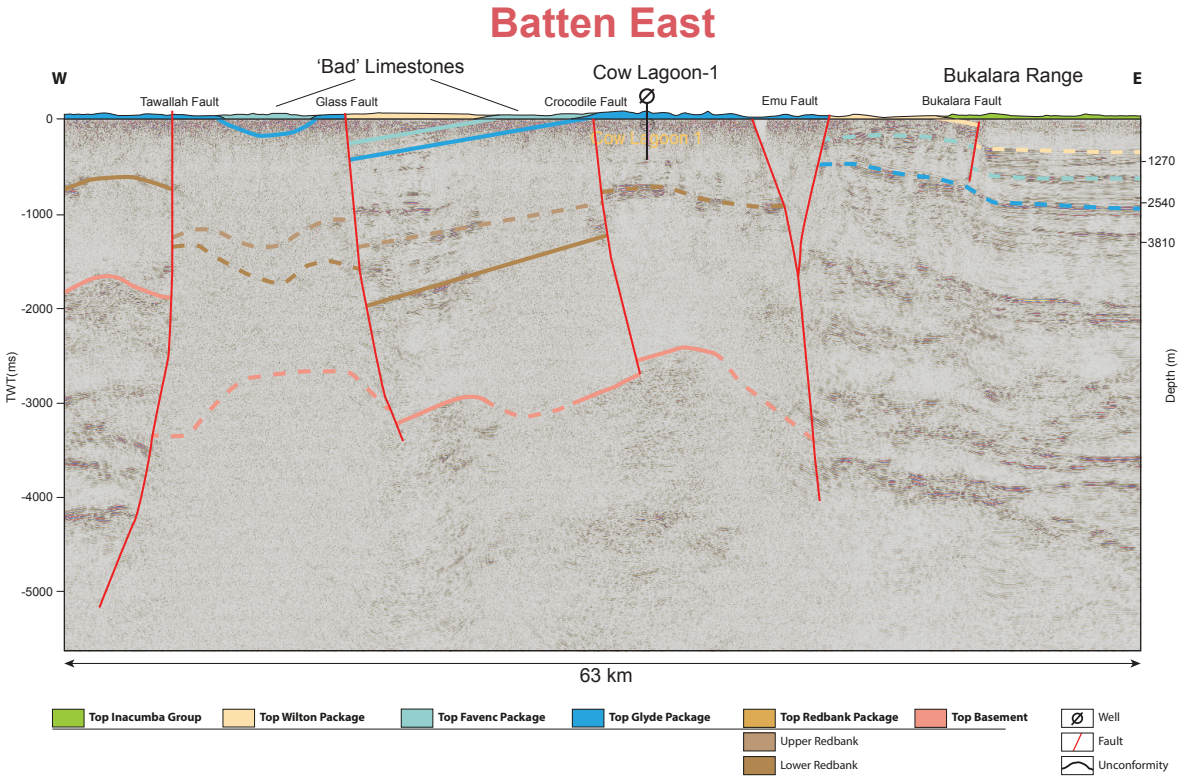

Figure 3.5: The Batten East section of the composite line.

Batten West

West of the Tawallah fault the image quality remains good (figure 3.6). This section can be divided in two parts: above and below the horizons interpreted as the basement (around 2000ms). Above the basement different horizons can be observed that could be correlated to package boundaries in outcrops at the surface. The horizons above the basement and between the Eighteen Creek and Tawallah Faults have been interpreted as the Lower Redbank Package with no Upper Redbank package on top. The contact between the Glyde and Lower Redbank Package does crop out south to the seismic line, also with no Upper Redbank Package in between (map view in figure 3.6). In addition, the seismic line is curved, this means that part of the convex shape of the Upper Redbank horizon is caused by the changing orientation of the seismic line. Hence the horizon dips to the north, which is also consistent with the dip observed on the surface.

The Upper Redbank Package is found mainly at topographic lows and is generally absent at topographic highs with respect to the Lower Redbank Package. This observation guided the interpretation of the Upper and Lower Redbank Packages in the seismic image when no clear horizons were present. The Upper Redbank Packages can be seen pinching out when nearing a topographic high of the Lower Redbank Package.

West of the Four Mile Lagoon Fault the formations begin to dip towards the west as part of the Bauhinia Syncline. The outcrops of the Wilton and Glyde Package can be traced from the surface to the seismic. The Favenc Package is locally eroded here.

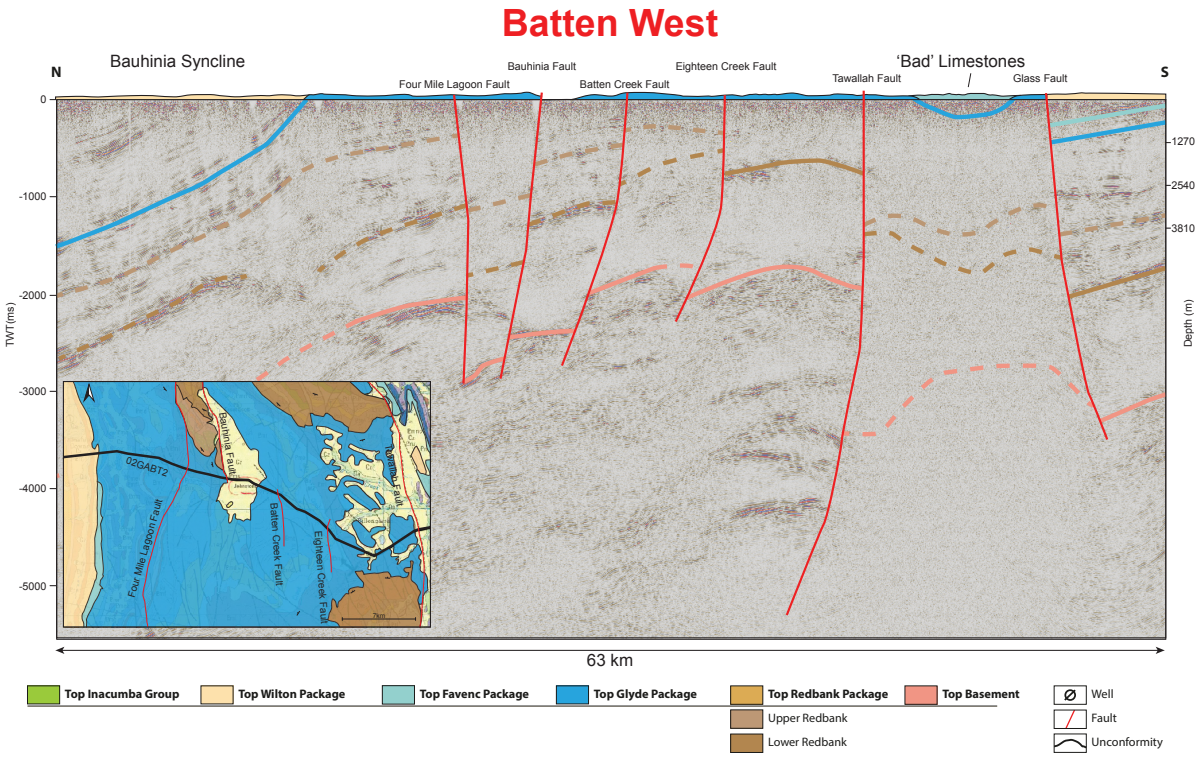

Figure 3.6: The Batten West section of the composite line, including a map section to indicate the curvature of the line.

Broadmere
This part of the composite line consists of three different seismic lines of two surveys. There are multiple folds from east to west:

- Bauhinia Syncline
- Broadmere Anticline
- Limmen Bight Syncline

No major faults have been observed neither at the surface nor in subsurface. The images from the Broadmere 1983 survey are of lower quality compared with the other two surveys, especially below 1000ms the images of the survey do not show clear reflections. The transition between the three surveys is good. From the MSCAN13 to the Broadmere 1983 almost all of the seismic reflections coincide with each other.

There is an asymmetry between the Limmen Bight and the Bauhinia Syclines. In this section this is exaggerated by the seismic line 83-115 which is oriented subparallel to the fold axis, elongating the shape of the fold. The flanks of the folds contain outcrops that can be traced on seismics to the subsurface. The Favenc Package pinches out on the eastern flank of the Bauhinia Syncline. This is observed at the outcrops, where the Glyde Package is unconformably overlain by the Wilton Package. But this changes along the strike of the fold limb. At other locations the Favenc Package is present.

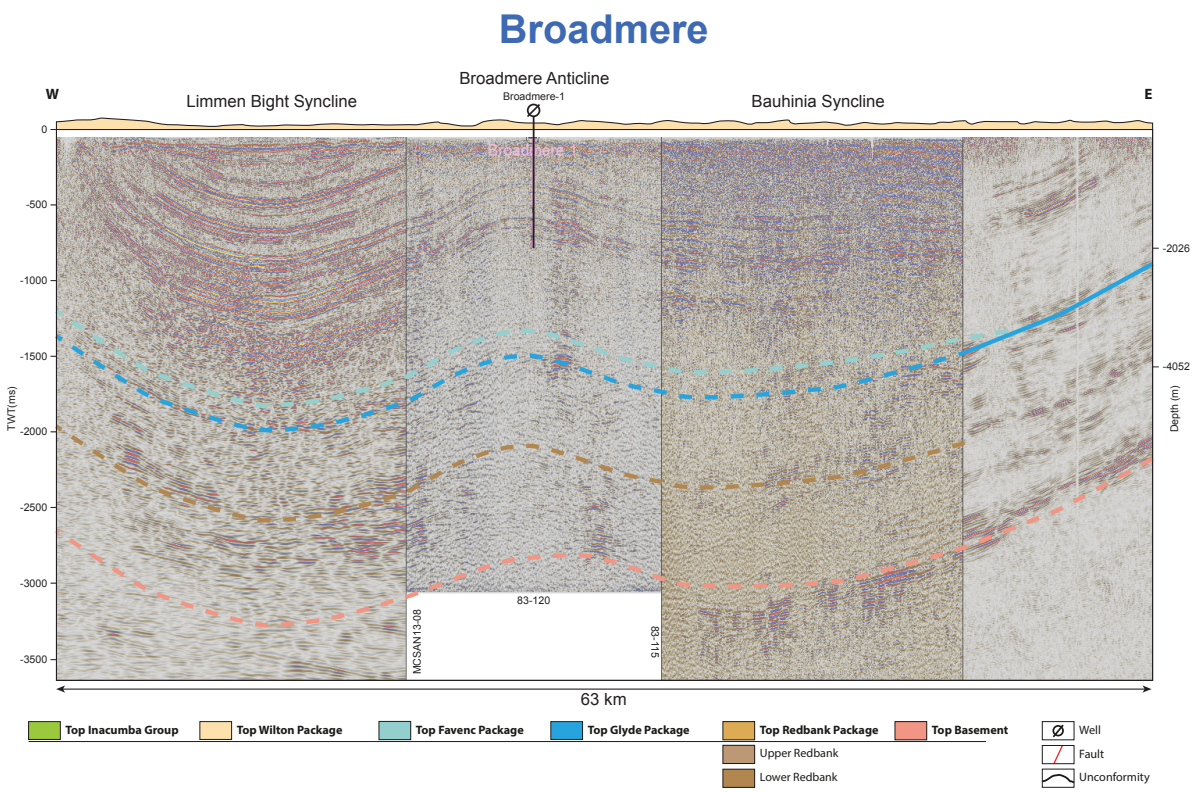

Figure 3.7: The Broadmere section of the composite line.

Beetaloo East
This section links the outcrops with the subsurface (figure 3.8). The western flank of the Limmen Bight Syncline flattens out and the horizons remain horizontal. Here a major toplap structure is observed between the interpreted Favenc Package and underlying formations. This toplap is referenced in the report as the Calymmian Unconformity. At a greater depth another unconformity is observed, in this report referred to as the Orosirian Unconformity. This is however part of the basement and thus not within the scope of this study.

A series of faults are observed that offset the sedimentary packages and the basement. The basement is uplifted compared to the surrounding areas. Especially the Mallapunyah Fault has a displacement of ±630 ms (TWT) or an estimated 1700m. This faulted zone is called the Mallapunyah Fault Zone. There are no outcrops of packages of the McArthur Basin west of the of the fault, because of the large fault throw. This marks the beginning of the Beetaloo Sub-basin.

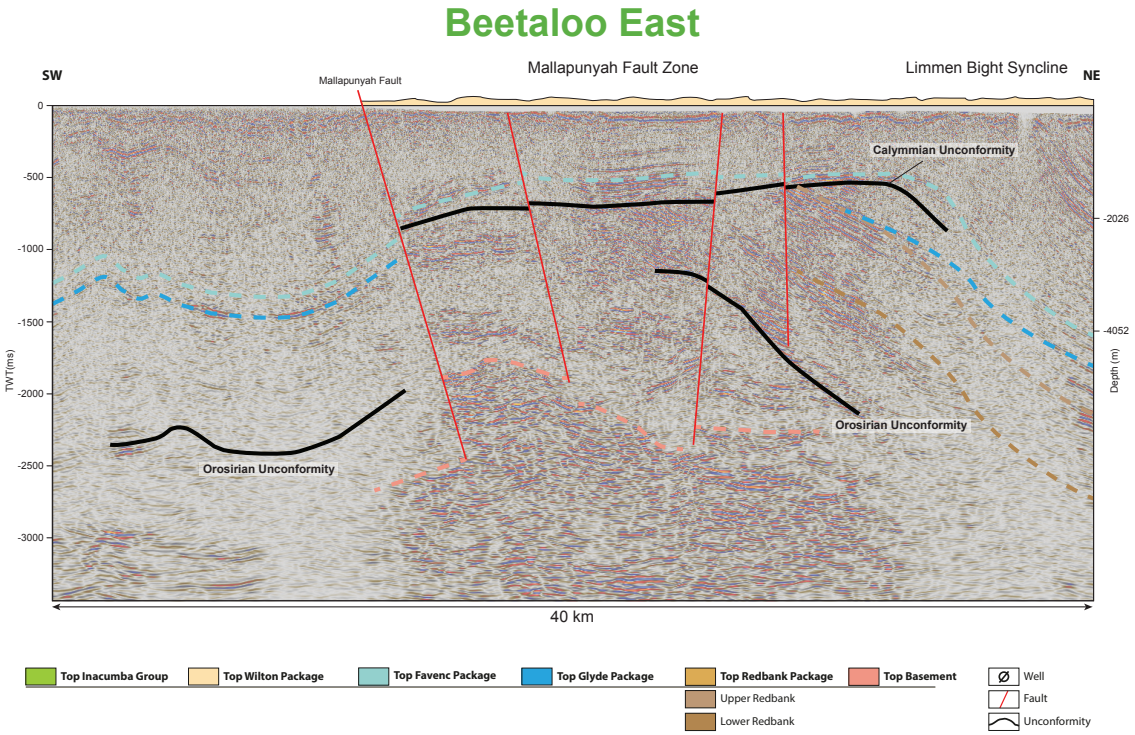

Figure 3.8: The Beetaloo East section of the composite line.

Beetaloo West

This section (figure 3.9) is oriented from south to north and contains part of the Beetaloo Sub-basin. The seismic reflections are clear and form a layer cake system. At the edges the layers are dipping upwards. The Tanumbirini-1 well, which coincides with a seismic line perpendicular to this section, gives valuable information on the upper formations of the Wilton Package and the Inacumba Group.

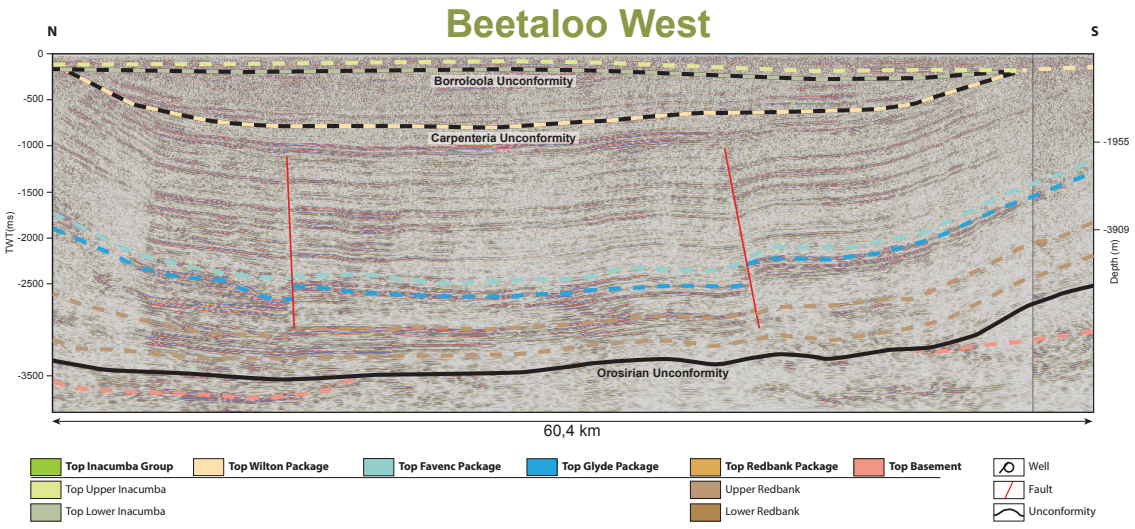

Figure 3.9: The Beetaloo West section of the composite line.

In this upper part two unconformities are interpreted, the Carpenteria and Borroloola unconformities. Towards the base of the Wilton the successive layers are disturbed by offsetted horizons and other deformational structures. FrogtechGeoscience (2018) interpreted this as the top of the Glyde Package. The boundary between the Lower Redbank Package and the basement is marked by the Orosirian Unconformity.

3.4. Magnetic and Gravity surveys

The NTGS has done extensive geophysical surveys, two of these (magnetic and gravity surveys) proved to be helpful in identifying faults in the Beetaloo Sub-basin. In combination with seismic and outcrop data faults can be traced in between seismic lines, which increases the quality of the geo-model.

The magnetic survey (figure 3.10) consist of airborne-acquired TMI (Total Magnetic Intensity) data. The features seen are either faults or igneous rocks. The feature interpreted as the Antrim Plateau Volcanics still shows the paleogeography in detail. This plateau covers a large part of the Beetaloo Sub-basin, but not the eastern part. This is proved by the absence of these rocks in the Tanumbirini-1 well and the presence in the Burdo-1 well. This also seen on the magnetic data.

The gravity map (figure 3.11) is also based on airborne acquired data. The colors often correlate with the depth of the basement. Faults are visible too, but also at locations were they are not detected by the magnetic survey. For example a series of faults can be seen in figure 3.11 which are also visible on seismic images.

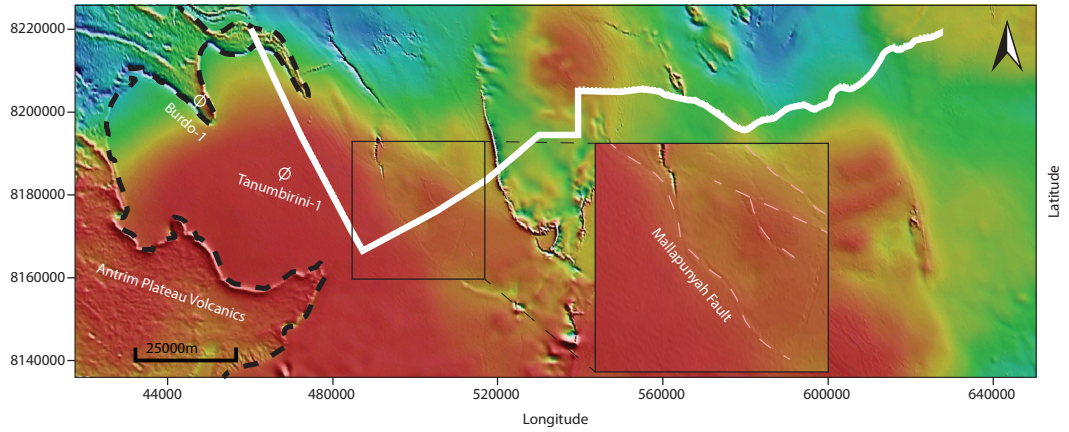

Figure 3.10: Magnetic TMI survey from the NTGS and the seismic composite line.

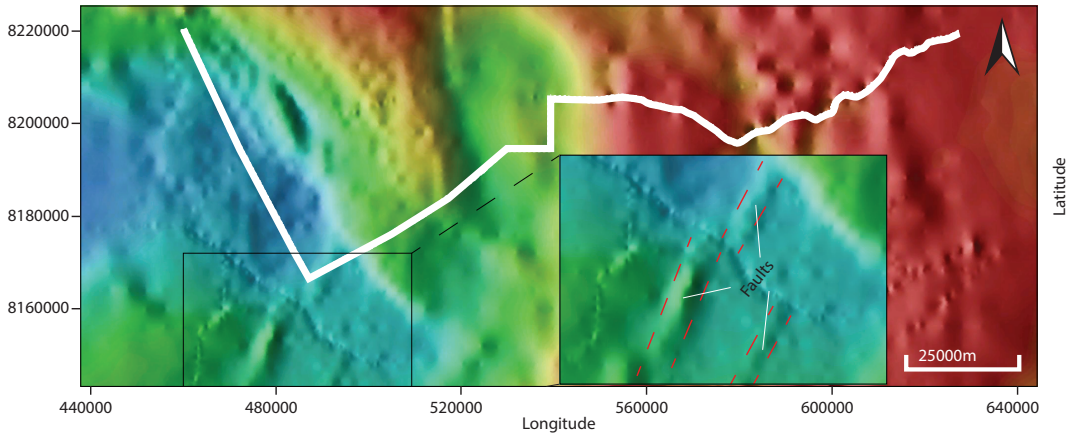

Figure 3.11: Gravity survey from the NTGS and the seismic composite line.

3.5. Vertical movements based on AFTA data

Two vertical movement curves (figure 3.12) at well locations are available from literature (Duddy, 2015, Duddy et al., 2004). These are situated at the Broadmere-1 and Jamison-1 wells. The curves are based on AFTA (Apatite Fission Track Analysis) data and is correlated with VR (Vitrinite Reflectance).

AFTA is a method to study the time of cooling after rocks have been exposed to a certain temperature. When Uranium-238 in a apatite crystal releases high charged particles during fission, they leave a track in the crystal. The time that has passed since the apatite crystal has been formed can be calculated, as the rate of fission is strictly time depended. When the grains are exposed to temperatures between 60 and 120°C, the length of the fission tracks begins to decrease as they start to heal (also called annealing). When reaching a temperature of 120°C the tracks have disappeared. The length thus becomes analogous to the exposed temperature. This also means that events prior to a thermal maximum can no longer be observed.

The Jamison-1 curve is based on 18 samples taken from depths between 519 and 1669.8m. The Broadmere-1 well has 6 samples taken from depth ranging from ±500 to ±2000m. In both curves two subsidence and two uplift events are visible. The Cambrian Event caused subsidence that was greater in the Jamison-1 than in the Broadmere-1. The following uplift, the Triassic-Jurassic Event, was also different at the two locations. It stopped during the Jurassic and was followed by a new phase of subsidence during the Cretaceous. During this phase the subsidence in the Broadmere-1 well is greater than in the Jamison-1 well. Renewed uplift during Tertiary continues to the present day.

The Cretaceous Event marks a major exhumation phase that also led to erosion. But the events that led to the generation of the fractures in the Wilton Package cannot be inferred from the AFTA data as they happened before the Cambrian.

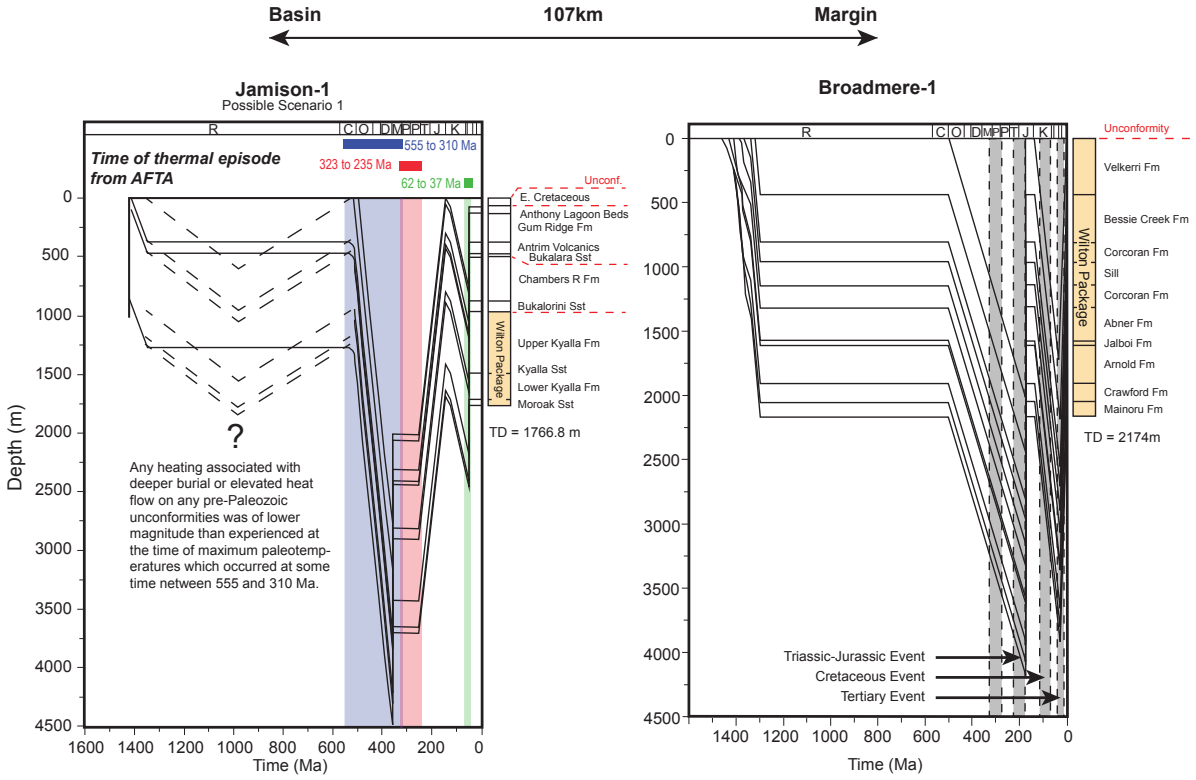

Figure 3.12: Vertical movement curves for the Jamison-1 well (left) and the Broadmere-1 well (right). Modified from Duddy (2015) and Duddy et al. (2004) respectively.

3.6. Backstripping

Backstripping is a method where the formations are removed one by one from younger to older formations. It is an useful tool to create a vertical movement curve, an example is given in figure 3.13. The depth of the formation is plotted on the vertical axis while the time on the horizontal axis. Different types of radiometric dating techniques provide the time of deposition of formations, which is the time when formations where at the surface. Unconformities indicates an erosional surface, i.e. a formation has come to the surface where it is only partially eroded after which it eventually subsides again. New formations are then deposited on top of this eroded surface. Unconformities can represent change of a tectonic phase, especially at a large scale setting. This method will be used in chapter 4.

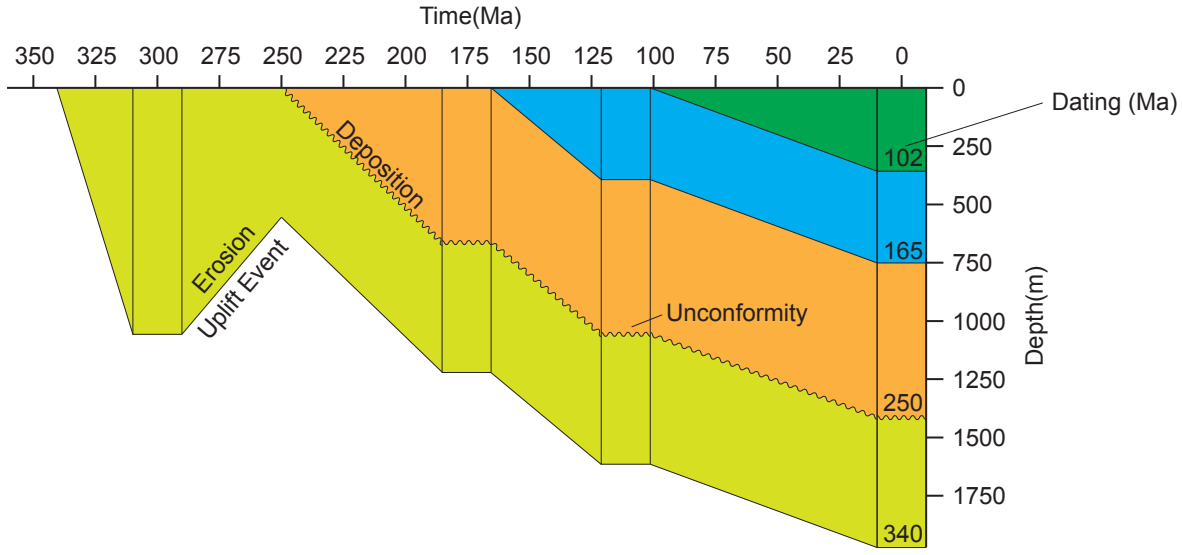

Figure 3.13: Example of a vertical movement curve.

4

Geological History

In this chapter the results obtained from the cross section are discussed as well as the Tanumbirini-1 backstripping results. The geological history is reconstructed based on literature and data integration. Only the large scale events are discussed, however more attention will be paid to the evolution of the Wilton Package and the Inacumba Group.

Within the scope of this thesis the interest in fracture geometry extends only to the formations of the Wilton Package. Fractures are generated by deformation phases affecting this package during and after its deposition. The deformation events are related to the vertical movement of the rocks.

4.1. Cross Section

The interpreted cross section and corresponding map are presented in figure 4.1. The focus of this study is on the large scale structures. Smaller scale faults, observed in the seismic, are not incorporated.

In the east the Bukulara Range is undeformed, flat and is bounded by the Emu Fault. In contrary to Rawlings et al. (2004) the Emu Fault has been reinterpreted as a negative flower structure. In figure 4.2 the cross section through the Emu fault shows that the core of the flower structure is thrown down with respect to the formations in the east and thrown up with respect to the formations of the west. The eastern branch of the fault acted as a 'reverse' fault similar to the Mallapunyah Fault. The region east of the eastern fault branch subsided more than the region west during basin wide subsidence.

The Batten Fault Zone is marked by a series of reverse faults, i.e. the Tawallah and Scrutton Faults. The packages start to form smaller folds towards the centre of the cross section, this is the Broadmere Complex. West of the complex a large angular unconformity separates the Favenc Package from the underlying packages. The Mallapunyah Fault forms the boundary between the Beetaloo Sub-basin and the other sections. The thicknesses of the packages change across this fault. The Redbank and Glyde packages are far thicker in the Batten Fault Zone as it was their depocentre. The depocentre shifted towards the Beetaloo Sub-basin during the deposition of the Wilton Package. The package is far thicker here than in the fault zone.

Accurate thicknesses of formations can be obtained from the Broadmere-1 and the Tanumbirini-1 wells. But no formation is penetrated by both wells. The thickness of the Velkerri Formation could be established at both well locations in combinations with seismics and surface geology (figure 4.3). The thicknesses are 1481.98m and 250m at the Tanumbirini-1 and Broadmere-1 well locations respectively. This thickness variation is also visible on the cross section. The Velkerri Formation is also thicker in Marmbulligan-1 than in the Broadmere-1 well. The total thickness in the Marmbulligan-1 well is however unknown as the well does not penetrate the underlying formation. This observation implies that thickness change is not solely caused by the Mallapunyah Fault but rather the Mallapunyah Fault Zone. This zone consist of smaller scale faults and is not included in the cross section but can be seen on the composite seismic line.

Thickness variations are also observed in the Glyde and Upper Redbank Packages. The actual thicknesses are not known and the cross sections indicates an interpreted thickness. The packages either become thinner or pinch out on structural highs of the Lower Redbank Package. Thickness variations are important when they occur above and within the Wilton Package. The variations below do not impact fracture generation in this package.

There are three orders of folding present. The first order ($10^2 km$) is an anticline of which the flanks correspond to the Beetaloo Sub-basin(west) and the Bukalara Range(east). The second order folding ($10^1 km$) is a series of folds like the Broadmere Complex but also the anticlines west of the Tawallah Fault and west of the Emu Fault. The third order ($10^0 km$) folds are smaller folds including the folds contained in the Broadmere Complex, i.e. the Limmen Bight and Bauhinia Synclines.

Four unconformities have been observed that are described in this study (figure 4.1). The Borroloola and the Carpenteria Unconformities are very close to each other. The Borroloola Unconformity separates the Upper from the Lower Inacumba Group. The Carpenteria Unconformity separates the Inacumba Group and the Wilton Package. The Calymmian Unconformity separates the Favenc Package and underlying Packages. The Orosirian Unconformities separates the basement and the overlying formations.

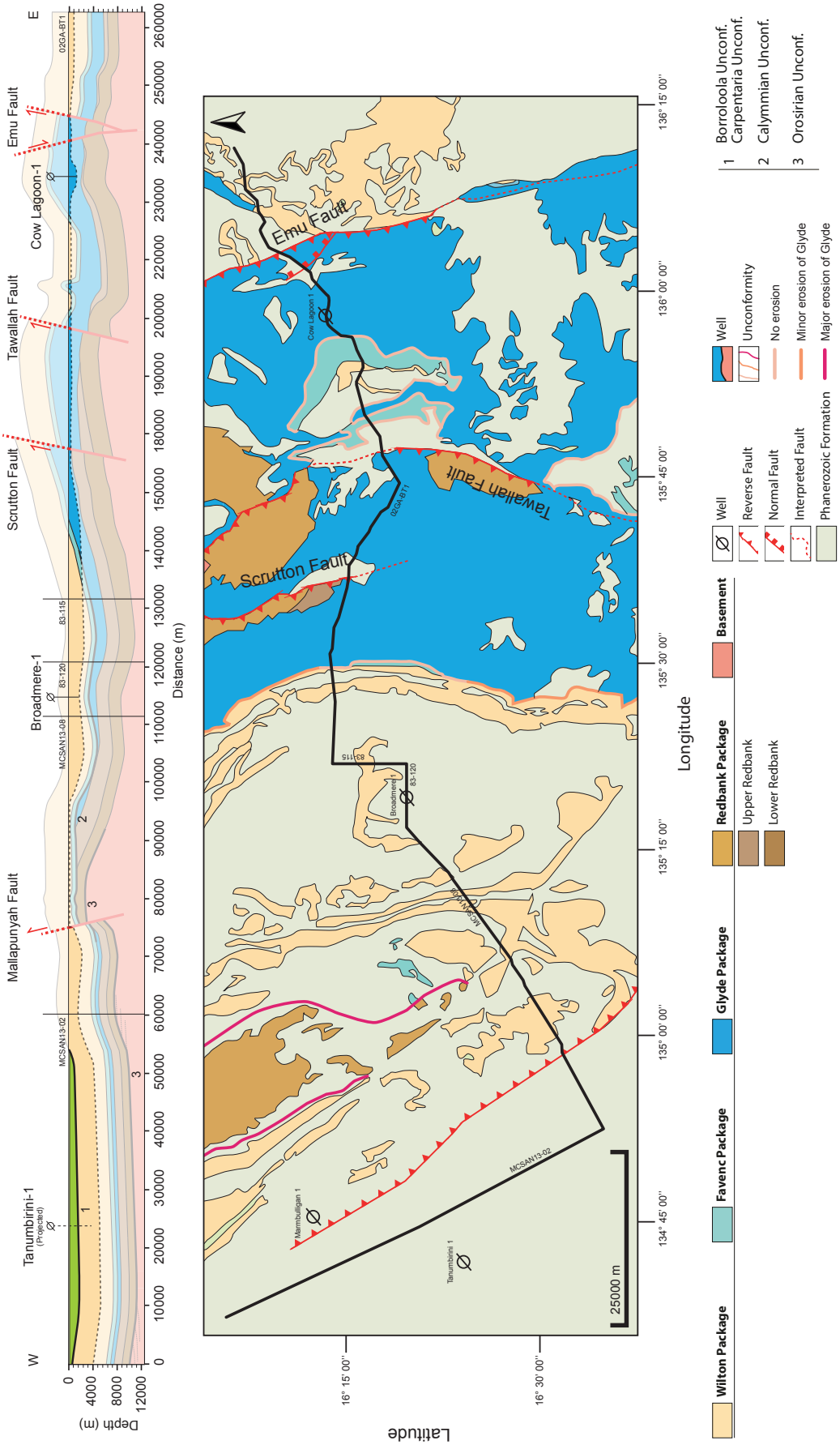

Figure 4.1: (top) Geological map of the large scale structures and the location of the composite seismic line. (bottom) The geological cross section linking the outcrop areas with the subsurface. There is no vertical exaggeration.

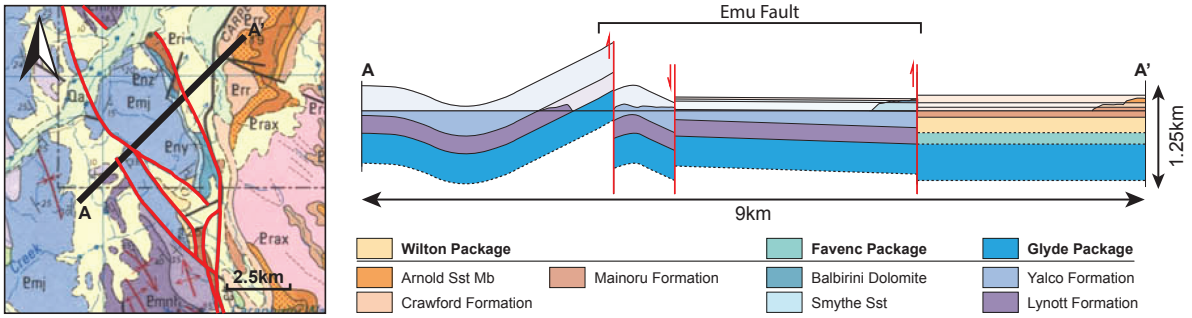

Figure 4.2: Surface geology map of the Emu Fault nearby the location of the seismic composite line and a cross section through the fault.

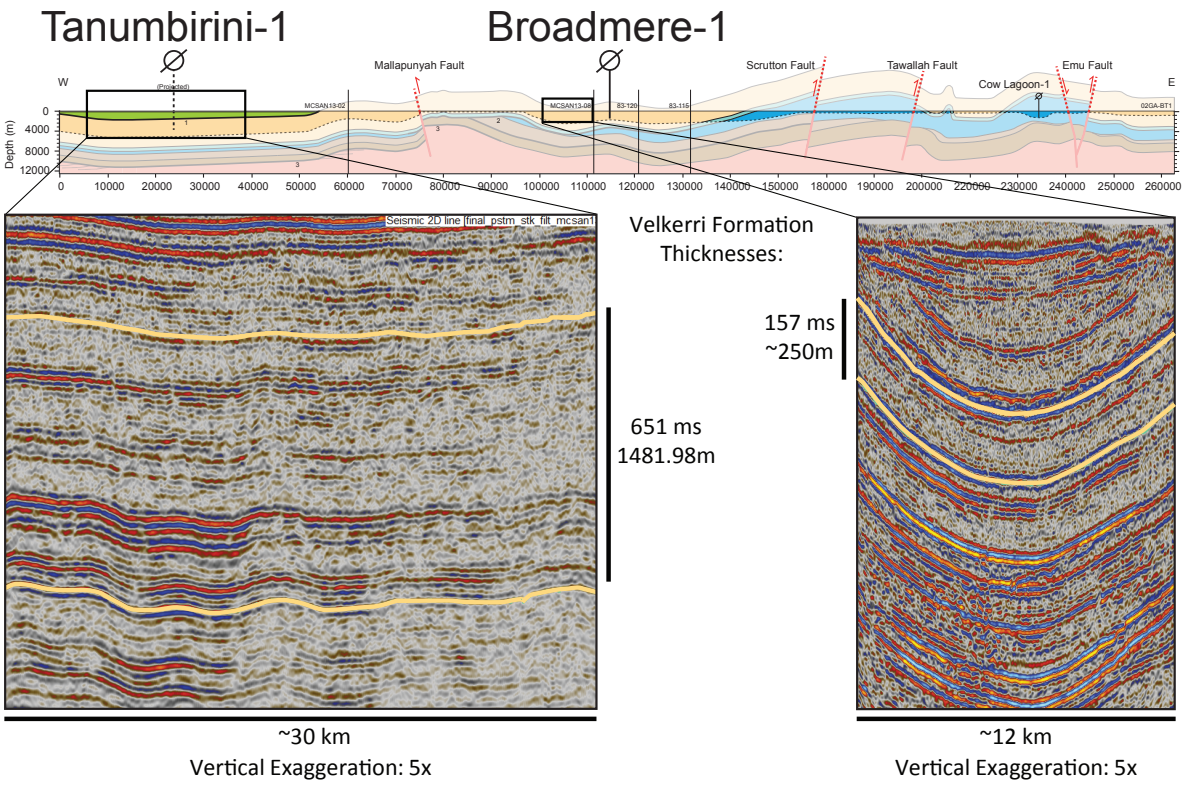

Figure 4.3: Sections of the composite seismic lines neighboring the Tanumbirini-1 and Broadmere well. Based on the seismic and well tops the thickness of the Velkerri Formation is established.

4.2. Intergrated vertical movement curve of the Tanumbirini-1

The Tanumbirini-1 was backstripped to quantify the deformation history of the McArthur Basin as the vertical movements and deformation phases might be correlated. Two AFTA based vertical movement curves from literature have been presented in section 3.5. They give values for subsidence at the margin and centre of the Beetaloo Sub-basin. Because of the limitations of the AFTA method, only data younger than ±555Ma exists. The gap between the deposition of the Wilton Package and ±555Ma is filled by integrating data from literature and seismics. The results are visualized in a vertical movement curve of the Tanumbirini-1 well.

Natural processes involved with uplift and subsidence, like decompacting exhuming formations or isostasy of the underlying crust, are included when backstripping. However, within the scope of this thesis none of these were used. The Tanumbirini vertical movement curve (figure 4.4) shows two uplift events before 555Ma, the Carpenteria and the Borroloola Events, corresponding to the two unconformities discussed in section 3.2. They are discussed in the next section. The timing of the first event can be constrained using recent published data, but further research is need to further constrain the second event.

The Jamison Sandstone has been dated by Yang et al. (2018), giving ages for both the Upper (959±18 Ma SHRIMP U-Pb) and Lower Jamison Sandstone (1092±16 Ma SHRIMP U-Pb). The younger Hayfield Mudstone and Bukalara Sandstone have yet to be accurately dated. However Yang et al. (2018) showed that the Hayfield Mudstone and the Upper Jamison Sandstone have the same provenance, in contrast to the provenances of underlying formations. Hence it is more likely that the Hayfield Mudstone is deposited 'shortly' after the Jamison, in addition no unconformity is found between these two formations. This first event, the Carpenteria Event, took place between ±1200 (initiation of the Musgrave Orogeny (Wade et al., 2008)) and 1092±16 Ma (maximal age Jamison Sandstone).

The Bukalara Sandstone has been previously identified as a Cambrian formation. New research on this topic shows that the Bukalara Sandstone has the same provenance as the (Upper) Jamison and Hayfield (T.J. Munson, personal communication, May 18th, 2018). This makes it less likely that it was deposited 400 Ma after the Jamison Sandstone. An unconformity does separates the Hayfield Mudstone and the Bukalara Sandstone, representing a time gap during which the Borroloola Event took place. The paleo thickness and the paleo depth of the Hayfield Mudstone and the Bukalara Sandstone remains unknown. The large uncertainty in timing and paleo thicknesses are expressed in figure 4.4 with error bars. The maximal age is given by the age of the Hayfield Mudstone which should be close to the age of the Upper Jamison Sandstone (959±18 Ma). Hence the two events are at least separated by ages of the upper and lower Jamison Sandstone, which is 133 Ma.

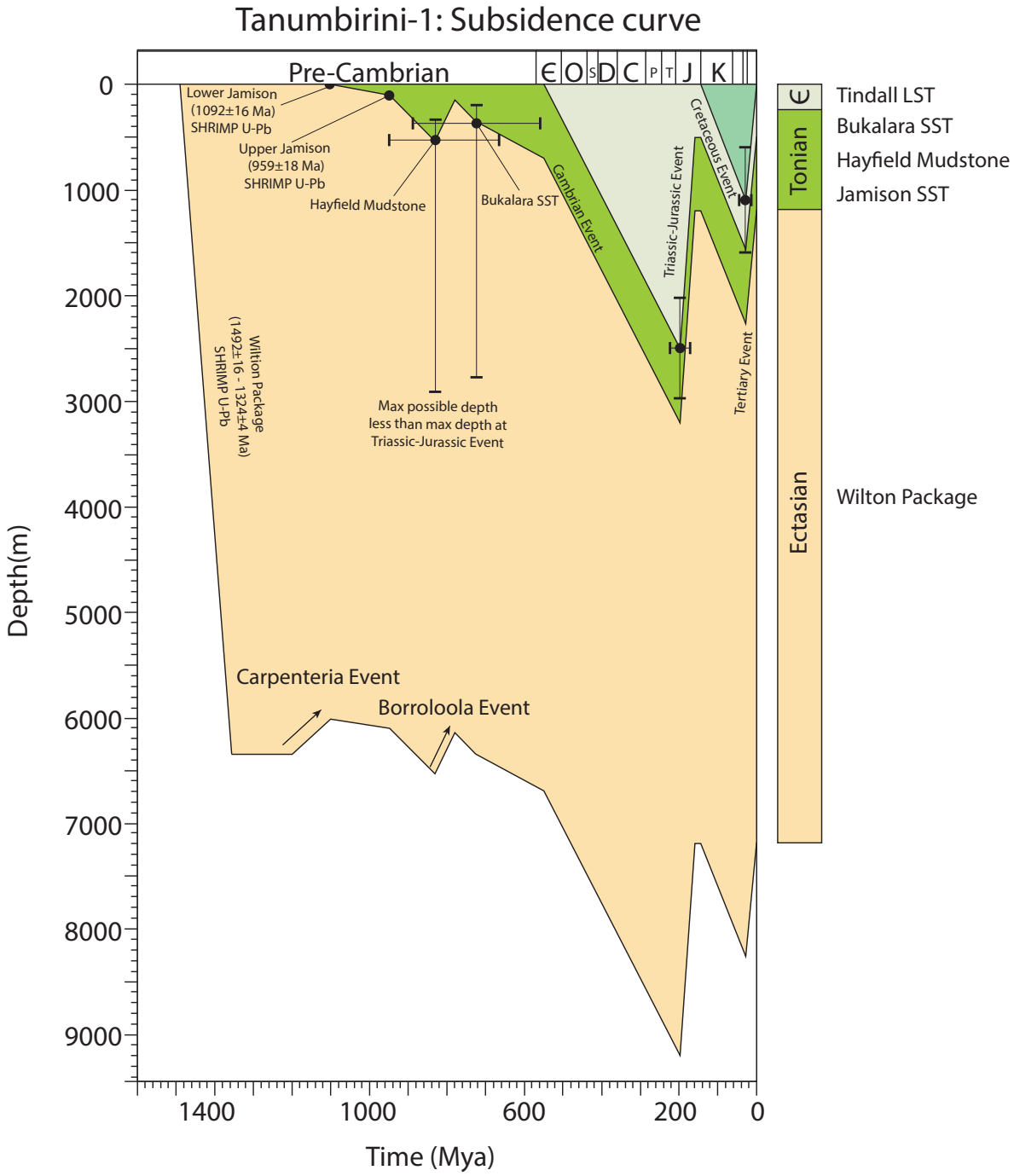

Figure 4.4: Vertical movement curve of the Tanumbirini-1 well based on backstripping.

4.3. Geological History

The geological history focuses on the large scale deformation events in line with the scope of this study. However, the period during and after the deposition of the Wilton Package receives more attention as this has a large impact on the generated fractures within the package.

±1851-±1710 Ma: Redbank

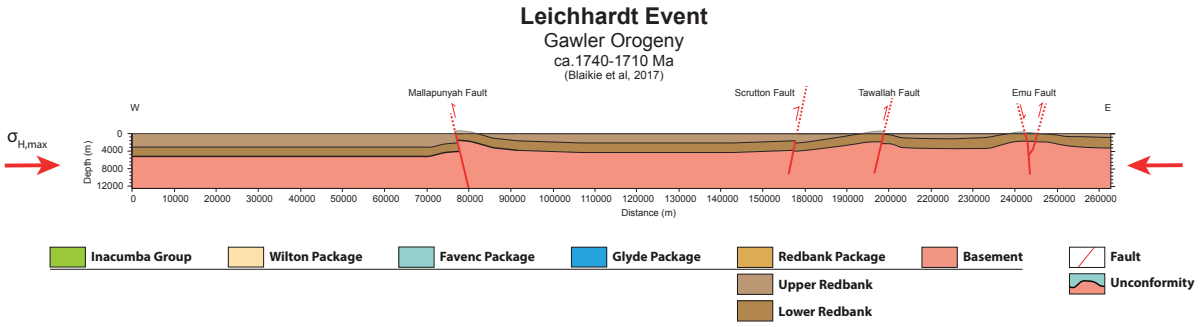

Figure 4.5: Geological reconstruction during the Leichhardt Event.

The basement is either part or contemporary to the Murphy Inlier. The inlier consists of metasedimentary rocks and has been dated to 1851±7 Ma based on U-Pb zircon dating (Page et al., 2000). During this period the North Australian Craton (NAC) started to collide in the south east with the Numil terrane (see section 2.2). This caused far field stresses to initiate rifting ±1500km inland north west from the margin. There were two main successive stress orientations: first during a short timeframe an E-W oriented extension was dominant, which was followed by a short period of N-S oriented extension (Blaikie et al., 2017). During these extensional periods the lower Redbank package was deposited.

An E-W compressional stress regime began to develop when the plates began to converge. Between 1740-1710 Ma this led to the formation of the Gidyea Suture and previous deposited rift sediments were inverted (Blaikie et al., 2017). Uplift of Lower Redbank followed and fault blocks ($10^0 km$ scale) became topographical highs (Rogers, 1996). This event has been identified as the Leichhardt Event (Blaikie et al., 2017). When extension continued the Upper Redbank package was deposited into the topographical lows. The resulting situation is illustrated in figure 4.5. The Upper Redbank Package is pinching out on the structural highs of the Lower Redbank Package.

±1710-1492 Ma: Glyde and Favenc

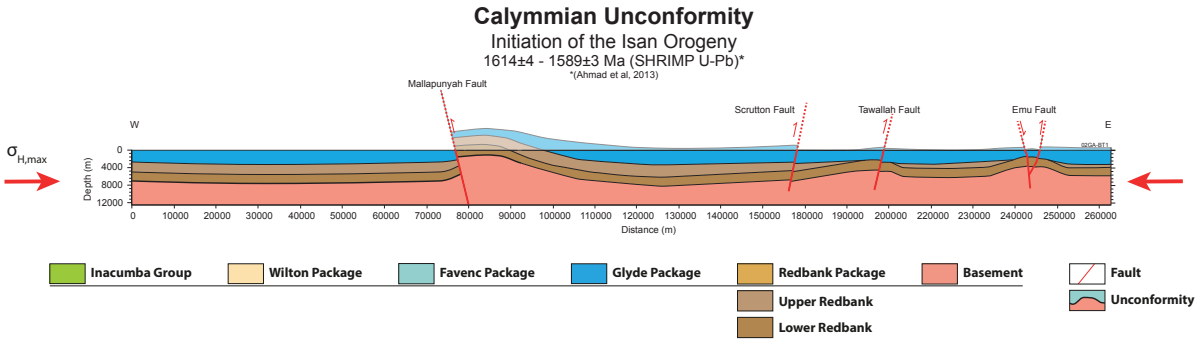

Figure 4.6: Geological reconstruction during the Calymmian Unconformity.

The uppermost age of the Redbank Package is dated to 1713±6 Ma (SHRIMP U-Pb) (Page and Sweet, 1998). The initial deposition of the Glyde Package conserved the paleogeography, meaning that more sediments were accumulated in the lows than at the highs. Locally E-W oriented faults were still active as thickness variations ($10^2 m$) across faults are observed (Rogers, 1996). These E-W extensional faults formed small blocks bounded by NNW transfer faults. Similar to the Redbank Package, siliciclastic sedimentation was still dominant. During this period a NW-SE extensional regime was dominant (Betts and Giles, 2006). When rifting stopped the basin entered a sag phase and carbonates started to dominate sedimentation. The Glyde deposition ended around 1614±4 Ma (U-Pb SHRIMP), while the Favenc package deposition started around the same time (Page et al., 2000) and ended at 1589±3 Ma (U-Pb SHRIMP) (Page et al., 2000).

The boundary separating the two packages is marked by the Calymmian Unconformity. At the Mallapunyah Fault Zone this unconformity even separates the Favenc and the Redbank Packages (figure 4.6). In figure 4.7 a cross section is shown through an outcrop of this unconformity based on surface geology. The whole Glyde Package, which in the Batten Fault Zone is 5km thick, is missing. The time span of erosion is very short (couple of millions years). A large outcrop of the Lower Redbank Package is located 30km to the north of this outcrop with the overlying Upper Redbank Package missing. This supports the presence of a structural high here, formed by the Leichhardt Event. The Glyde Package, affected by the paleogeography, was thinner at the highs. This makes it more reasonable for it to be eroded within such a short timeframe.

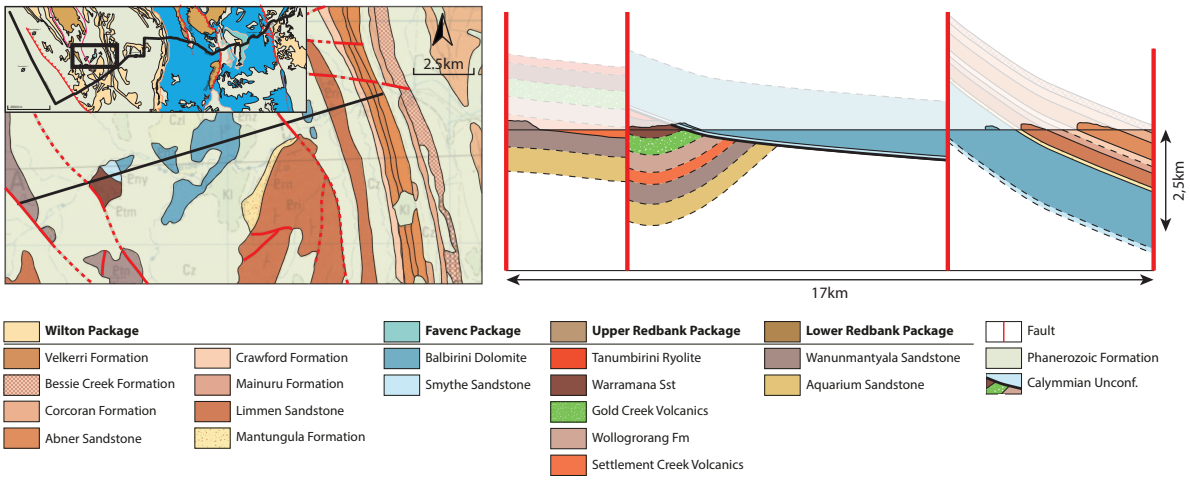

Figure 4.7: Cross section through an outcrop in the Mallapunyah Fault Zone.

The Calymmian Unconformity was caused by the Isan Orogeny, which initially induced an NNE-SSW compressive regime (Betts and Giles, 2006). The sediments were deformed along the major faults. The carbonate-dominated Favenc Package was deposited shortly after. A second unconformity, representing an estimated 80-90 Ma time break between the Favenc and Wilton Package, has been interpreted to be also related to the Isan Orogeny (Jackson et al., 1999). It was caused in a later phase of the orogeny which was dominated by an E-W orientated stress field (Ahmad et al., 2013, Lindsay, 1998).

1492-959: Wilton and Inacumba

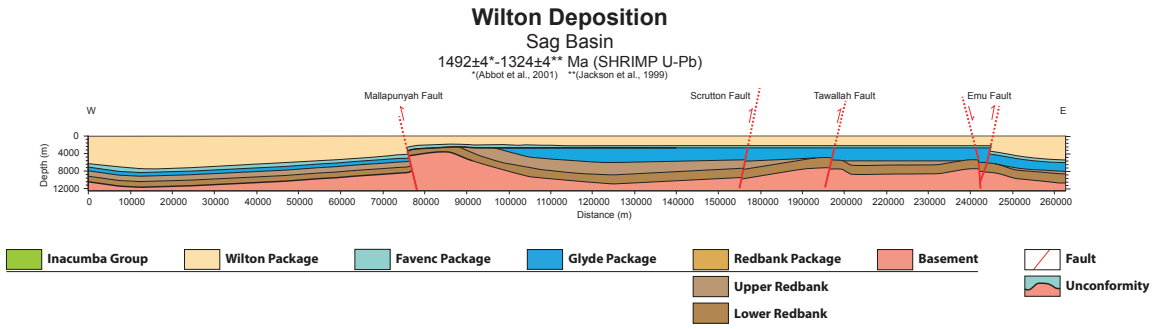

Figure 4.8: Geological reconstruction during the deposition of the Wilton Package.

The Wilton Package was deposited between 1492±4 and 1324±4 Ma during a basin sag. In contrast with the Favenc and Glyde packages it was rich in siliciclastics (Abbott et al., 2001). Major faults, including the Mallapunyah Fault, were responsible for asymmetric subsidence variations (figure 4.9). The Mallapunyah Fault was reactivated during the deposition of the Wilton Package (Silverman and Ahlbrandt, 2011). The extent of this variation east of the Broadmere Complex is difficult to assess as the Wilton Package has largely been eroded away, with the exception of some formations at the Abner Range. The thickness variations are however preserved across the Mallapunyah Fault. Where, as stated before in section 3.1, west of the fault the Velkerri Formation (Wilton Package) is 3 times thicker compared to the east of the fault.

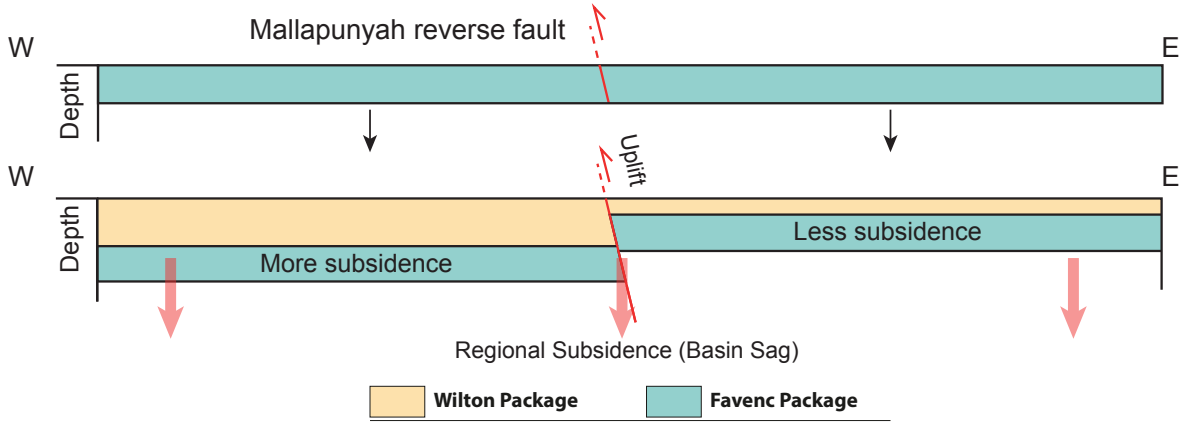

Figure 4.9: Asymmetrical subsidence causing thickness variation at the sides of the Mallapunyah Fault.

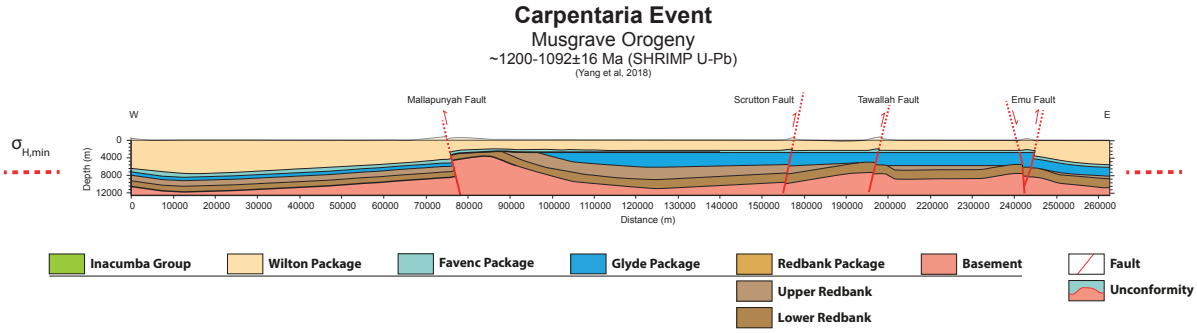

Figure 4.10: Geological reconstruction during the Carpenteria Event.

No deformation occurred up to the end of deposition of the Wilton Package (figure 4.8). The Corcoran Sill is an intrusion that was formed during this time and is dated to 1324±4 Ma. The sill was deformed alongside the Wilton Package, giving a maximal age of deformation. A minimal age for the deformation can be found in the overlying formations of the Inacumba Group (see section 2.5). These are only conserved in the Beetaloo Sub-basin. Seismic data indicate an unconformity between the Wilton Package and the overlying Jamison Sandstone of the Inacumba Group. The Lower Jamison Sandstone is dated to 1092±16 Ma (Yang et al., 2018). The deformation hence took place between 1324±4 and 1092±16 Ma and coincides with the Musgrave Orogeny (figure 4.10), which is dated to ±1200 Ma (Wade et al., 2008). This unconformity is caused by the Carpentaria Event and occurred between ±1200 and 1092±16 Ma.

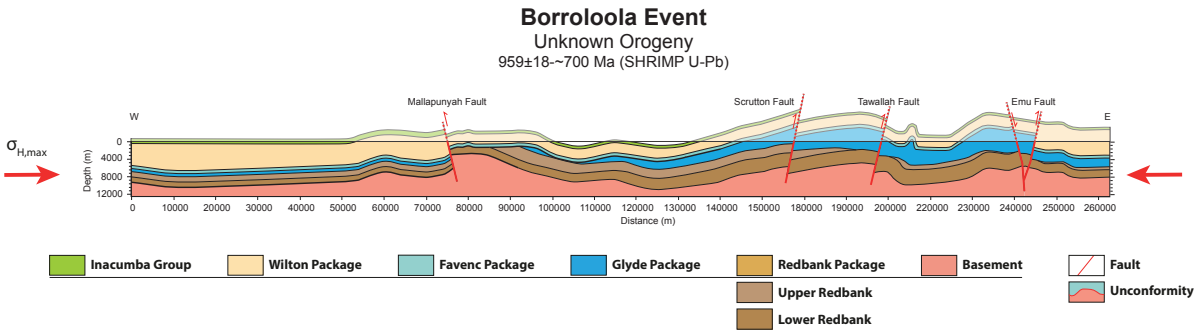

Figure 4.11: Geological reconstruction during the Borroloola Event.

The Hayfield Mudstone lies conformably on top of the Jamison Sandstone. Another unconformity separates the Hayfield and the overlying Bukalara Sandstone. This second event, called the Borroloola Event, took place after the deposition of the Jamison and Hayfield formations i.e. 959±18 Ma (figure 4.11). The lower limit of the event is not well constrained, but can be assumed to be within the Neoproterozoic as the Bukalara Sandstone belong to the Inacumba group. The Bukalara Sandstone is negligibly deformed after deposition, which means that the Wilton Package was only deformed by the Carpentaria and Borroloola Events.

The cross section in the Beetaloo Sub-basin (figure 4.12) shows these two unconformities (events). The erosion during the first event is mainly visible on the shoulders of the basin (e.g. between the 45 and 50km mark in the figure). This is typical during a basin sag phase. Away from the shoulders the angle of the unconformity becomes less.

The cross section also gives information on the chronology of the events. Small anticlines are visible in both the Wilton Package and the Lower Inacumba Group. Hence the anticlines are generated after the Carpenteria Event. The lack of deformation of the Bukalara Sandstone proves that the anticlines have been created during the Borroloola Event.

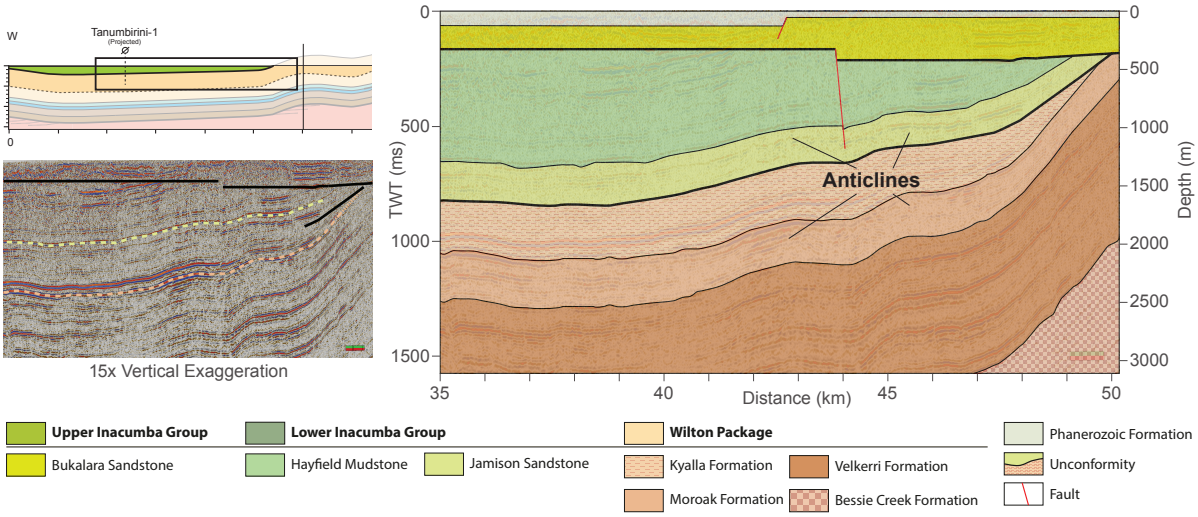

Figure 4.12: Zoom of the seismic line and cross section (interpretation) of the Beetaloo Sub-basin indicating the two unconformities.

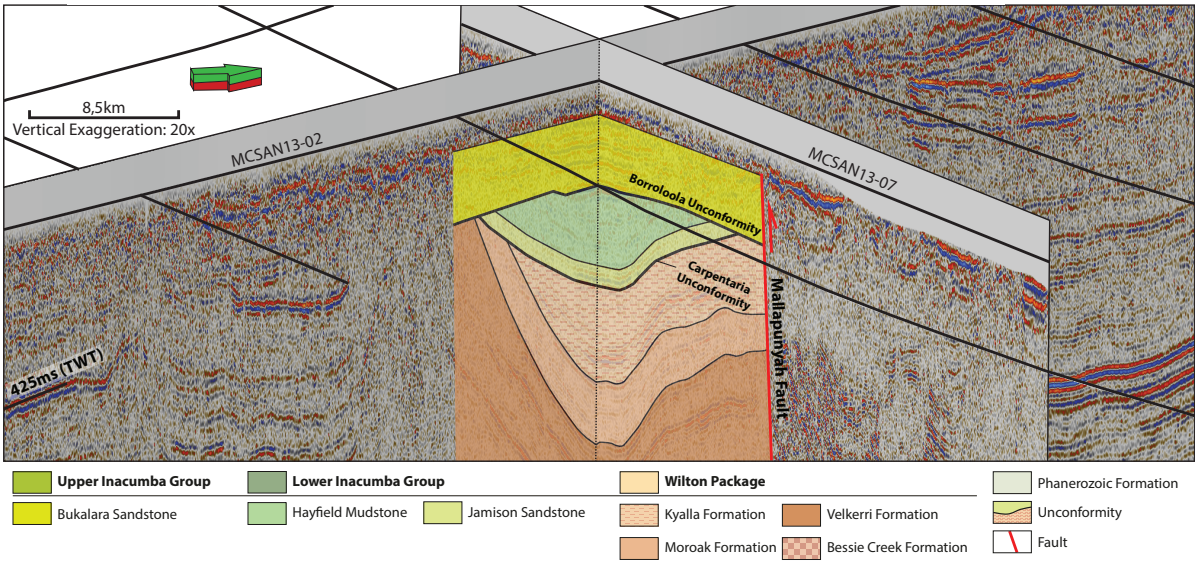

Figure 4.13: 3D view of the section in figure 4.12. MCSAN13-02 is intersection with MCSAN13-07

In figure 4.13 the two unconformities are interpreted on intersecting seismic sections of the MCSAN13 survey. The Carpenteria Unconformity is not present in the E-W direction. At other locations there is an unconformity in the E-W direction. However this occurs either at the corners of the basin or close to faults where this is expected. Additionally the unconformity is more consistent in the N-S direction. Hence the Carpenteria Event is interpreted as a mainly N-S compressional deformation phase. Literature is not clear in which direction the Musgrave Orogeny happened. But from Aitken and Betts (2009), fault orientations in the Musgrave Province support a N-S direction. This is another argument for the N-S deformation seen in the Broadmere Complex to be linked to the Carpenteria Event as they both are dated to the same age.

In figure 4.13 the Borroloola Unconformity is present in the N-S and the E-W direction. This could mean that there also was a smaller N-S deformation component. However the structures (e.g. the anticlines described earlier) found in both the Wilton Package and the Lower Inacumba Group are caused by the Borroloola Event. These structures are far more pronounced in the E-W direction than the N-S. Therefore the event is interpreted as an E-W compressional deformation phase.

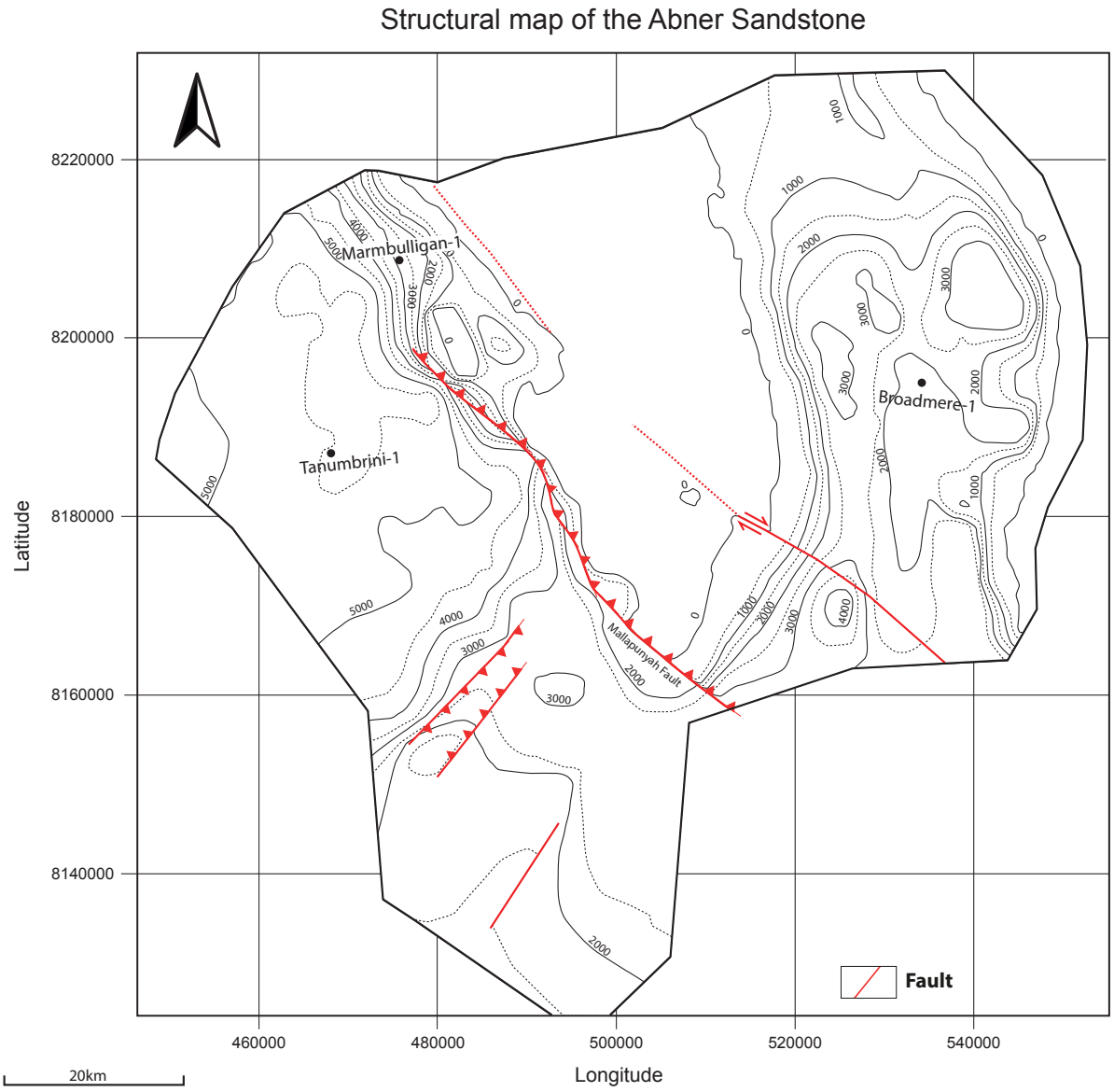

Figure 4.14: A depth map of the Abner Sandstone.

In figure 4.14 a depth map of the Abner Sandstone (Wilton Package) is shown based on the 3D model (figure B.1 in appendix B). The many folds in the Broadmere complex are visible too. The geological history is summarized in figure 4.15.

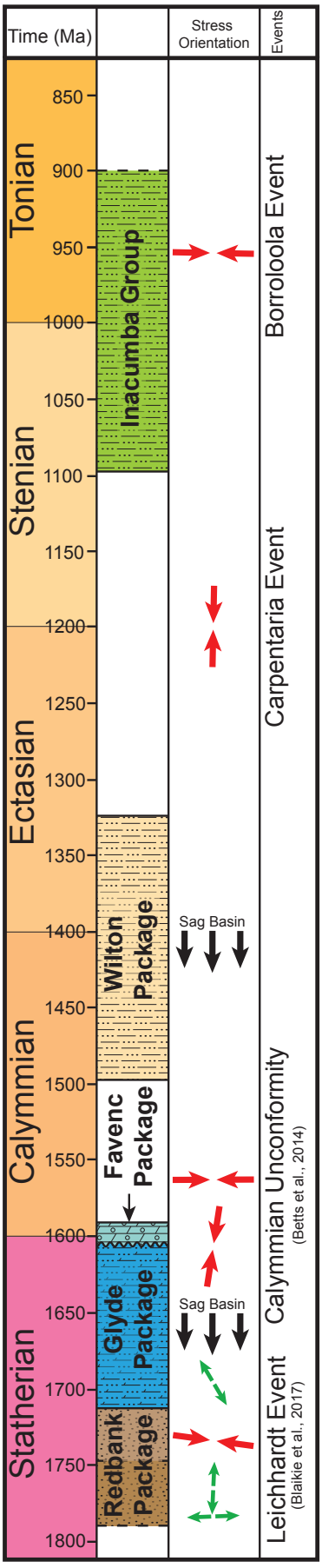

Figure 4.15: Stratigraphical column including the major deformation phases.

5

Fracture analysis in the surface and subsurface

In this chapter the fieldwork is discussed. An overview is given on the outcrops that were visited and the advantages of using a drone as tool to acquire data. The observations made during the fieldwork are discussed in section 5.3

5.1. Fieldwork

A two week outcrop study in the area of interest was conducted in May 2018. The goal was to acquire drone aerial images of pavements containing fractures. But also measuring fracture orientations and characteristics with conventional means. The team focused on outcrops in the Broadmere Complex. Additionally two outcrops were visited at the Western and Southern Lost Cities. In table 5.1 a summary is given of the outcrops.

Initially outcrops were chosen such that they were located at different limbs and crests of an anti-cline/syncline and near faults. This would make it easier to identify the characteristic fracture geometries associated with different drivers, as discussed in chapter 6. Accessibility is another criteria whether outcrops can be visited or not. The Northern Territory is a vast rural area with sparse roads. Outcrops must be located near roads to be easily reached. During the fieldwork some outcrops were not reached because travelling on foot proved to be too far and too dangerous. Some outcrops could not be reached because they are part of protected sacred sites and access was not granted.

Name	Location	Formation	Potential Driver	Aerial Data
WLC	Western Lost City	Abner Sst	Fold	Yes
SLC	Southern Lost City	Bessie Creek Fm	Fold	Yes
BRO1	Broadmere Complex	Bessie Creek Fm	Fold	Yes
BRO3	Broadmere Complex	Bessie Creek Fm	Fault	Yes
BRO4	Broadmere Complex	Abner Sst	Fold	Yes
BRO5	Broadmere Complex	Abner Sst	Fold	Yes
BRO6	Broadmere Complex	Bessie Creek Fm	Fold	No
CAR1	Broadmere Complex	Bessie Creek Fm	Fold	No
CAR2	Broadmere Complex	Bessie Creek Fm	Fold	Yes
ABN	Abner Range	Abner Sst	Regional	No
Marmbulligan-1	Broadmere Complex	Velkerri Fm	Fold	No
Tanumbirini-1	Beetaloo Sub-basin	Velkerri Fm	Regional	No

Table 5.1: Details of outcrops visited during fieldwork.

5.2. Advantage of drone acquired imagery

Fracture pavements can be observed on different scales, by the geologist ($10^0 m$) or with satellite images ($10^3 m$). However observations at the $10^{1-2} m$ scale was traditionally difficult to make or expensive. With the advent of affordable drone technology this became possible. In figure 5.1 the same area is imaged by both the satellite and a drone. There is a clear increase in the fidelity of the image. Another advantage is the large amount of data that can be acquired in a short amount of time. An area of 200 by 200m can be imaged in ±25 minutes, leading to less time spent per outcrop which results in more outcrops overall during a fieldwork.

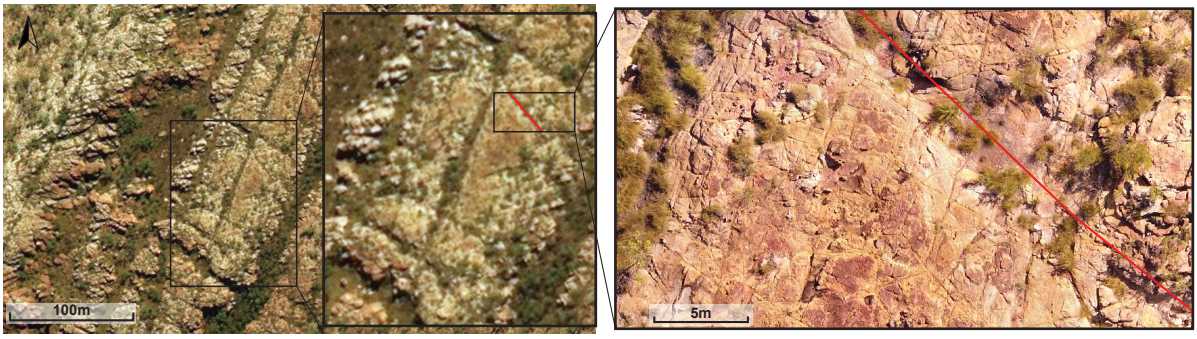

Figure 5.1: The same area in the Southern Lost City imaged by both a satellite and the drone. The same fault is indicated on both images.

The drone that was used is the DJI Phantom 4 (figure 5.2). The Pix4D Capture App was used to configure a flight plan for the drone. The app controls the drone through its path, automatically taking overlapping georeferenced pictures along the way. Any point on the outcrop is photographed from different angles and locations. Agisoft PhotoScan software was used to analyze the pictures and convert them to a point cloud while also stitching the separate pictures into one outcrop stretching image. The images were imported in QGIS where fractures are then traced. FracPac was used to analyze them further. FracPaq software is a Matlab package that automatically analyzes traced fractures and outputs the relevant geometry parameters (Healy et al., 2017).

Figure 5.2: DJI Phantom 4 drone flying over the Southern Lost City.

In total 7 fracture pavements were imaged without difficulty. Even with wind the drone managed to fly and complete its missions. A total amount of 15 GB of pictures was acquired. The amount proved to be to large to all be analyzed during this study. But it provides sufficient data for further research. Steijn (2018) already used some of the data to analyze fracture geometries.

5.3. Fieldwork observations and results

In figure 5.7 the locations of all the outcrops are shown. Included are a cross section connecting the Tanumbirini-1 and Broadmere-1 well (figure 5.5), a N-S cross section through the Broadmere Complex (figure 5.6) and a cross section connecting the outcrops at the Western and Southern Lost Cities. Most outcrops are located in the western flank of the Broadmere Complex and will form the focus of this study. The cross sections connect different outcrops with each other or with wells. They also indicate the type and style of deformation. All observation are made on either the Bessie Creek Formation and the Abner Sandstone. Fracture interpretation from wells were done in the Velkerri Formation.

Direct measurements on the outcrops were made in structural stations, where geologists spent some time in the field measuring fracture dips and azimuths. Some features or configurations indicate paleo orientations of the principal stresses. Conjugate fractures sets give information on $\sigma_1/\sigma_{H,max}$ and σ_3. To prove that fracture sets are conjugate three criteria are needed:

- (Shear) Movement
- Striation
- Angle of 50-70°between fractures

Small movements occur along conjugate shear fractures, which can be observed by other features like beds that have been offset. When movement occurs striation takes place. Moreover striation also gives a direction of movement if it is observed in situ (i.e. not on a loose piece of rock). The angle at which fractures intersect should be between 50°and 70°if they are part of a conjugate system. This relationship is described by the Mohr-Coulomb failure criterion (figure 5.3).

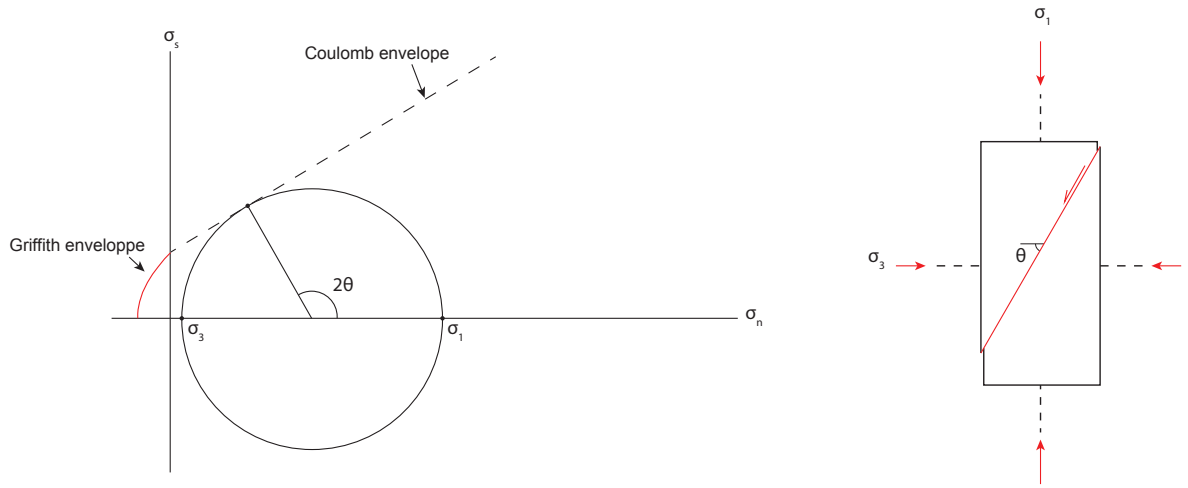

Figure 5.3: Mohr Coulomb criteria describing the relationship between angle and failure (fracture generation). Figure is modified from Fossen (2016)

Movements along fractures have been observed at outcrops in the field, e.g. outcrop SLC1.2. Here older fractures where offset by fractures of a conjugate system. At other outcrops striations were present, for example in outcrop BRO5.2. In the majority of outcrops sets were observed that make an angle of 50-70°with each other. The presence of additional criteria increases the validity of them being a conjugate set. It thus becomes more ambiguous when only one or two criteria are met. Therefore all outcrops have been graded, with each criteria worth 1 point. A 'perfect' outcrops scores 3/3. All the stereonet plots and field observations have been integrated per outcrop or station. The stereonets were created with Stereonet 10.0 (Allmendinger et al., 2011). They can be found in appendix C.

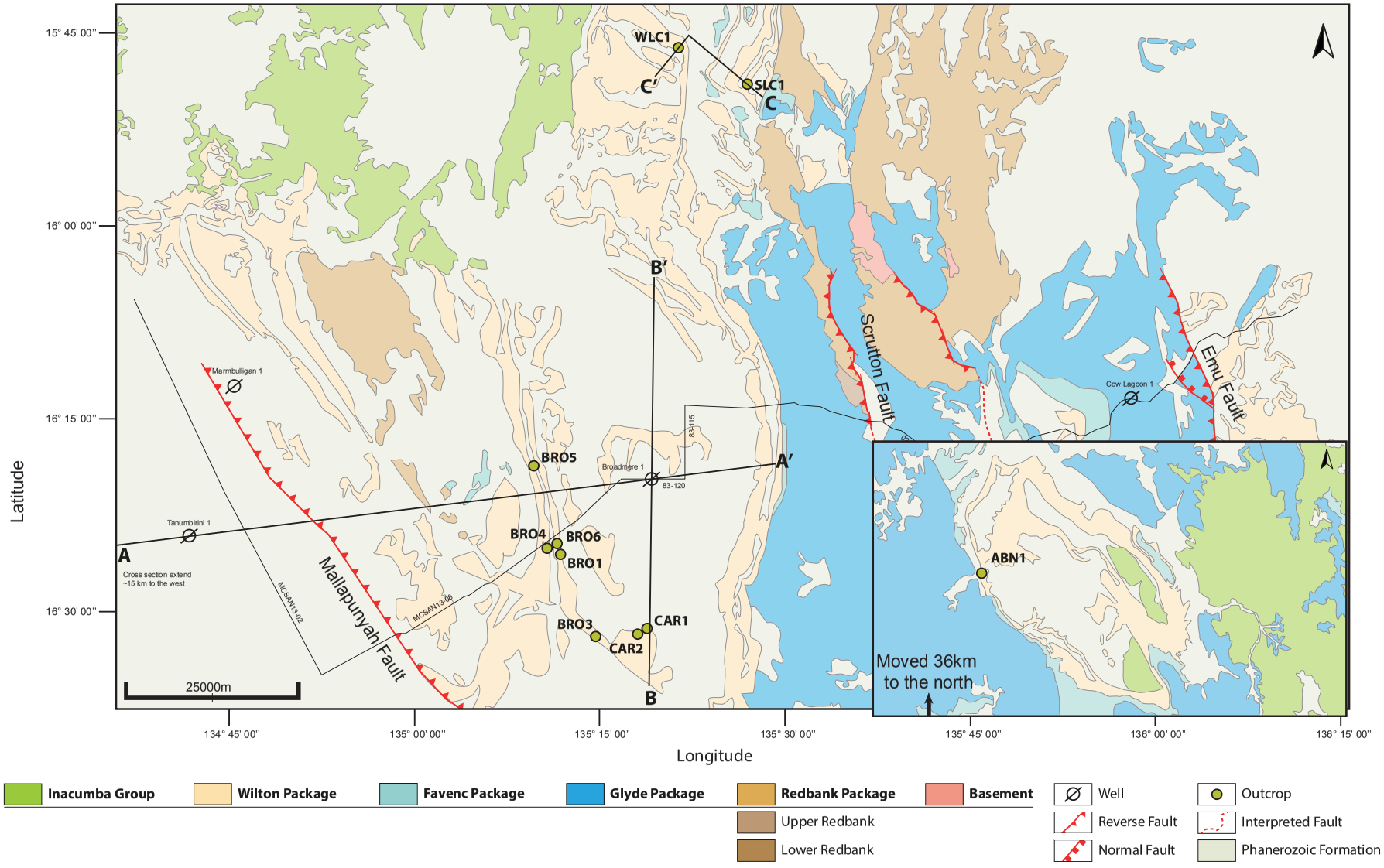

Figure 5.4: Geological map of the area of interest showing all the outcrops and interpreted well locations.

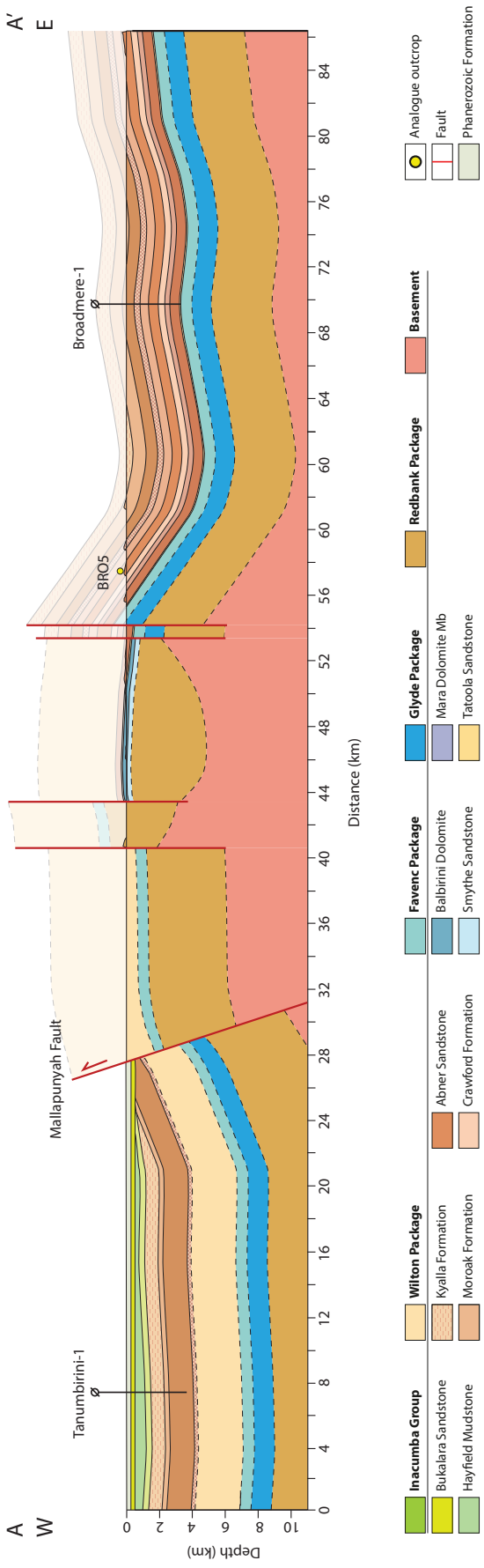

Figure 5.5: Cross section connecting the Tanumbirini-1 well and the Broadmere-1 well.

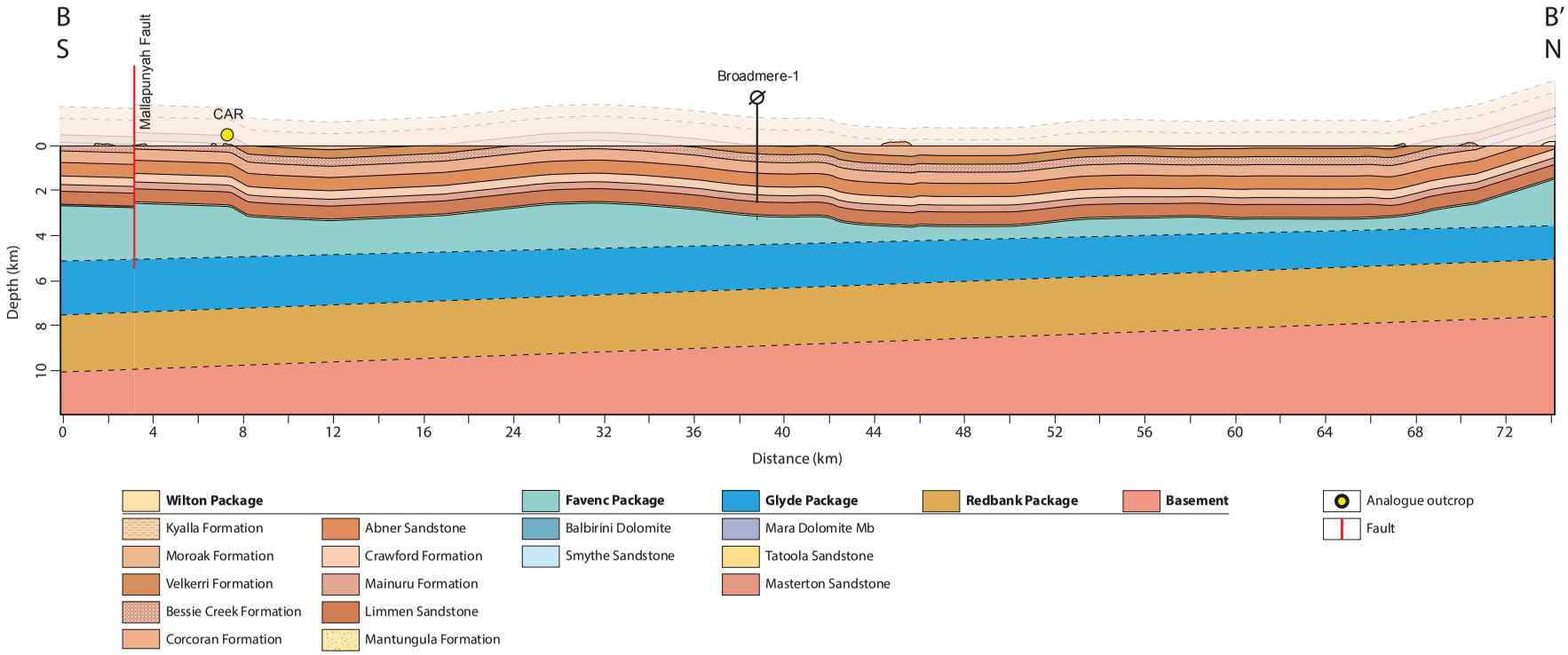

Figure 5.6: Cross section through the Broadmere Complex parrallel to the N-S fold axis.

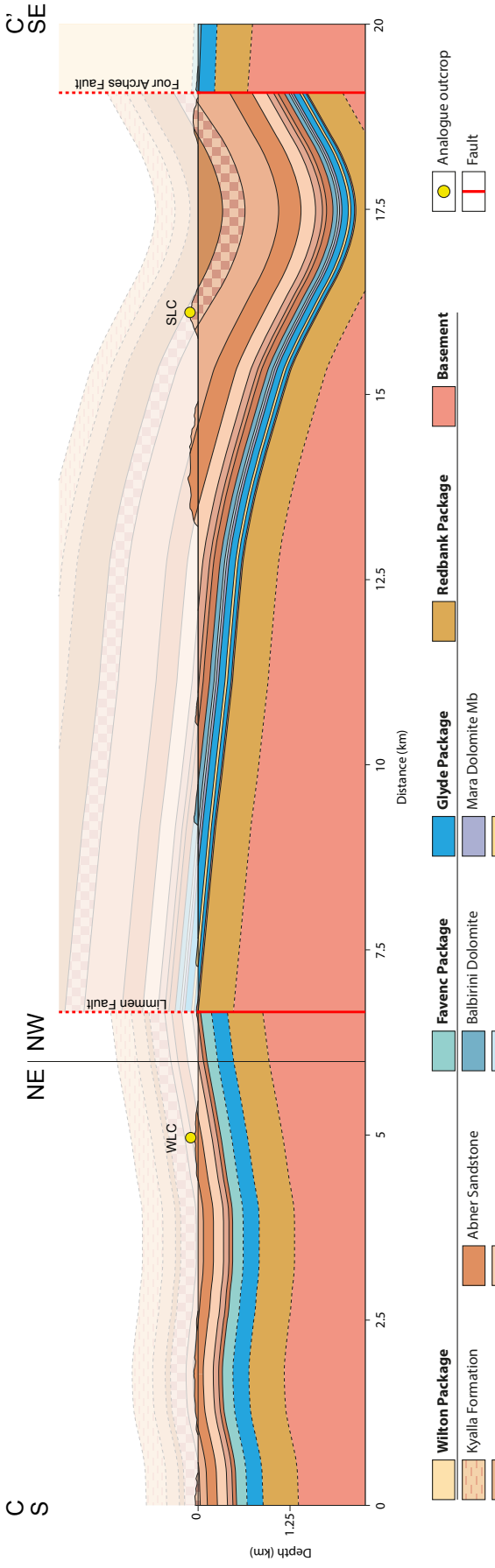

Figure 5.7: Cross section connecting the SLC and WLC outcrops in the Nathan Range.

5.4. Fracture interpretation from wells

BHI logs are available for the Tanumbirini-1 (FMI) and Marmbulligan-1 (UBI) well. They give 1D fracture data in the subsurface. This means that from the three criteria stated before only the angle between the fractures can be observed. Any conclusions should hence be taken with caution. The dip and azimuth were measured and created evidence for paleo principal stress directions.

The Marmbulligan-1 well is situated on the left flank of an anticline. The Tanumbirini-1 well is located at an undeformed area, where only regional stress field induced fractures are expected. The depth of 3.9km at this well will also give insights whether surface observations can be used to predict the fracture geometry in the subsurface. This concept was discussed in chapter 4. The first well has been interpreted with TechLog. A short tutorial on the software package can be found in appendix E. Importing the FMI log of the second well was unsuccessful, the interpretation was done manually. The stereonets of the wells can also be found in appendix C.

6

Linking vertical movements and fractures in outcrops

The relationship between vertical movements, stress and strain must be understood to predict fractures in the subsurface. In this chapter theoretical background is given which is used for choosing the outcrops discussed in chapter 5. The concept of structural drivers influencing the fracture geometry is also defined here. Identifying drivers and their corresponding fractures sets is key to predict fracture distributions.

6.1. From vertical movements to stress fields

The concepts of stress and strain are closely linked. It is important to understand how fractures are formed and which mechanisms influence them.

Strain is the relative change of a rock body in the final configuration with respect to the initial configuration. (Paleo)Strain cannot be directly measured, but is revealed by strain markers. As a rock body is strained deformation structures appear like cleavage, shear zones and fractures. Deformation can occur localized (e.g. fault) or distributed (e.g fractures) (figure 6.1). A geologist can try to interpret what the rock would have looked like before it was deformed (Fossen, 2016).

Strain is caused by stress, which is the expression of forces acting on a surface area of a rock body. There are different reference states of stress. The most simple model is the lithostatic reference state. The stress is controlled by the density and thickness of the overburden. More complex processes affect the state of stress such as thermal effects, burial and exhumations of rocks and residual stresses. Natural deviations of the state of stress are due to tectonic stresses. Regionally these stresses are consistent over large areas but locally they are influenced by folds and faults (Fossen, 2016).

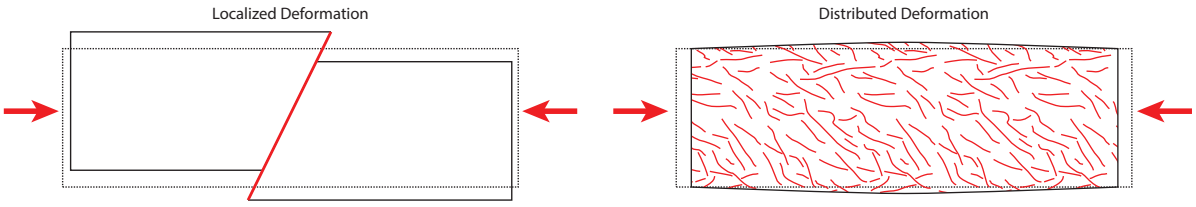

Figure 6.1: (left) Localized deformation by the means of a fault. (right) The rock body is deformed by small fractures that are distributed throughout the rock.

6.2. Fractures and drivers

Fractures are planar discontinuities where one dimension is far narrower than the other two. There are three types of fractures e.g. tensional, sliding shear and tearing shear fractures (Fossen, 2016). They are also known as mode I, mode II and mode III fractures respectively. As mentioned in the previous sections fractures are generated by stresses. Tectonic stresses are constant over a large area but can locally be influenced by folds and faults. These are called drivers. In theory each driver has its own characteristic fracture pattern. These patterns can be 'superimposed' when multiple drivers are present (figure 6.2). Identifying these patterns is the task of the geologist.

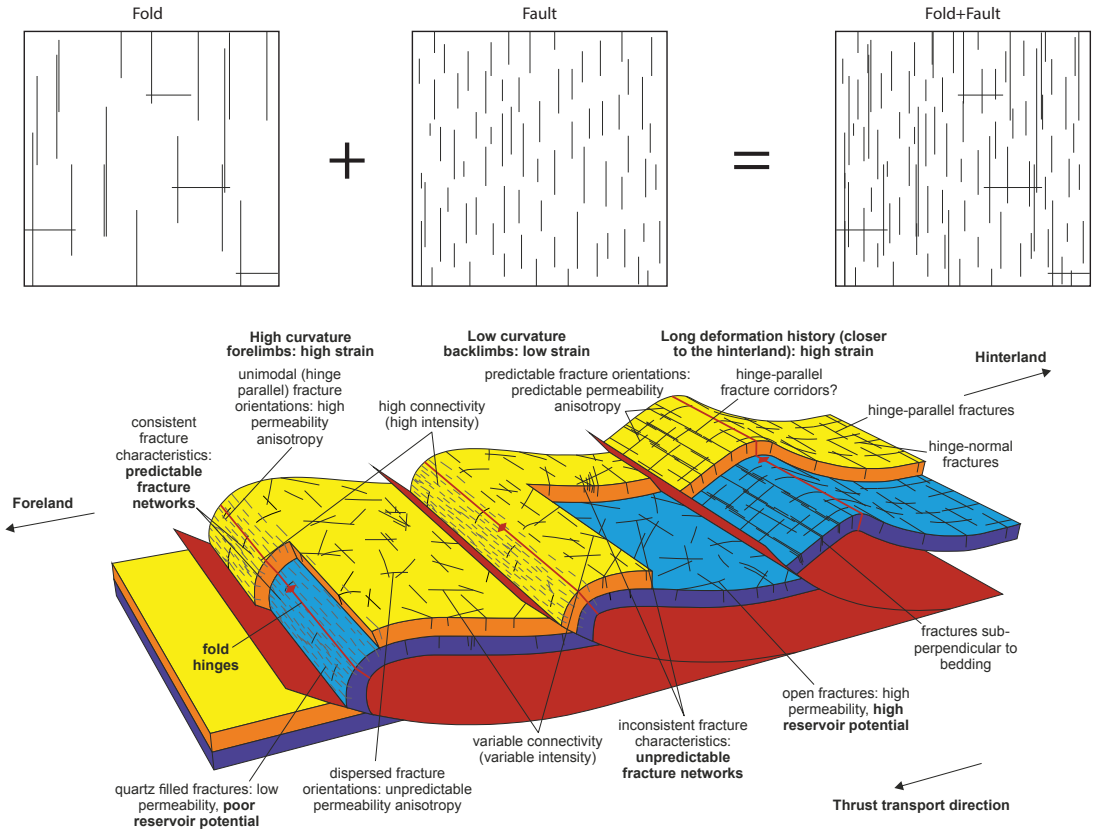

Figure 6.2: Illustrating the concept of driver superposition. Lower image modified from Watkins et al. (2017).

The relationship between faulting styles and stress regimes has been described by the Andersonian Model (Anderson, 1951). This also applies to fracture generation. The fracture geometries generated by different orientations of the principal stresses are illustrated in figure 6.3. The largest stress direction is σ_1 while the smallest is σ_3. For this study stresses in the horizontal plane are caused by tectonic process and the vertical stress is generated by the overburden.

The fracture geometry changes when the vertical stress becomes σ_1 or σ_2. This only happens when the vertical stress is larger than the stresses in the horizontal plane. Depth is thus an important characteristic when correlating fractures geometries at different locations. The depth is increased when there is a thicker overburden. Correlating between two locations with different stress regimes becomes unreliable.

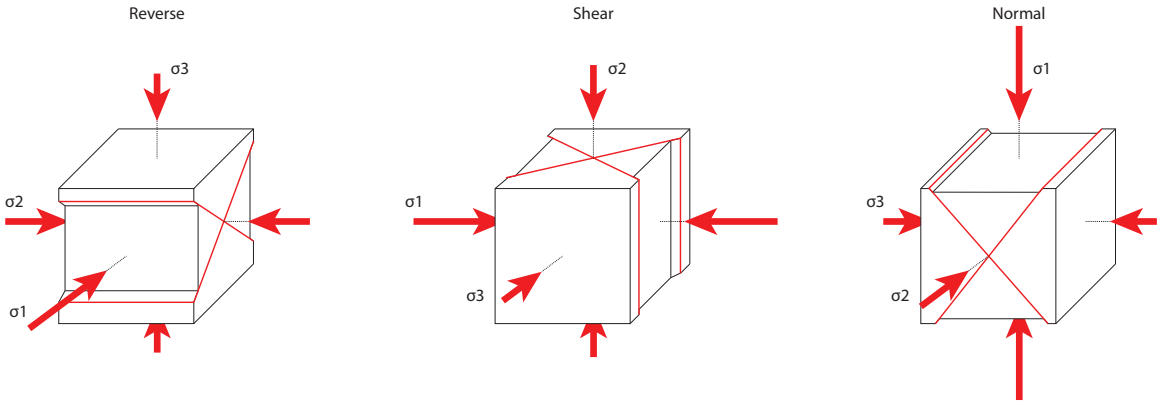

Figure 6.3: The Andersonian model also be applies for fractures.

6.3. Linking Outcrop to the Subsurface

Outcrops are ideal to observe fracture geometries in 2D and 3D, in contrast to wells which only give 1D information. The main objective for an outcrop study is to identify the characteristic fracture pattern of each driver. An fracture network on an outcrop could be similar to the pavement shown right of the equal sign in figure 6.2. The geologist's job is to identify the individual components (left of the equal sign) that make up the pavement. These components are the characteristic fracture geometries generated by individual drivers. The lower part of the figure shows that in reality this is very hard to do as there is a lot of heterogeneity involved.

Correlating to the subsurface is still difficult even when the characteristic fracture patterns have been identified. Increasing depth can change the stress regime, resulting in a different style of fracturing. Correlating between two different stress regimes is unreliable. Wells can be used to determine the stress regime in the subsurface. Fractures can be observed with borehole image logs like FMI (Formation Micro Imager) or UBI (Ultrasonic Borehole Imager). The fracture orientations can be used to identify in which regime of the Andersonian model the well is located. Outcrop geometries can be correlated to the subsurface if they are also in the same regime.

Large thickness variations occur in the area of interest, because of asymmetrical subsidence west and east of the Mallapunyah Fault. This means that there is a risk that the vertical stress in the Beetaloo Sub-basin is large enough to become either σ_1 or σ_2. Fortunately the Tanumbirini-1 well is located west of the fault and the Marmbulligan-1 just east of the fault. And both contain borehole image logs. These will be used to assess in which Andersonian regime they are and to which extent the surface observations can be used for a subsurface prediction.

7

Fracture characterization and the geological history in the McArthur Basin

In this chapter the data from the fieldwork is discussed and the results are presented. Additionally the same is done with fracture interpretation of intervals within the Tanumbirini-1 and Marmbulligan-1 wells. The results are placed within the geological framework discussed in chapter 4. Two drone acquired pavements from the SLC and WLC outcrops are analyzed and compared with two pavements from the BRO1 outcrop described in Steijn (2018). Based on this a prediction is made of a subsurface fracture geometry.

7.1. Surface fracture interpretation

The results of the fieldwork are synthesized in sheets containing (unfolded)stereonets, observations, pictures and a score. These can be found in appendix C. The unfolded stereonets are superimposed on the geological map in figure 7.1. Conjugate fracture sets were observed at both WLC and SLC outcrops, associated with an E-W σ_1. Movement can be seen along fractures of the conjugate system at the outcrop SLC1. The BRO5 outcrop is an east dipping pavement where striation was observed. The striation together with the right angle between the two sets suggests that they are part of a conjugate system where σ_1 is roughly oriented E-W. The outcrops BRO1, BRO4, BRO6 are located close together. The interpreted σ_1 at BRO1 and BRO4 is oriented E-W. In contrast the σ_1 at BRO6 has a N-S orientation. The outcrops CAR1 and CAR2, located further south, also show the same N-S orientation. No conjugate systems were observed at the ABN1 and BRO3 outcrops.

Orientations of individual fractures within sets are not consistent in all cases. This causes some ambiguity in regards to whether it is a normal or shear conjugate system. In figure 7.3 this is seen in the stereonet of BRO1.1. The bold lines suggest that this is a shear conjugate system. The thin lines however would be interpreted as a normal conjugate system. Another type of ambiguity is seen at BRO6.1 where the two fracture sets form a high angle shear conjugate system. The number of fractures that are observed during the fieldwork also impacts the interpretation. In SLC1.2 the number of fractures is far higher than at most other places. Within one fracture set deviations occur, but stay within a certain limit.

The σ_1 orientations per outcrop are shown in figure 7.2. At most outcrops σ_1 is roughly oriented perpendicular to both the strike of the bedding and to the fold axis. An exception to this trend is outcrop BRO6 where a N-S orientated σ_1 is observed. But this outcrop is also scored lower than most others.

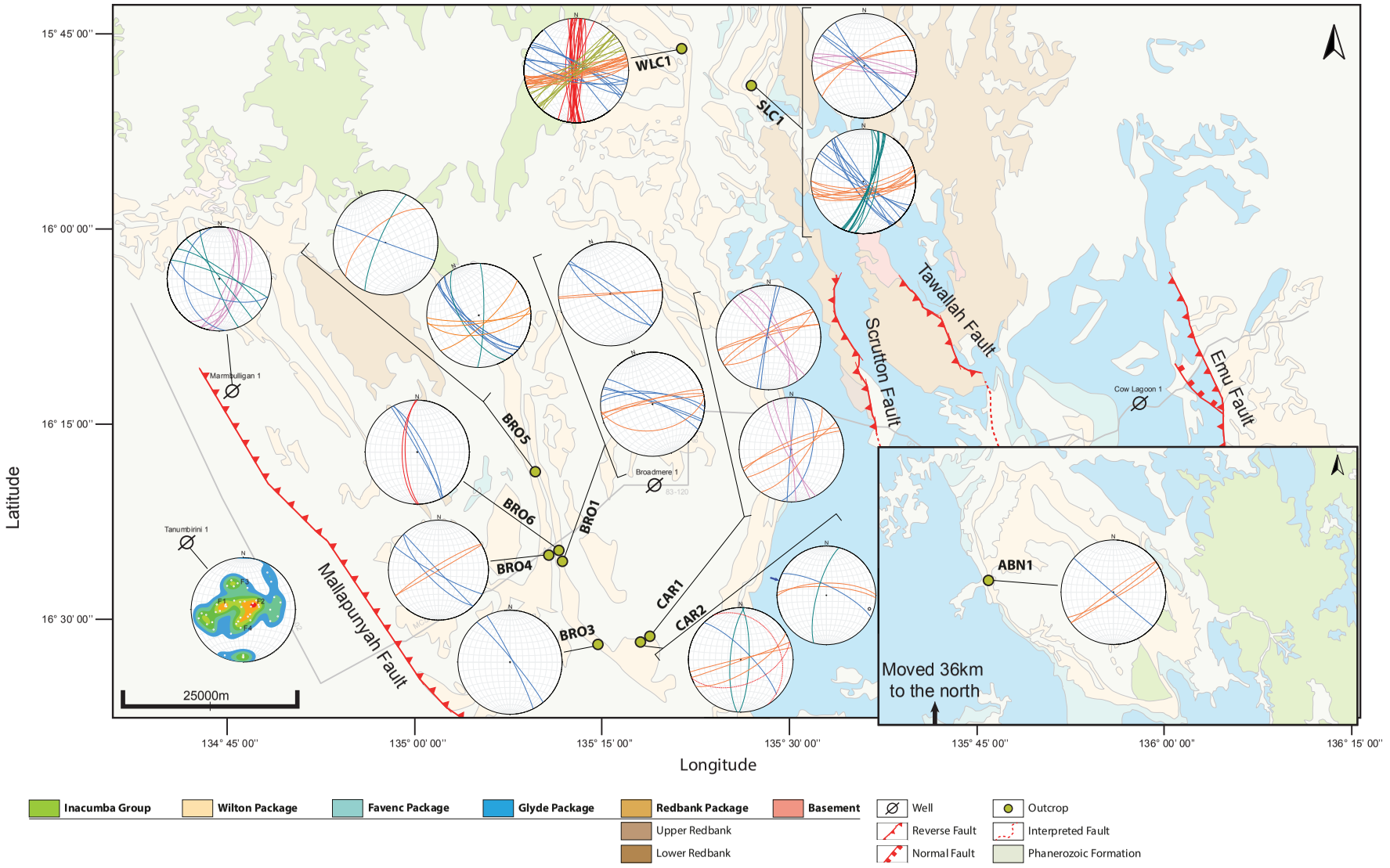

Figure 7.1: Geological map of the area of interest containing the unfolded stereonets of fractures observed on outcrops during the fieldwork. Stereonets of fractures interpreted from the two wells are also included.

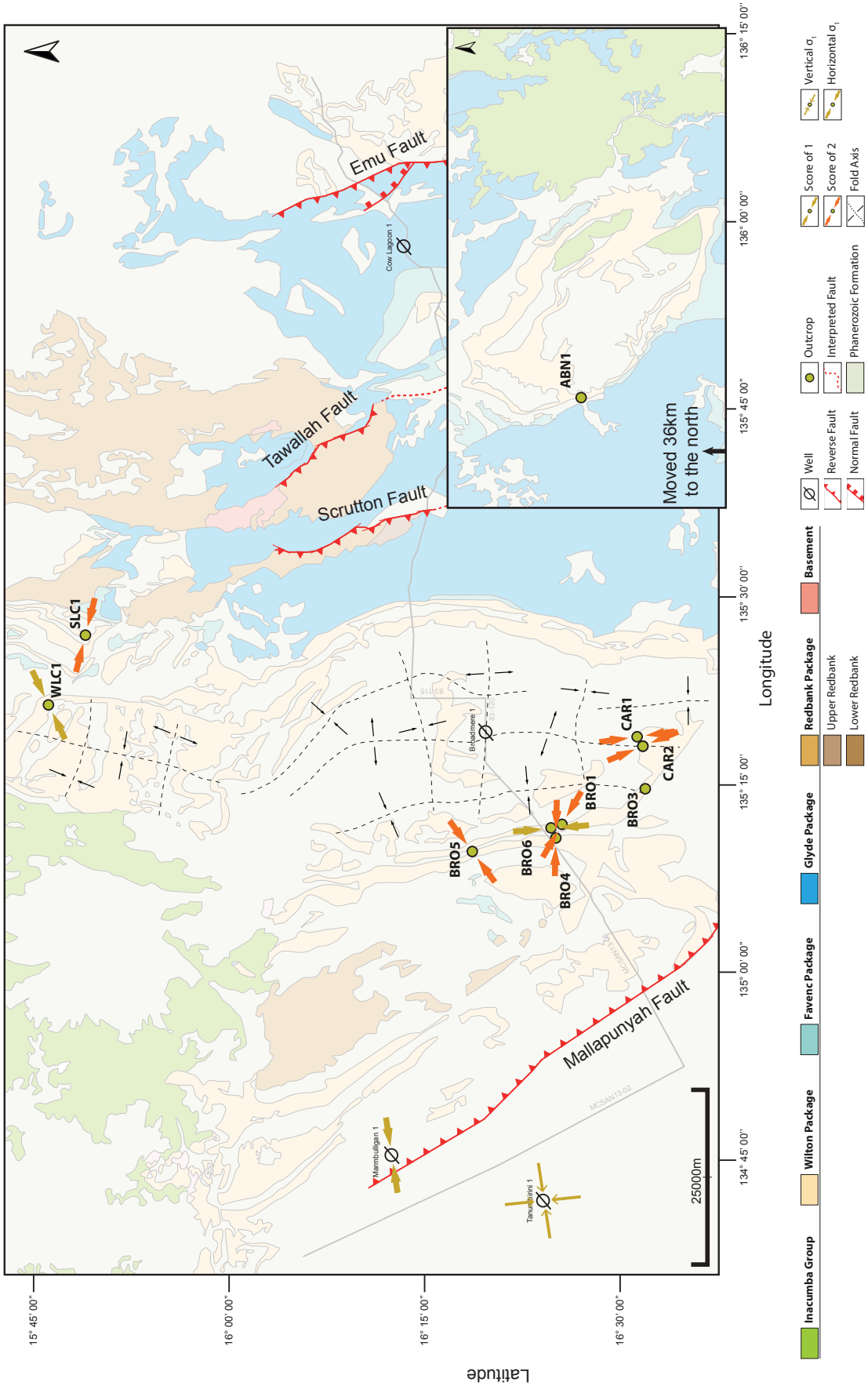

Figure 7.2: Geological map of the area of interest containing the $\sigma_1/\sigma_{H,max}$ at the outcrops visited during the fieldwork and at the two interpreted wells.

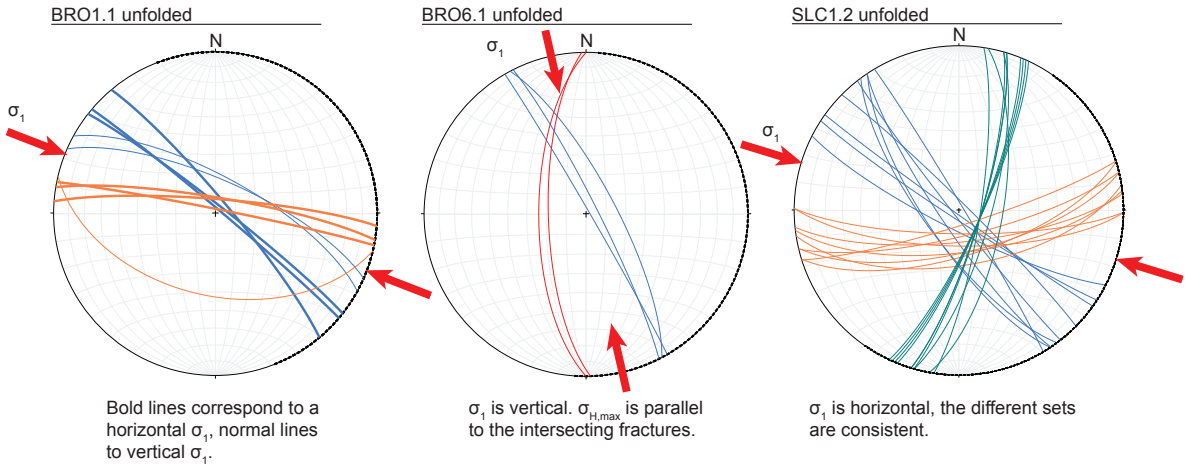

Figure 7.3: The unfolded stereonets of the BRO1.1, BRO6.1 and SLC1.2.

7.2. Subsurface fracture interpretation

The fractures in the Marmbulligan-1 well are grouped into three sets (figure 7.4). Because the well data is in 1D it is hard to establish which sets are conjugate. The most numerous sets, F2 and F3, form a shear conjugate system with σ_1 oriented E-W. Additionally fractures of F3 are very consistent w.r.t. the other sets. Such a σ_1 orientation agrees with the surface observations, i.e. being perpendicular to the fold axis. At this depth the σ_1 is not vertical, possibly the vertical stresses are comparable with the situation at the outcrops.

Fractures interpreted in the Tanumbirini-1 well are at a far deeper interval (±2400-3900m). The number of fractures and their orientations proved too chaotic to group in sets. They therefore have been plotted as poles in a stereonet (figure 7.4). The stereonet contains a contour map which shows a '+' pattern. The angle between F1 and F2 is ±50°while F3 and F4 make an angle of ±65°. The angle between the sets is in the vertical plane, σ_1 is thus oriented vertically. σ_2 or $\sigma_{H,max}$ is oriented perpendicular to the line connecting two sets within one conjugate system.

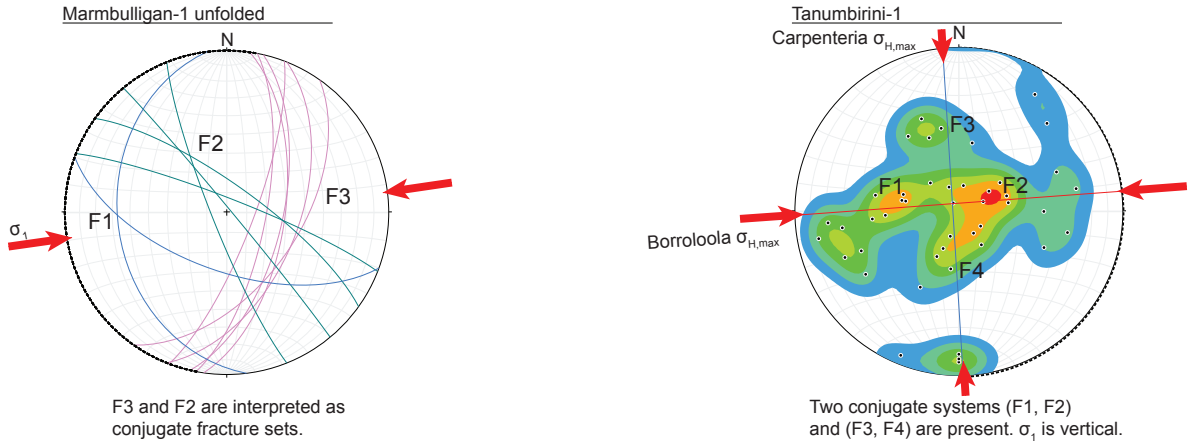

Figure 7.4: Unfolded stereonets of the Marmbulligan-1 and Tanumbirini-1 wells.

7.3. Integration within the geological framework

The results of the fieldwork need to the be integrated within the geological framework that has been discussed in chapter 4. This will help when correlating between the surface and subsurface.

The outcrops either contain N-S or E-W conjugated fractures. These are related to two separated events, the Carpenteria and Borroloola Events. Folding controls the fracture generation perpendicular to the fold axis, this is due to Layer parallel Shortening (LPS). The fractures are the precursor to folding. Fracturing in fold limbs is often denser than in unfolded or non-faulted areas, excluding fracturing due to exhumation. In the area of interest any fracturing associated with the Carpenteria event preceding folding or faulting will be underrepresented as this event was less severe than the Borroloola Event. Fractures observed at BRO6 could be caused by the Carpenteria Event. In the three neighbouring outcrops the fractures are caused by the Borroloola Event. The fold axes are illustrated in figure 7.2. There are folds in both N-S and E-W direction. These are also generated by the two different events.

The conjugate fractures seen in the Marmbulligan-1 well correspond to the Borreloola Event. The conjugate sets F1-F2 (N-S $\sigma_{H,max}$) and F3-F4 (E-W $\sigma_{H,max}$) of the Tanumbirini-1 well were created by the Carpenteria Event and Borroloola Event respectively.

7.4. Pavement Characterization

The fractures on pavements can be traced in QGIS and then analyzed in FracPaq software. This is a time consuming process. Interpreting all the acquired images was not feasible within the time frame of this thesis. Therefore this study only looked at two smaller sections in the SLC and WLC outcrops (figures 7.6 and 7.5). Additionally a bachelor thesis has done a more extensive study on the outcrop of BRO1 (Steijn, 2018). The imaged outcrops provide fracture geometries at different locations. Comparing them will allow to better understand the response of the rocks from comparable stress fields. Choosing only outcrops from the same location will create a bias towards the traced fractures. The trace length of the four outcrops/stations are in figures 7.7 and 7.8. The P20 (fractures per unit area) are in figures 7.11 and 7.13.

The sections that were interpreted in the WLC and SLC outcrops are chosen such that they contain an uninterrupted pavement. Erosion and vegetation can make tracing fractures difficult. The areas also cannot be too large as this will consume too much time. Fractures are traced when they are visible. The level of detail at which the pavements have been imaged allows for analysis on small fractures as well as larger ones. To avoid interpreting fractures on different scales, the tracing was done within a certain zoom level in QGIS.

Fracture length varies within an outcrop and between outcrops. Figures 7.7a and 7.7b are both from interpreted sections of the outcrop BRO1. Differences in distributions is controlled by fracture orientations. Fractures in the outcrop of a certain direction are consistently larger. This is seen in figures 7.9a and 7.9b. There is a strong correlation between length and orientation. Fractures oriented 60-240°are short when compared to those oriented 150-330°. The latter are also present in BRO1.2 but are not that large. The same is seen in the outcrops SLC and WLC (figures 7.10a and 7.10b). In the cross plot of the WLC outcrop the fractures form two groups at 120°and 180°. The cross plot of the SLC does not contain contains the large fractures and does not form peaks.

The fracture intensity varies within the interpreted outcrops. This can be seen in figures 7.5 and 7.6. The intensity can be expressed as the number of fractures within an unit area or fracture density (also called p20). The p20 plots of the BRO1.0 and BRO1.2 are shown in figures 7.11a and 7.11b. Rose diagrams showing orientation frequencies of the two stations are illustrated in figures 7.12a and 7.12b. The same is done for the outcrops WLC and SLC in figures 7.13 and 7.14. The p20 plots are heterogeneous but show a correlation with fracture orientations which are indicated by the rose diagrams. This fracture density trend is present in all cases except in outcrop WLC. Here the fractures are also not oriented in a clear direction. The trends are roughly NW-SE for BRO1.0. BRO1.2 and WLC.

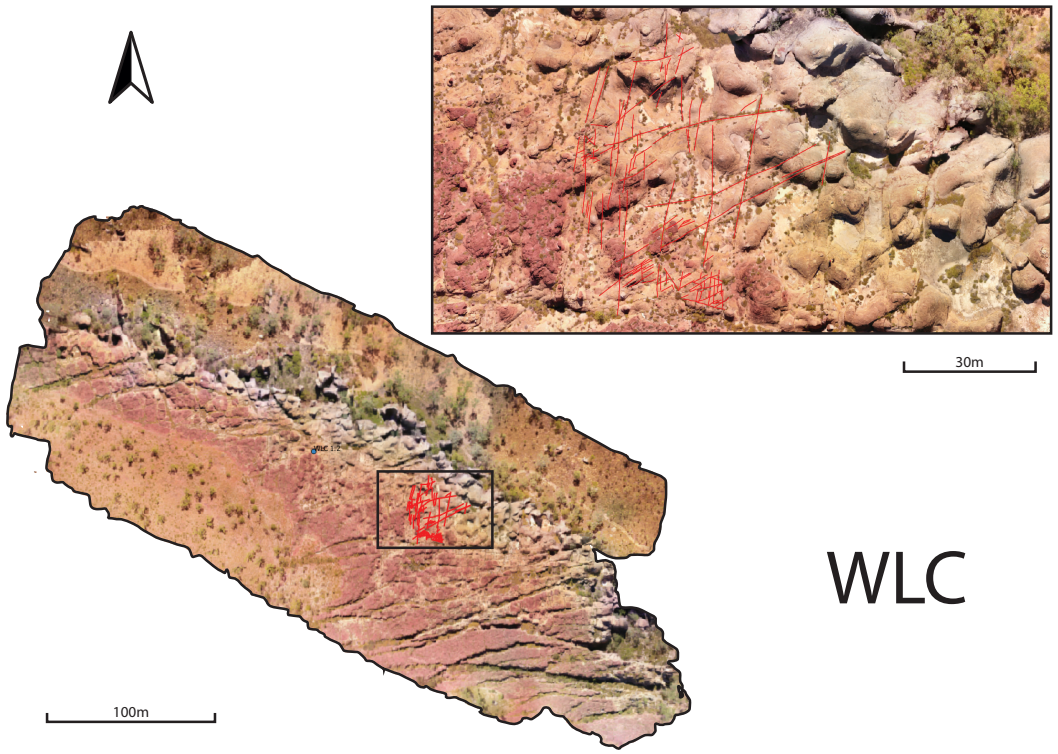

Figure 7.5: Pavement of the WLC outcrop and the interpreted section. A larger version can be found in appendix D.

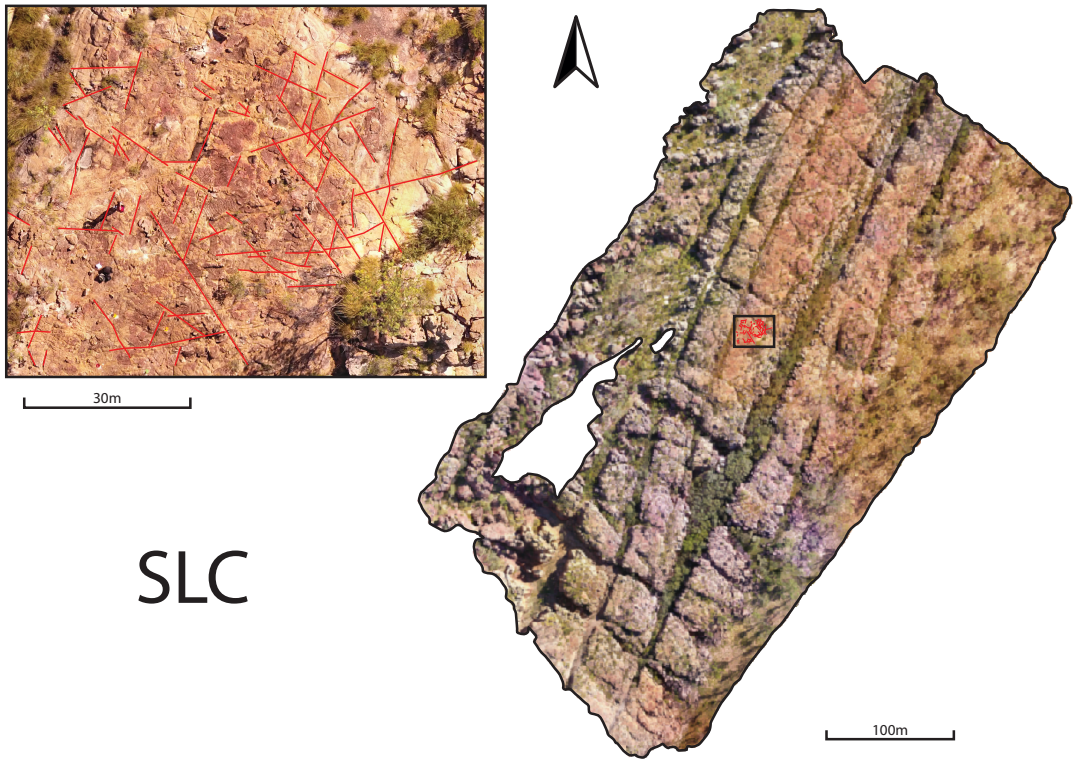

Figure 7.6: Pavement of the SLC outcrop and the interpreted section. A larger version can be found in appendix D.

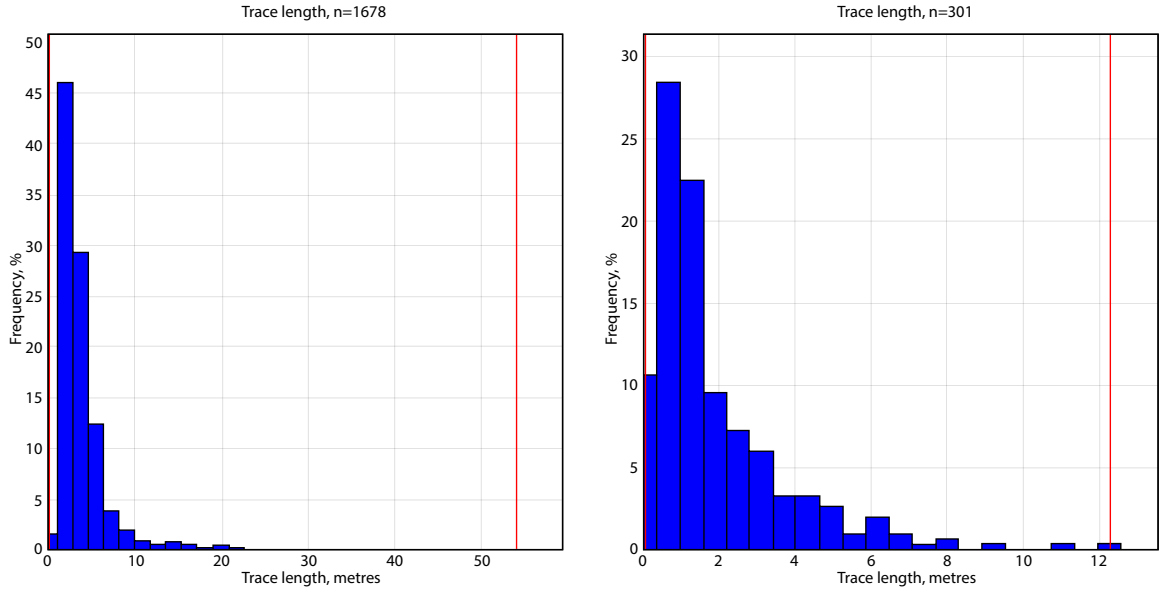

(a) (b)

Figure 7.7: Distribution of the trace lengths of outcrop BRO1 (a) and of station BRO1.2 (b). Both figures are from (Steijn, 2018).

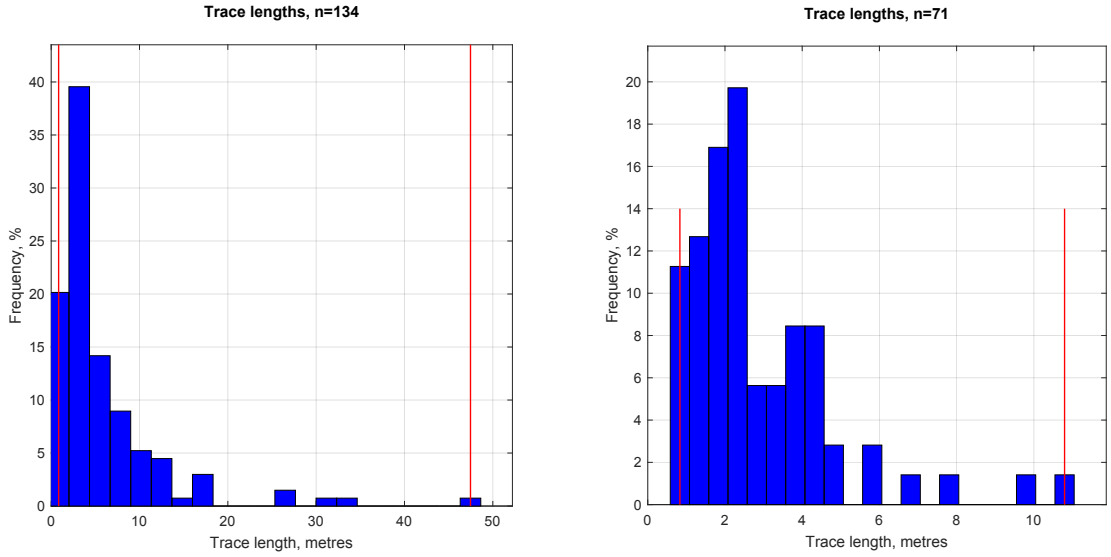

(a) (b)

Figure 7.8: Distribution of the trace lengths of outcrop WLC (a) and of outcrop SLC (b)

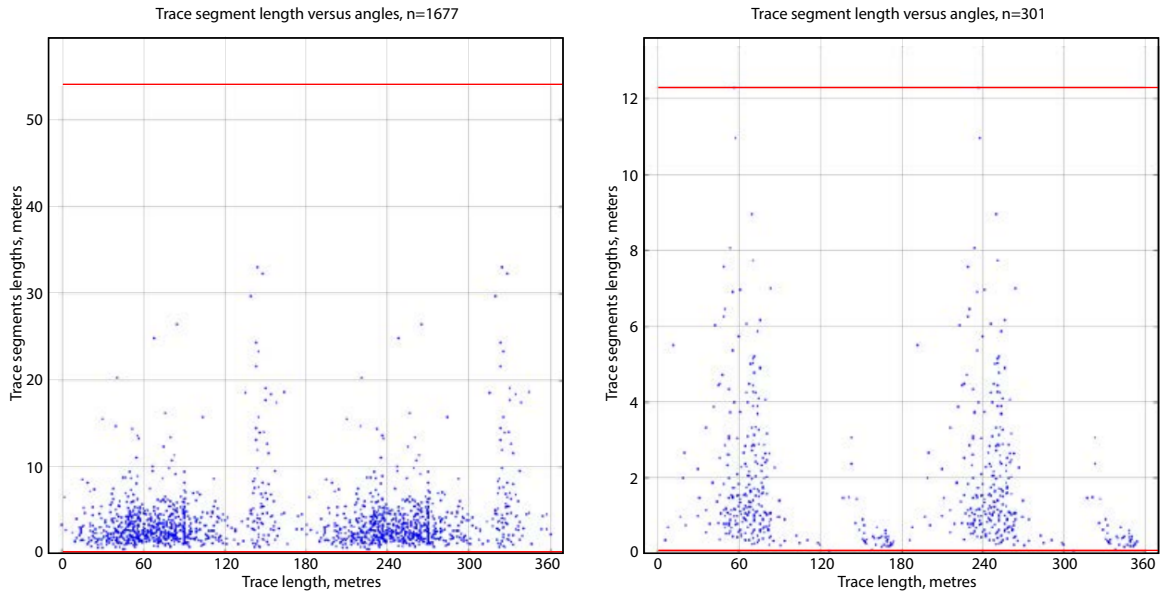

(a) (b)

Figure 7.9: Fracture orientation and length cross plots of outcrop station 1.0 (a) and of station BRO1.2 (b)

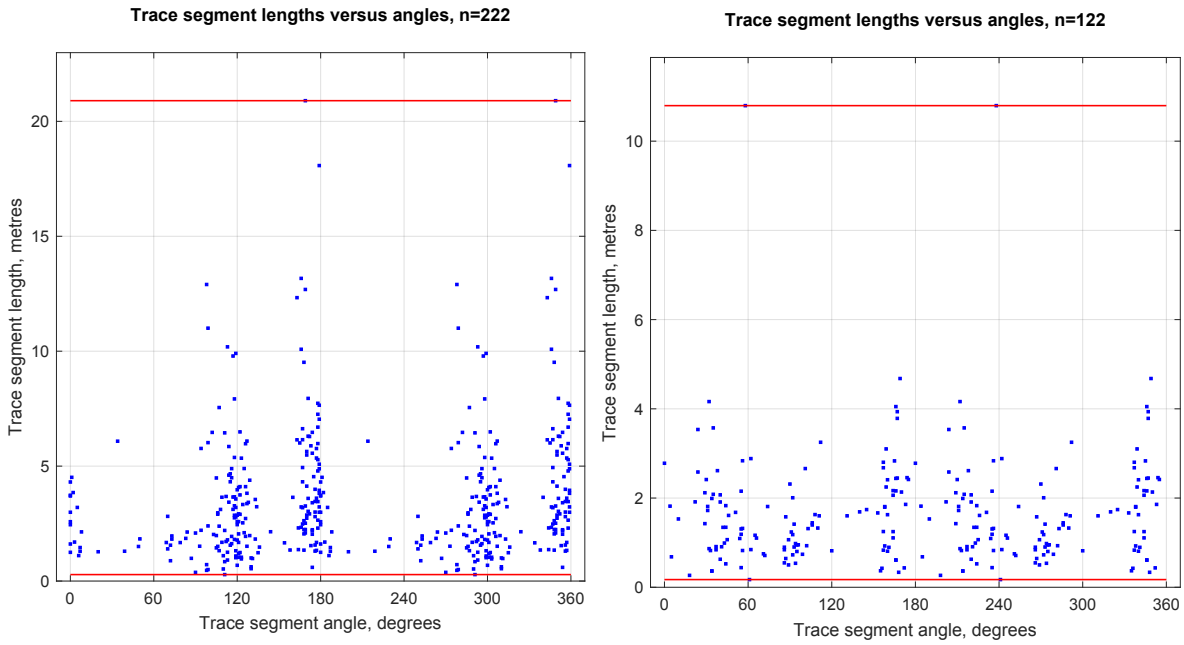

(a) (b)

Figure 7.10: Fracture orientation and length cross plots of outcrop WLC (a) and of outcrop SLC (b)

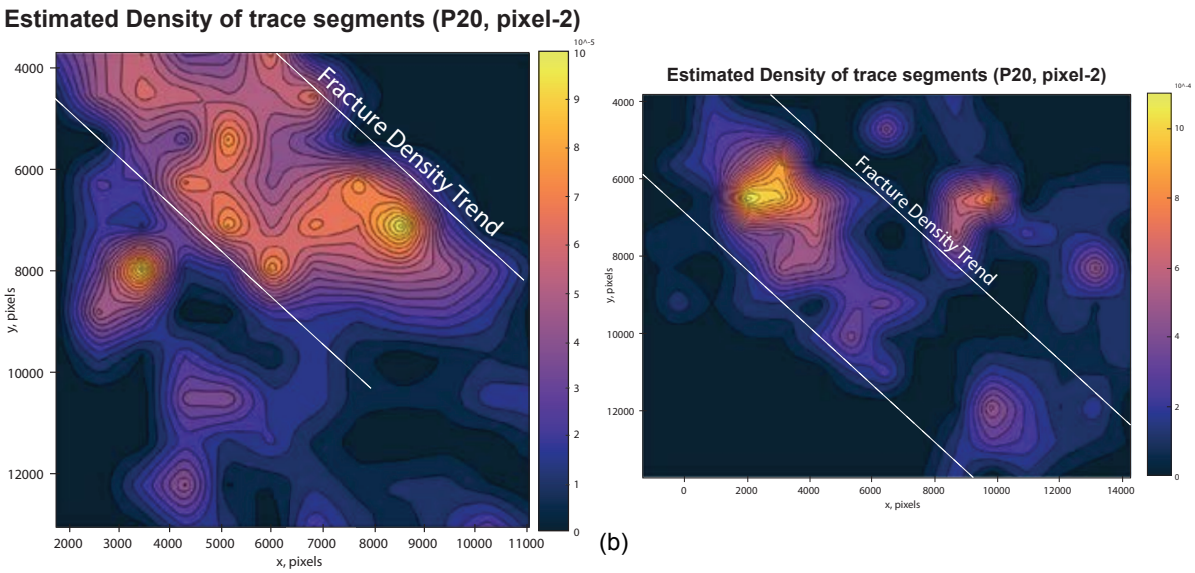

(a) (b)

Figure 7.11: P20 maps of outcrop BRO1.1 (a) and of outcrop BRO1.2 (b).

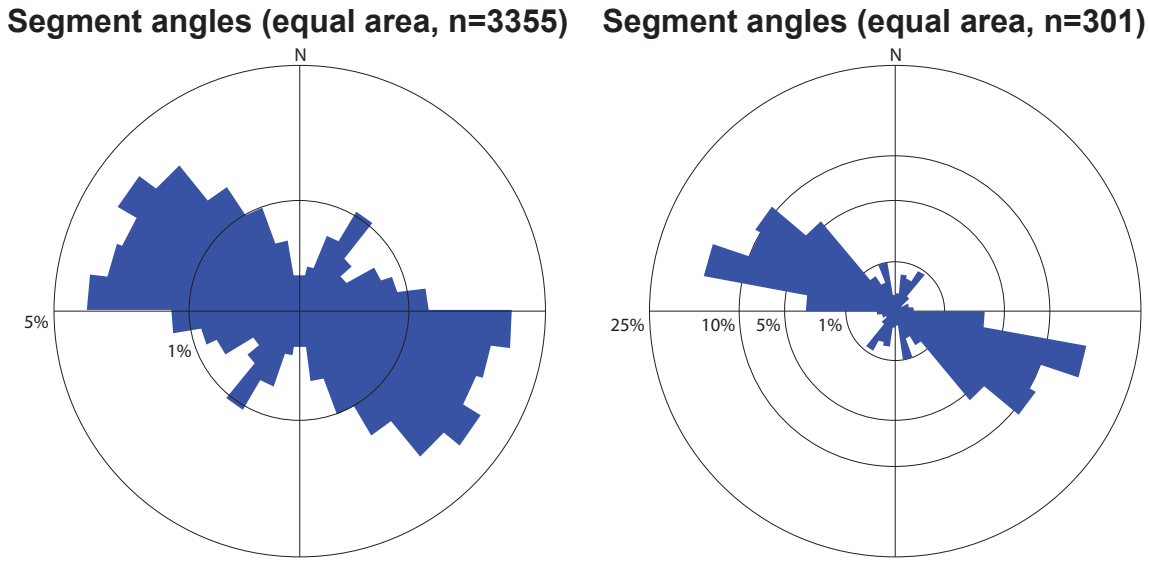

(a) (b)

Figure 7.12: Rose frequency diagrams of fracture orientations of outcrop BRO1.1 (a) and of outcrop BRO1.2 (b).

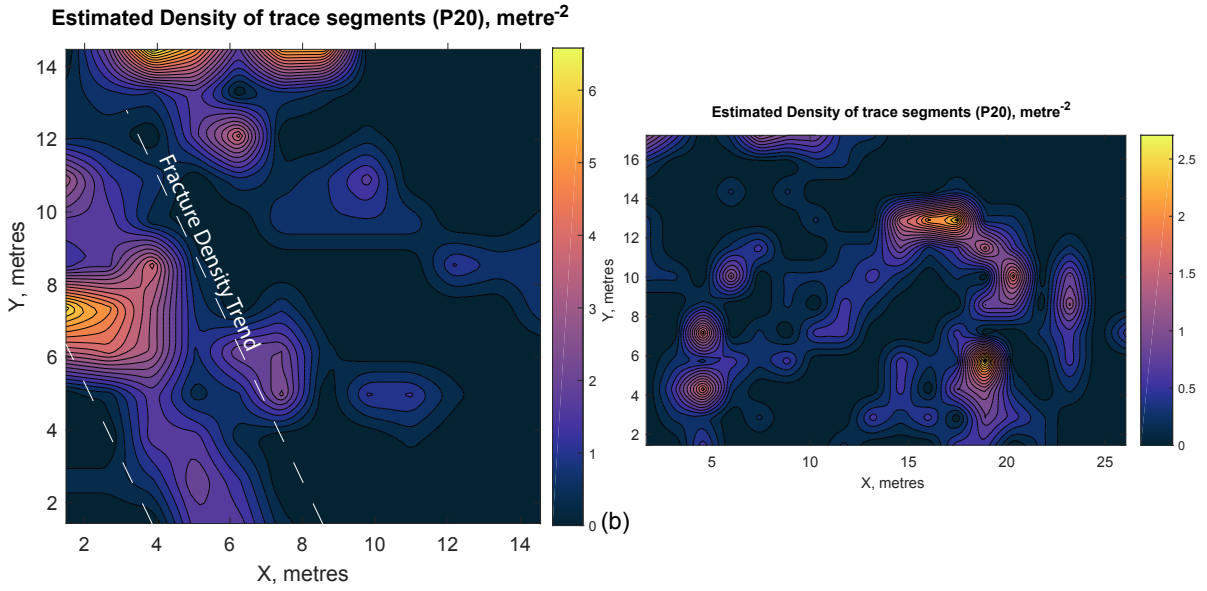

Figure 7.13: P20 maps of outcrop WLC (a) and of outcrop SLC (b)

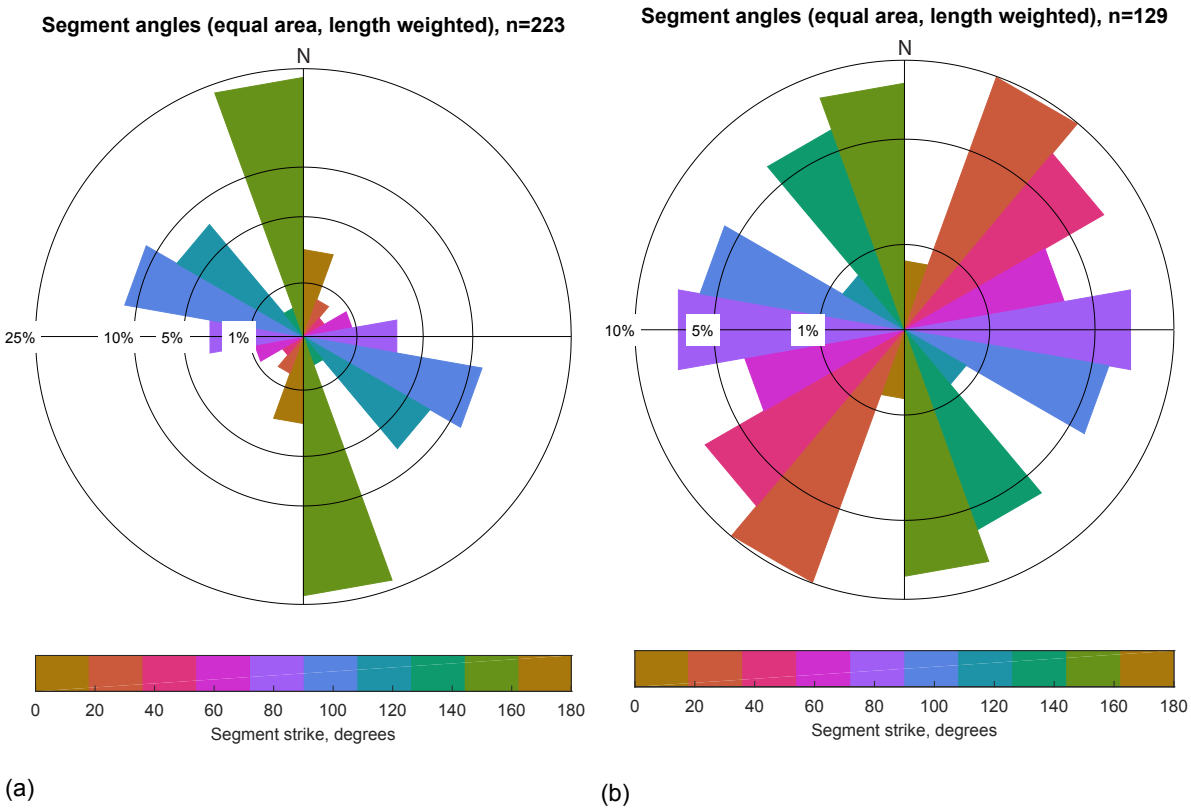

Figure 7.14: Rose frequency diagrams of fracture orientations of outcrop WLC (a) and of outcrop SLC (b).

The fracture density also impacts permeability. FracPaq outputs the permeability in direction of flow (figure 7.15). The 2D permeability tensor is represented as an oval whose axes (k_1, k_2) have the same ratio as the ratio of the permeabilities in those directions. In this case k_1 is three times larger than k_2. The azimuth of k_1 is 123°, close to the group of fractures at 120°seen in figure 7.10. The fracture density trend and permeability direction in the WLC outcrop are hence correlated.

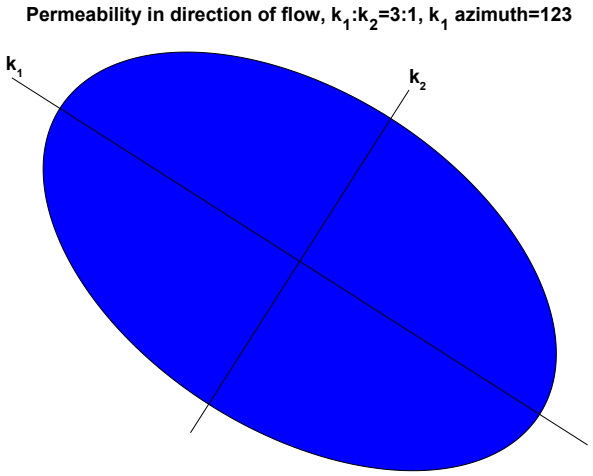

Figure 7.15: 2D Permeability tensor represented as an oval of the interpreted fracture geometry of the WLC outcrop.

7.5. Correlating the surface with the subsurface

One of the goals of this thesis is to correlate the fracture network at surface with the subsurface. This is possible based on the new insights gained in this study. The new insights are:

- There are two deformation events, the Carpenteria Event (N-S) followed by the Borroloola Event (E-W).
- The deformation during the Borroloola Event was larger.
- They each generated a conjugate fracture system.
- $\sigma_{H,max}$ is oriented perpendicular to the fold axis.
- The fracture density trend roughly follows in the direction of the dominant fracture sets.
- The surface observations formed in another stress regime than the subsurface. Any correlation should be done with caution.

This study assumes that the orientations observed during the fieldwork apply to the whole Wilton Package. The geometry parameters however do not apply on other formation within the Wilton Package.

The list above has been used to create a conceptual model that shows the qualitative properties of a fracture geometry in the subsurface at a location similar to the Tanumbirini-1 well. The prediction is shown in figure 7.16. The Tanumbirini-1 stereonet indicates that the fractures form a normal conjugate system. The fractures are thus parallel to each other in the horizontal direction and only cross each other in the vertical plane. Two conjugate sets are present in the well and are associated with the two deformation events. Throughout this report it is stated that the Borroloola Event (E-W) deformed the basin stronger than the Carpenteria Event (N-S). More fractures are expected to have been generated by the stronger event. Moreover the stereonet of the Tanumbirini-1 well (figure 7.4) also shows far more fractures present in the E-W direction than the N-S direction.

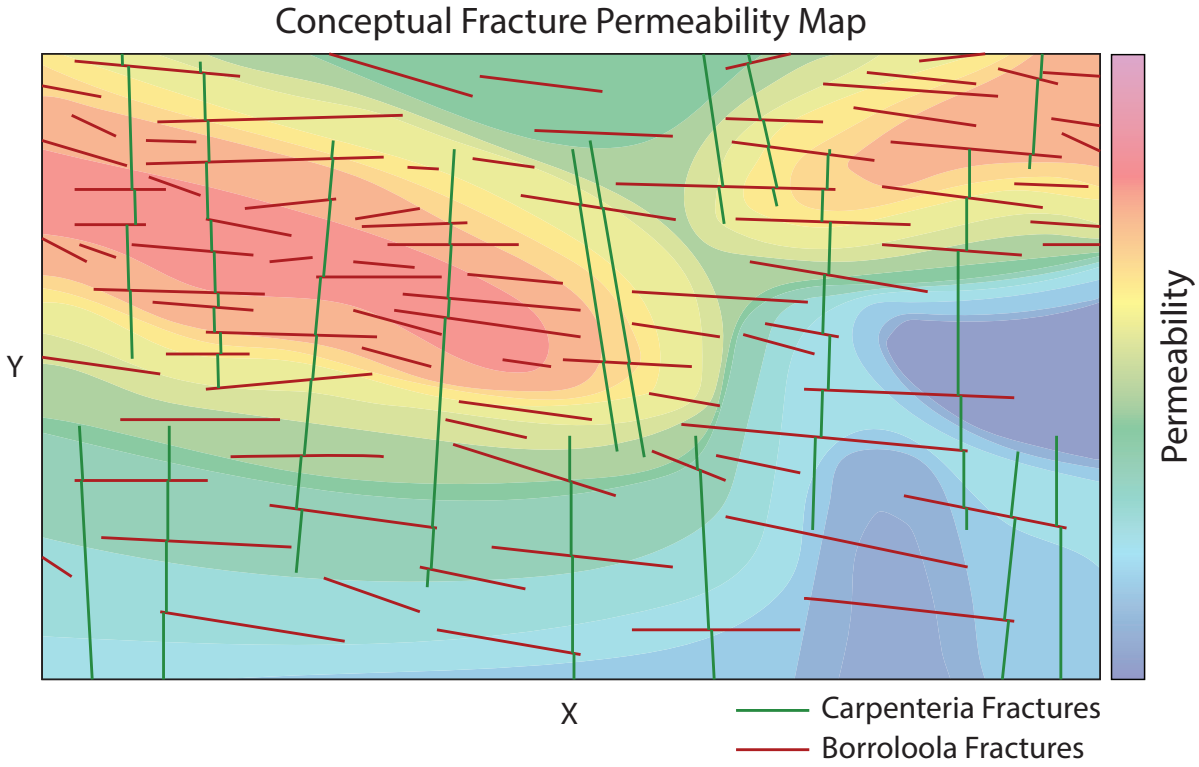

Figure 7.16: A conceptual fracture permeability map at an undeformed location in the Beetaloo Sub-basin.

The flow will be better in the E-W direction as most fractures are oriented that way. This is also seen at the interpretations of the outcrops presented in the previous section. The N-S oriented fractures improves the connectivity between E-W fractures. Some 'random' heterogeneity in fracture density can be expected as can be seen with the p20 figures in the previous section. Figure 7.16 shows the correlation in the form of a conceptual model of the a fracture network in the subsurface.

8

Discussion

This study presents two main findings, i.e. the two deformation events and the fracture response from these events. However a lot of assumptions and statements were made which need to be discussed as they influence the validity of the results.

8.1. Seismic Interpretation

The interpretation of the composite seismic line gives room for discussion. The packages reach depths of several km's, besides seismics no other information can be used to determine what is present at these depths. The amount of time that was available to interpret the seismic composite line was limited, this removed the option for example to create another model. The model that has been presented by Rawlings et al. (2004) for the Batten Fault Zone is totally different. The fault zone is presented as a thrust belt instead of an inverted extensional basin.

Further research could focus on seismic reprocessing to increase the fidelity of the seismic images. This study used only the OT Downs region of the Beetaloo Sub-basin. The sub-basin contains dozens of other seismic surveys. They can also be included in a 3D model. In addition neighbouring locations outside the study area also contains gridded seismic surveys similar to the McArthur River 2D 1983 survey. They can be studied to look if the two deformation events also produced unconformities there.

8.2. Deformation Events

Two deformation events have been identified that occurred after the deposition of the Wilton Package. The main axes of the folds in the Broadmere Complex are N-S oriented corresponding to a E-W deformation, this is supported by literature (Rogers, 1996). The same complex also has E-W oriented fold axes, one of these was observed during the fieldwork. There are only a few unlikely scenarios in which the different fold axes could have been created by one event. The two unconformities observed in the seimsic line MCSAN13-05 and the two conjugate fracture systems in the Tanumbirini-1 well supports the occurrence of two events. The well also provides the depths and formations at which the unconformities occur. The Carpenteria Event is situated between the Wilton Package and the Jamison Sandstone. The Wilton Package and the Jamison Sandstone have already been dated, giving an accurate time window of 232 Ma for the Carpenteria Event. The Borroloola Event separates the Hayfield Mudstone and the Bukalara Sandstone. With current data the time window of this event is 404 Ma. The formations above and below the Borroloola event have not yet been dated. Further research can focus on dating these formations to narrow the time window.

By looking at other areas of the Beetaloo Sub-basin more evidence could be found to (dis)prove the existence of the two events. Towards the center of the basin other formations are underlying and overlying the Jamison and Bukalara Sandstones. The unconformities become more pronounced towards the 'shoulders' of a basin, i.e. more erosion happens at these edges. Hence a more complete stratigraphical record can be found at the center of the basin. The original thicknesses of the eroded formation of the Wilton Package and Inacumba Group also could be found. Figure 4.4 only accounts for the three formations within the Inacumba Group. There were possibly more formations between the Hayfield Mudstone and the Bukulara Sandstone at this location. This increases the depth at which the rocks originally were. And depth corresponds to the vertical stress which impacts the fracture geometry.

8.3. Fieldwork

The fieldwork was a complex operation. The plan before leaving would have taken the team to the eastern flank of the Broadmere Complex and the Abner Range. The latter possibly has horizontal oriented formations, an ideal outcrop to study the response on the regional stress field. Because there is a lack of folding and faulting. The main improvement is to better estimate the route from the car to the outcrop. And not primarily in distance but also the type of terrain. The Abner range seemed doable on paper, but in reality however it proved to be further away and through dangerous terrain.

The drone did its job, but the Pix4D app does need to have the satellite images saved in cache. The app also has the tendency to crash often. It will be better for future fieldwork to have high resolution images of all important areas available offline. These should be used with software like QGIS. GPS points of the current position could be imported in to QGIS, helping find the outcrop. When driving off-road or walking through rough terrain this proved the key to success in reaching the outcrops.

8.4. Fracture Interpretation and Prediction

To decide whether or not two fracture sets are conjugate can be difficult. Therefore the outcrops were scored with regards how many of the criteria were met. Most scored 2/3, making it likely that but not certain that they are conjugate. The σ_1 of these sets were observed in both the E-W and N-S direction. This confirms the presence of the two fracture directions in the region. In Steijn (2018) three conjugate fracture sets were interpreted at the BRO1 outcrop, this is however only based on the angle between the fractures.

Many arguments suggest that the N-S fractures and E-W fractures are generated by the Carpenteria and Borroloola Events respectively. There are also some counter arguments. Although the two events are likely to have occurred, it remains up to debate whether they correspond to the observed unconformities. Both unconformities are visible in both the N-S and E-W direction, as has been discussed in chapter 4. It cannot be ruled out that both two fracture directions could have been generated by one of the two events. Formations that have only been deposited after the Carpenteria event should be investigated in further research. Observing only E-W fracture in the Jamison Sandstone or the Hayfield Mudstone will rule out this counter argument.

Unfortunately the FMI log interpretation of the Tanumbirini-1 well was done manually. This limited the amount of data that could be analyzed. The well almost contains 1500m of FMI log of both the Velkerri Formation and the Moroak Sandstone (both part of the Wilton Package). Additionally manual interpretation is prone to inaccuracies compared to interpreting in Techlog. Future research could focus on interpreting this well with Techlog to obtain a more complete and accurate dataset.

Fractures observed in the field have been grouped manually. This introduces bias from the interpreter and impacts the orientation of $\sigma_1/\sigma_{H,max}$. A new method described by Maerten et al. (2016) uses stochastic modelling to fit the observed data to a specific stress regime removing any bias from an interpreter. Unfortunately there was not enough time to successfully do this during this study. But could be used in subsequent research.

The 'weakest' result is the prediction of the fracture geometry at a location similar to the Tanumbirini-1 well. The observations discussed in section 7.5 gives a list of these. The existence of two events is supported by strong evidences and the corresponding two conjugate sets have both been observed in the field. The interaction between the two fracture geometries remains unknown. As stated in the previous section the Abner Range could have revealed this. The difference in fracture intensity between the two sets could also support or contradict the statement that the Borroloola Event was more extreme than the Carpenteria Event. The fracture density trend is only based on four interpreted sections of three outcrops. Further interpretation of the acquired data can give more evidence. This will either reinforce the trend or refute it.

An important concept is the REV or Representable Elementary Volume (figure 8.1). This is not investigated in this study but can be important for future analysis of the drone images. Figure 8.1 shows a generic fracture pavement. Interpreting sections at scale 1 will give different results depending on the location. The heterogeneity at this scale is large. Increasing the scale to 2 could decrease or increase the heterogeneity. But at scale 3 the different locations will not lead to a totally different result. This is the REV scale of this outcrop. This concept implies that only the REV scale needs to be interpreted. The process of interpreting the large images becomes more efficient. If the wrong scale is chosen the observed data is biased as it is not the REV. The main difficulty is to determine the REV scale. Knowing the REV will make interpreting the data more efficient and can be a criterion for selecting outcrops in future fieldworks.

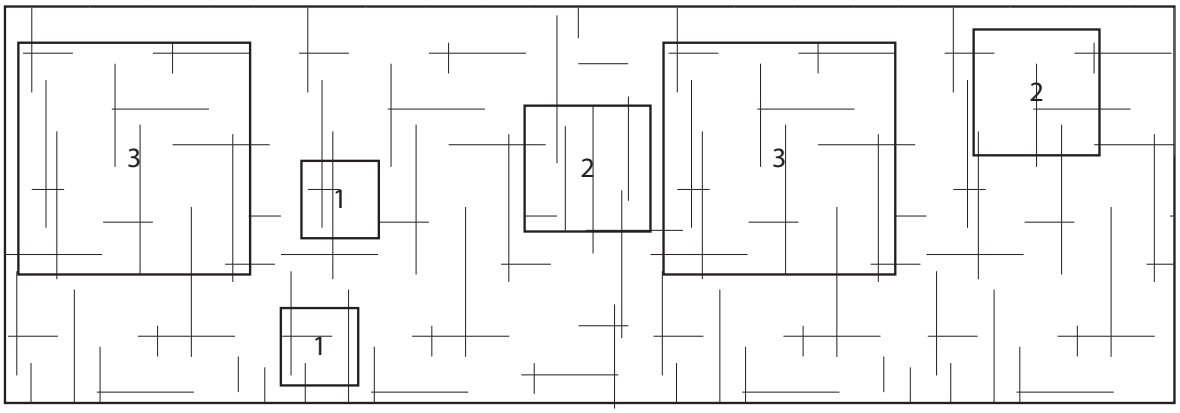

Figure 8.1: The heterogeneity decreases when the box is increased, this demonstrates the concept of REV.

8.5. Further research

The results of this thesis forms a good basis for future research. The discovery of the two deformation events can be used as a structural control for numerical modelling. It can be used to simulate the fracturing of the rocks and compare them with the real observations. Other researchers are actively developing methods to do this effectively (Favorskaya et al., 2017). Stochastic modelling of the fracture geometry based on statistics from the acquired field data could also be done. An example could be discrete fracture networks (DFN), which have been used before to successfully describe fracture geometries (Wilson et al., 2015). Open source DFN software (Alghalandis, 2017) is readily available and can be used to model the fractures in the McArthur Basin. Both numerical and stochastic modelling will improve the predictions made in this report. Any fracture model could also be used to study the behaviour of fluid flow. Understanding this will help in developing smarter field development plans in the Beetaloo Sub-basin. All these topics are interesting to investigate in future research.

Conducting the fieldwork proved to be important to answer the questions posed in this study. If hydrocarbon fields in the Beetaloo Sub-basin are developed it can reveal more data on the nature of the subsurface fracture networks. Actual well test results give an idea on the direction of the permeability field, which can be compared to the prediction made in this report. If it validates the prediction the approach of this study (geological history, fieldwork, outcrop and well fracture analysis) can be repeated in other regions.

9

Conclusion

This study posed two questions:

- *What is the structural history of McArthur Basin?*
- *How to predict the subsurface fracture network geometries in the Beetaloo Sub-basin from outcrop analogues?*

A literature study was conducted which led to a geological history of the basin. Subsequently a fieldwork in the area of interest led to acquisition of fracture data that could be linked with the geological history. The questions that were posed in chapter 1 have been answered.

What is the structural history of McArthur Basin?
The understanding of the polyphased deformation history of the McArthur Basin has been improved by new discoveries in this study. The Leichhardt Event (Blaikie et al., 2017) caused the Lower Redbank to be faulted and partly uplifted. These structural highs led to the deposition of the Upper Redbank in lows and pinch outs towards the highs. This paleotopography also influenced the overlying Glyde Package, which was thinner over the structural highs. The Calymmian Unconformity (Betts et al., 2014) eroded to various extent the packages underlying the Favenc Package. The events after the deposition of the Wilton Package and before the Cambrian were poorly understood. From literature one event was known. Rogers (1996) identified an E-W oriented deformation event based on field observations.

In this report different data sources were integrated. The Inacumba Group is proposed for the Jamison Sst, Hayfield Mudstone and Bukulara Sst as they have a similar provenance (Yang et al., 2018) (T.J. Munson, personal communication, May 18th, 2018). The seismic survey MCSAN13 revealed the presence of two unconformities or events. The Carpenteria Event (first) separates the Wilton Package and the Jamison Sandstone. The Borroloola Event separates the Hayfield Mudstone from the Bukulara Sandstone. The events can be timed by looking at the ages of the underlying and overlying formations. This puts the Carpenteria Event between 1324±4 and 1092±16. The Borroloola Event is less constrained, a maximal age is 959±18 Ma. A minimal age would depend on the age of the Bukalara Sandstone, which is not yet known. The events can be linked to the folds seen in the Broadmere Complex. The complex consists of N-S and E-W oriented folds. The N-S folds were created during the Carpenteria Event and the E-W folds by the Borroloola Event.

How to predict the subsurface fracture network geometries in the Beetaloo Sub-basin from outcrop analogues?
Fieldwork observations led to the conclusion that $\sigma_{H,max}$ is oriented perpendicular to the fold axes. The fracture orientations are strongly influenced by either the Carpenteria or the Borroloola Events. This also controls the orientation of the fractures of conjugate sets. Analysis of the drone acquired images led to the observation that the fracture density is oriented in the direction of dominant fracture set.

A

Seismic Images

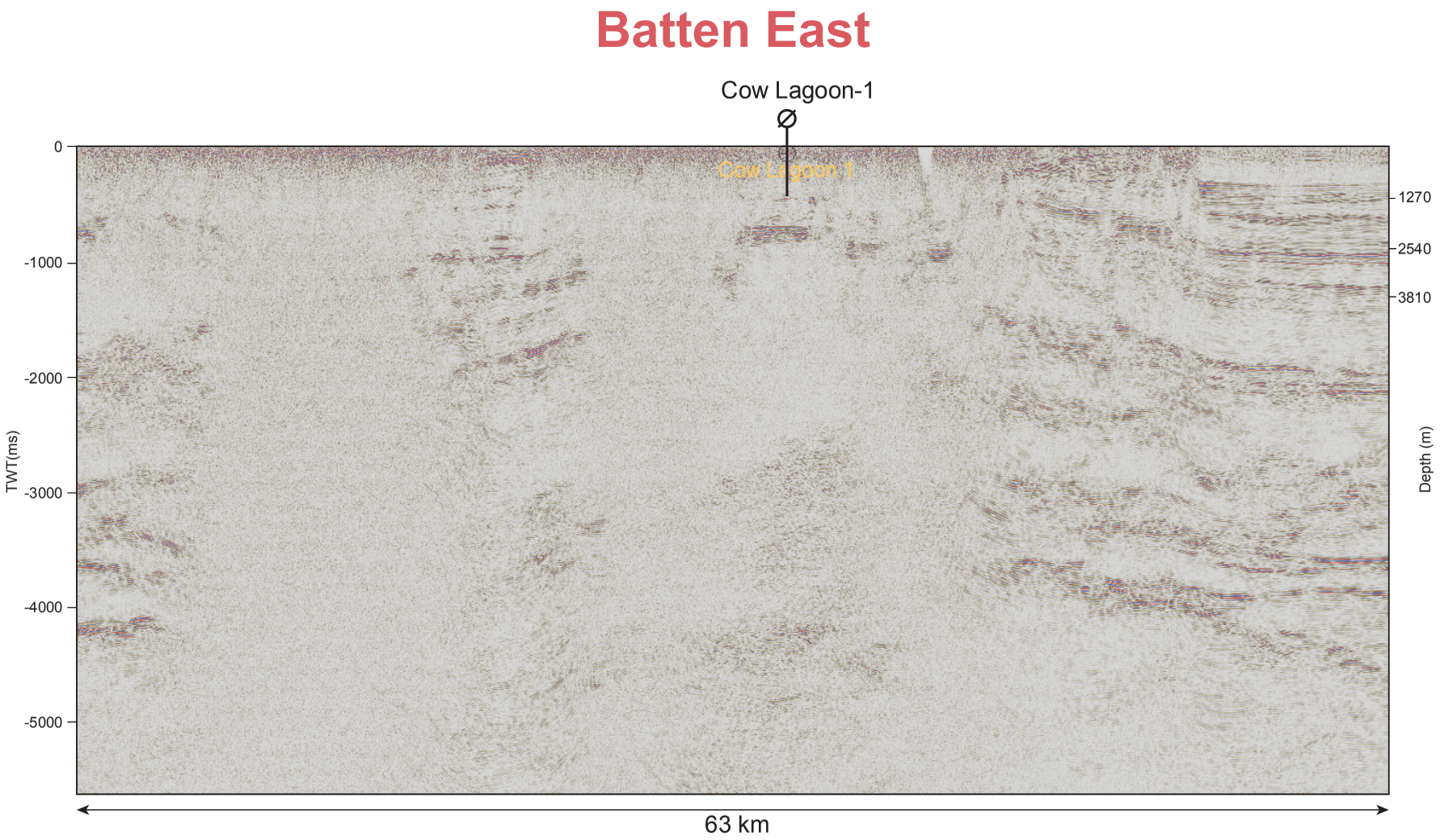

Figure A.1: Batten East section of the seismic composite line.

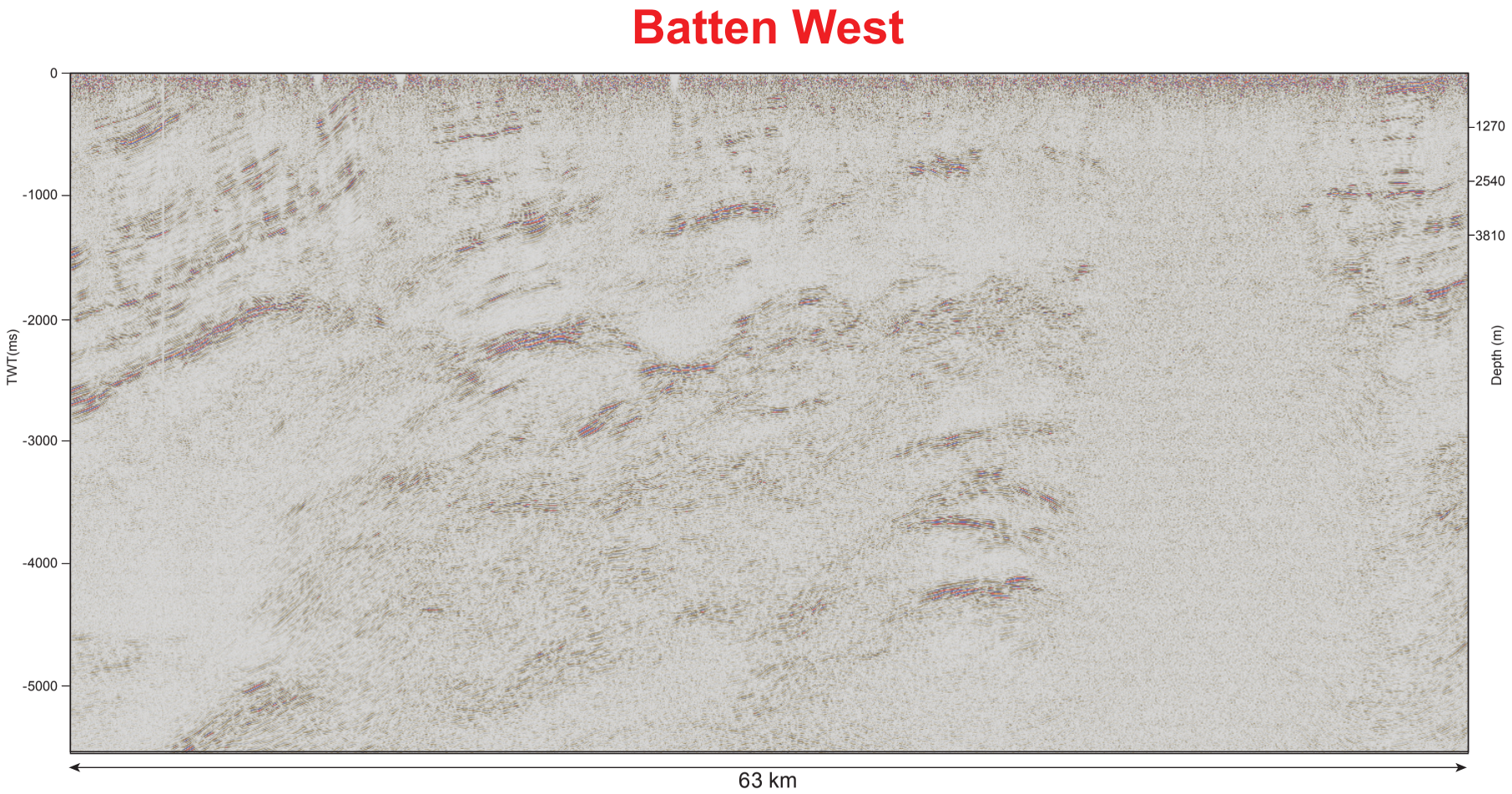

Figure A.2: Batten West section of the seismic composite line.

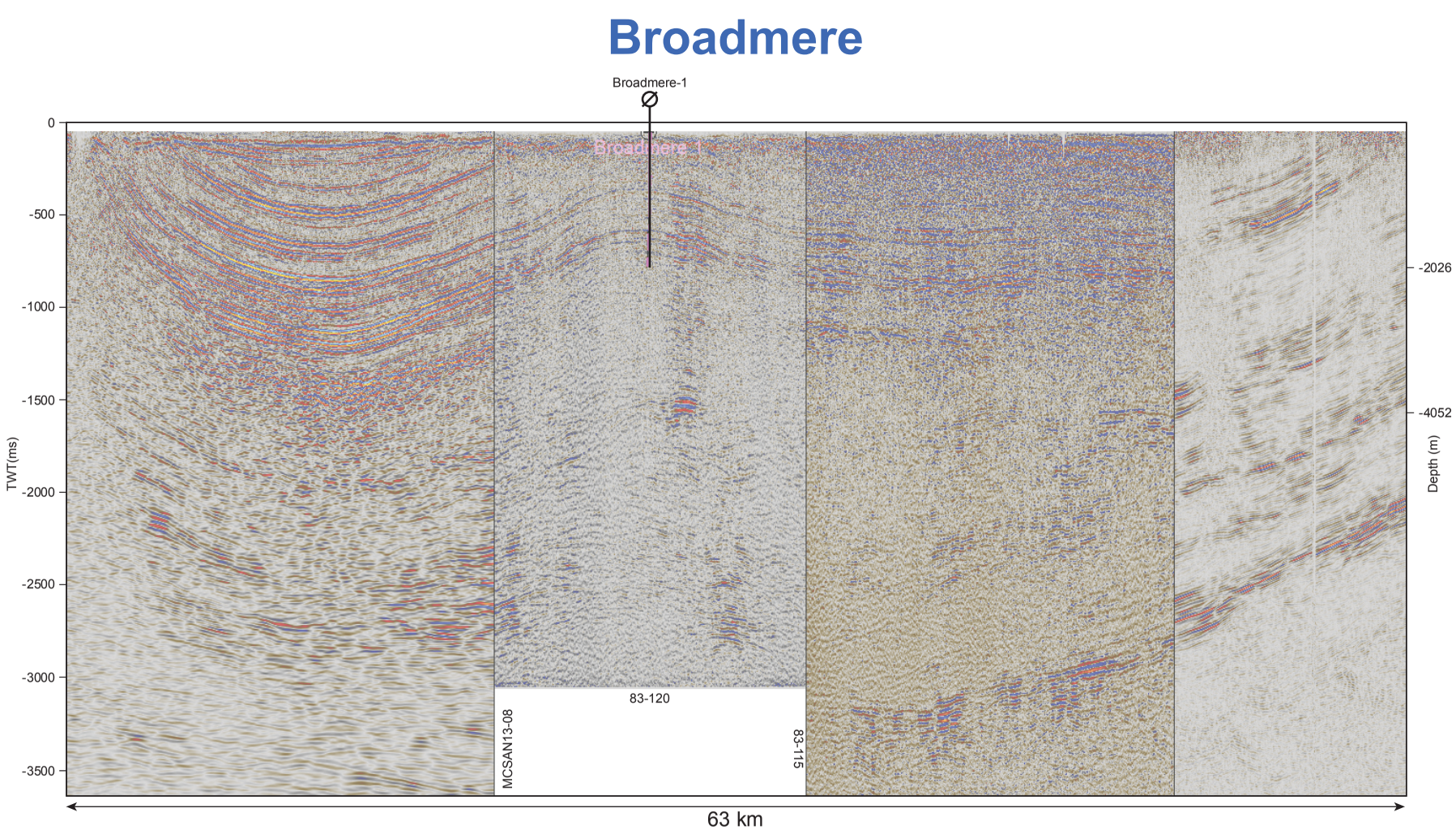

Figure A.3: Broadmere section of the seismic composite line.

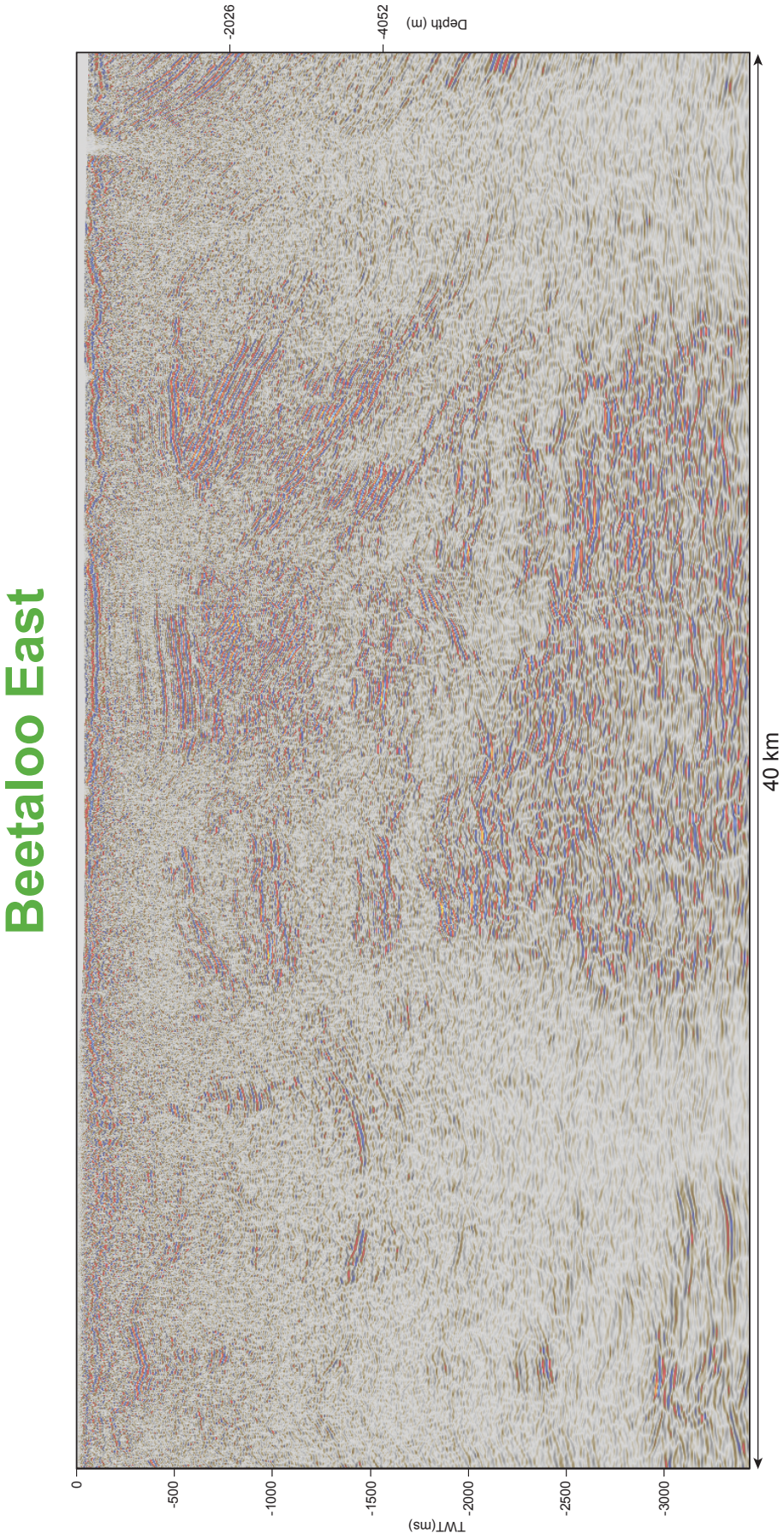

Figure A.4: Beetaloo East section of the seismic composite line.

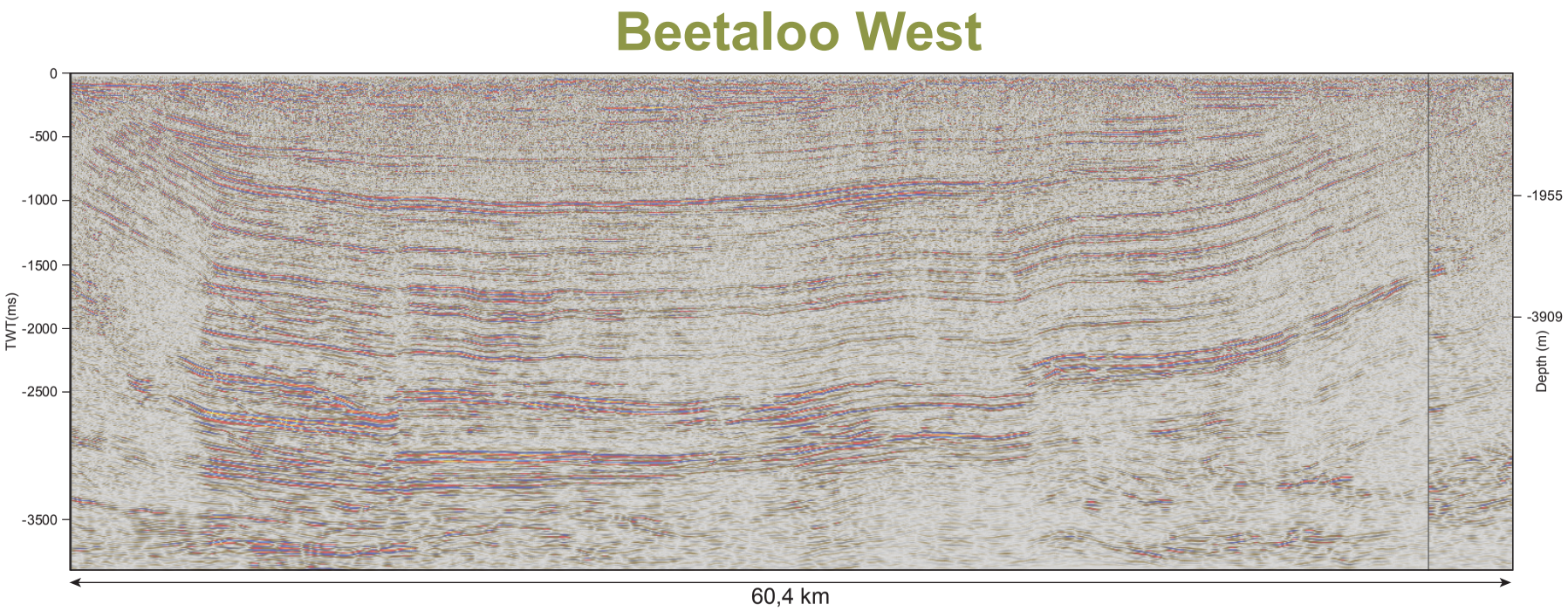

Figure A.5: Beetaloo West section of the seismic composite line.

B

3D Model

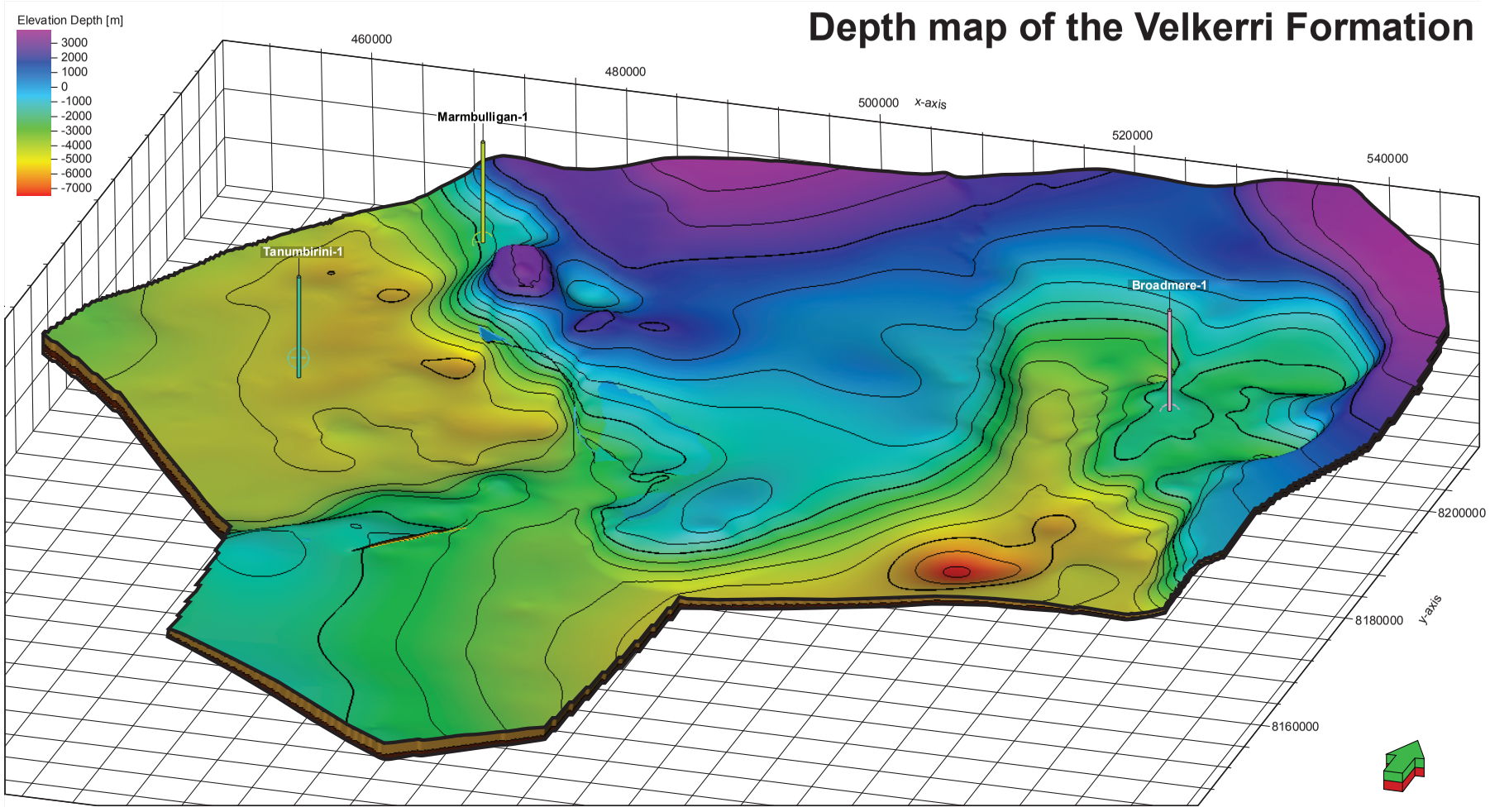

Figure B.1: The 3D model of the Beetaloo Sub-Basin and the Broadmere Complex. There is no vertical exaggeration.

C

Stereonets

Outcrop: ABN1

1/1

Station: ABN1

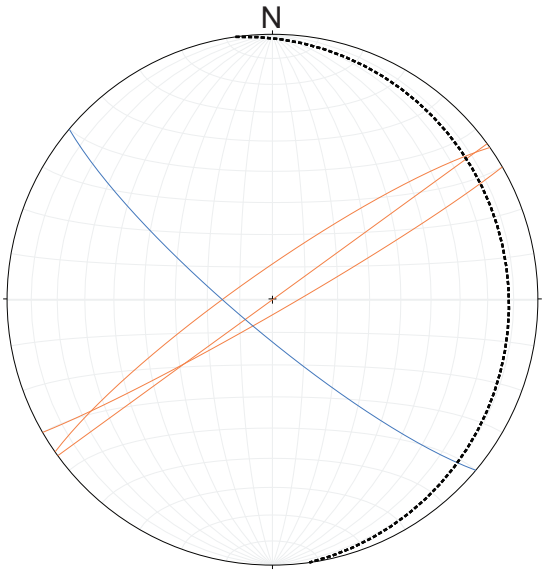

Unfolded w.r.t. bedding

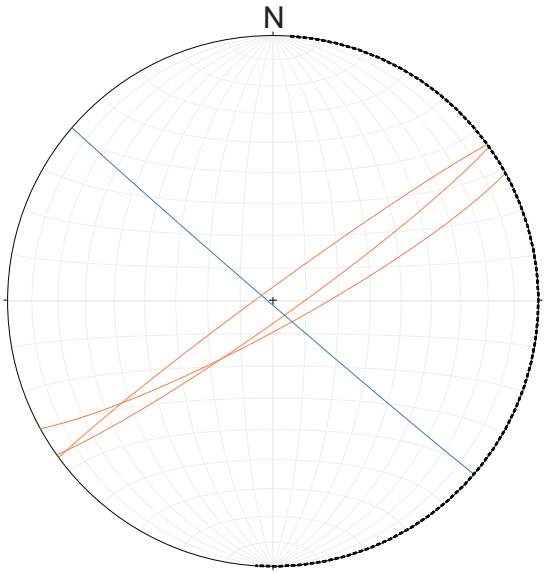

ABN1

Not reached the planned pavement, but took some measurement. Much better to have some representation:

- F1(056/86) is a NE-SW striking set.
- F2(130/80) is NW-SE striking set.

Bedding

Although the picture was taken without referencing direction. The corresponding GPS points was taken at 6:33 (GMT +1:00) time, which is 14:03 local time. Using Find My Shadow (https://www.findmyshadow.com/) the direction of the shadows could be determined. Together with the stereonet the sets seem to form a suborthogonal system.

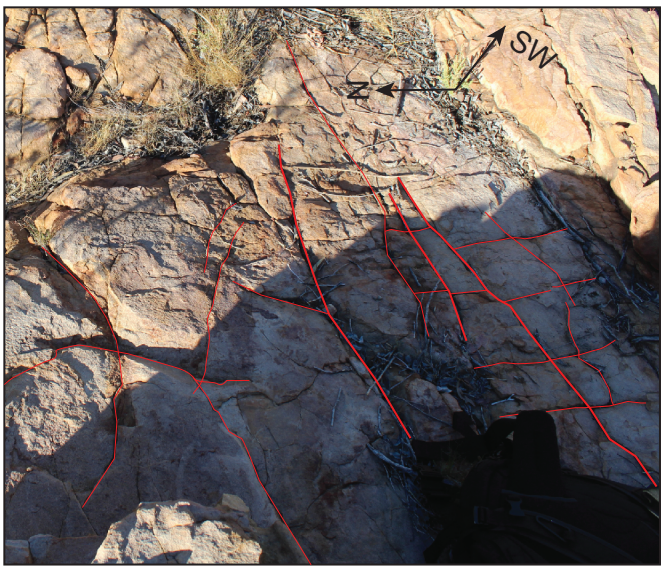

Angle: No	Movement: No	Striation: Yes	Score: 0/3

Figure C.1: Stereonet of ABN1.

Outcrop: BRO1

1/2

Station: BRO1.1

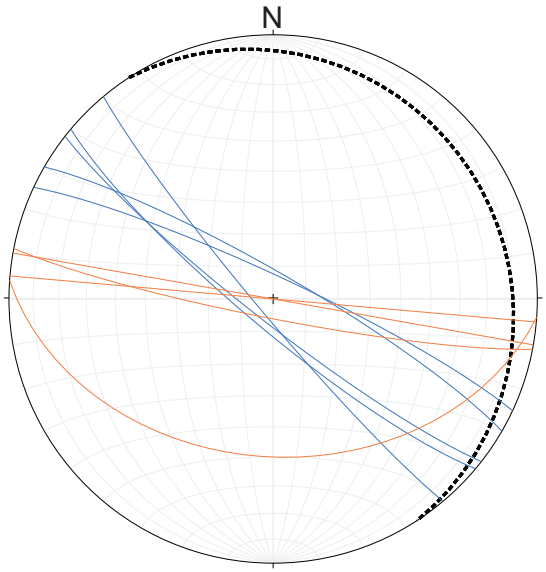

Unfolded w.r.t. bedding

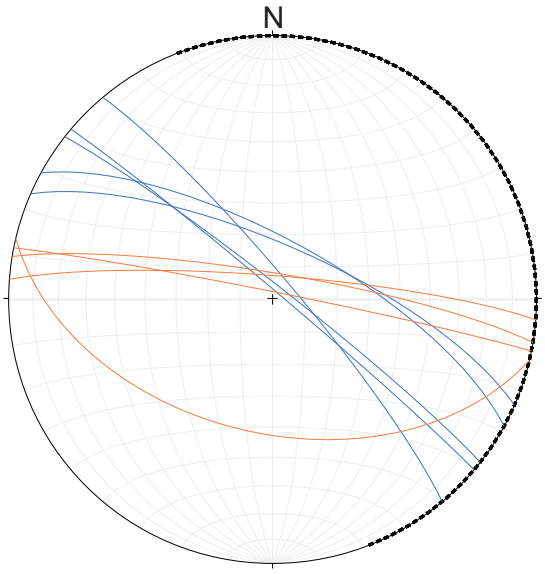

BRO1.1 (S16^{0}25.585' – E135^{0}11.885)

Bedding to the dipping NE and two fracture sets have been identified:

- F1(217/88) is a NW-SE trending that has shorter fractures that are often confined by F2 (see sketch)
- F2(188/76) is a E-W trending set.

Bedding

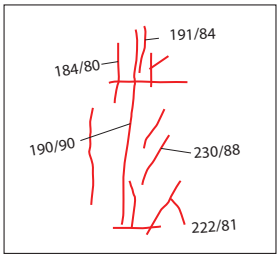

Figure C.2: Stereonet of BRO1.1.

Outcrop: BRO1 2/2

Station: BRO1.3

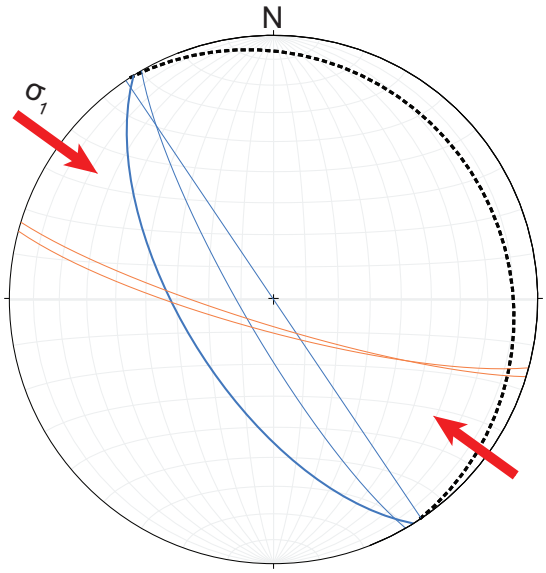

Unfolded w.r.t. bedding

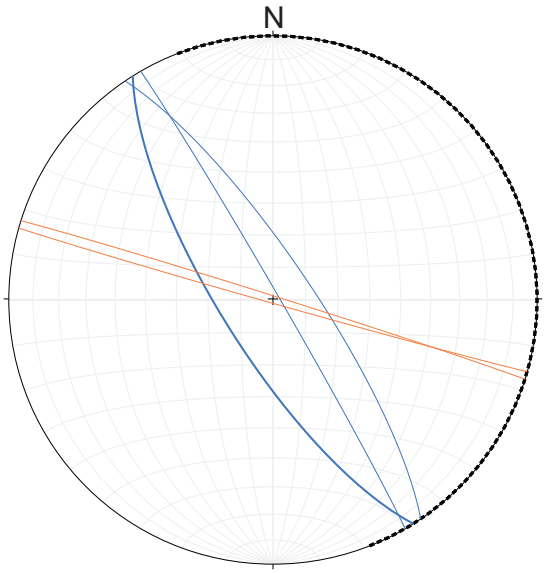

BRO1.3

F1(238/85) NW-SE trending set is long and binds F2 (seems the opposite to BRO 1.1)
F2(196/81) is a E-W trending set
Sinistral movement suggests conjugate with red arrow compression (black

Bedding

Sinistral movement suggests conjugate with red arrow (strike 300) compression (dark blue).

Systems of conjugate sets oriented parallel to the axis of the syncline. If conjugated then they are not LPS and thus are not related to the fold.

Sketch 1 the intersection of the fractures and the presence of horsetail splays.

Sketch 1

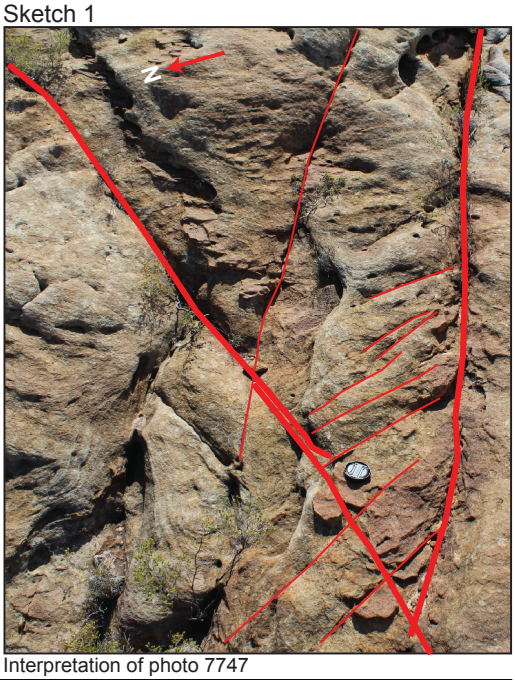

Interpretation of photo 7747

Angle: Yes	Movement: Yes	Striation: No	Score: 2/3

Figure C.3: Stereonet of BRO1.3.

Outcrop: BRO3

1/1

Station: BRO3.1

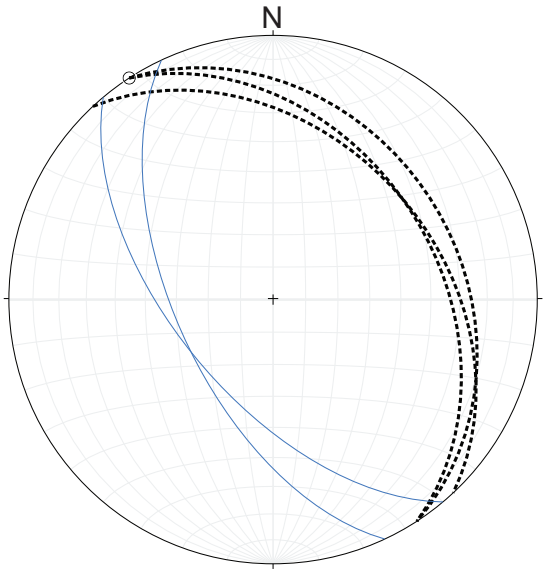

Unfolded w.r.t. bedding

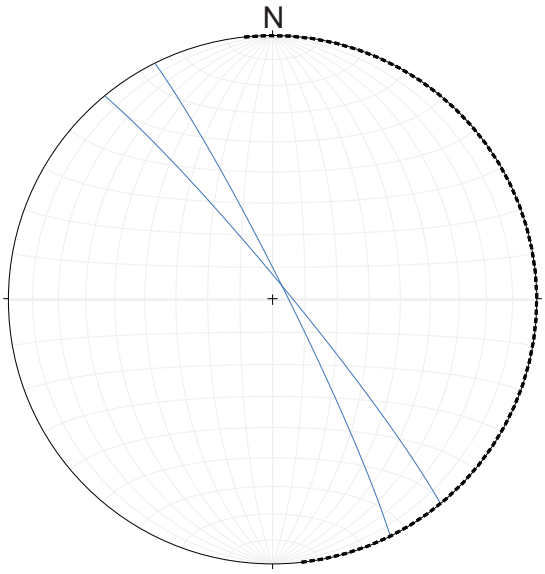

BRO3.1
South of the station, close to the road, outcrop on top of a parallel sister to the Malapunya fault). Small anticline (continuation to the NW not looked at): F1(238/60) is a ENE-WSW striking set.

Bedding

Ridge elongate NW-SE (indicated by ○) parallel to the general trend of the Malapunya fault (but also parallel to the strike in BRO1.1 ….). Fractures are parallel to the strike. Strong dips are peculiar; one bed has top to the SW (towards the hinge) compatible con local flexural slip.

The strikes are parallel to those (beds and some fractures) in BRO1.1 which is clearly away from the Mallapunyah Fault).

Angle: Yes	Movement: No	Striation: Yes	Score: 2/3

Figure C.4: Stereonet of BRO3

Outcrop: BRO4 1/1

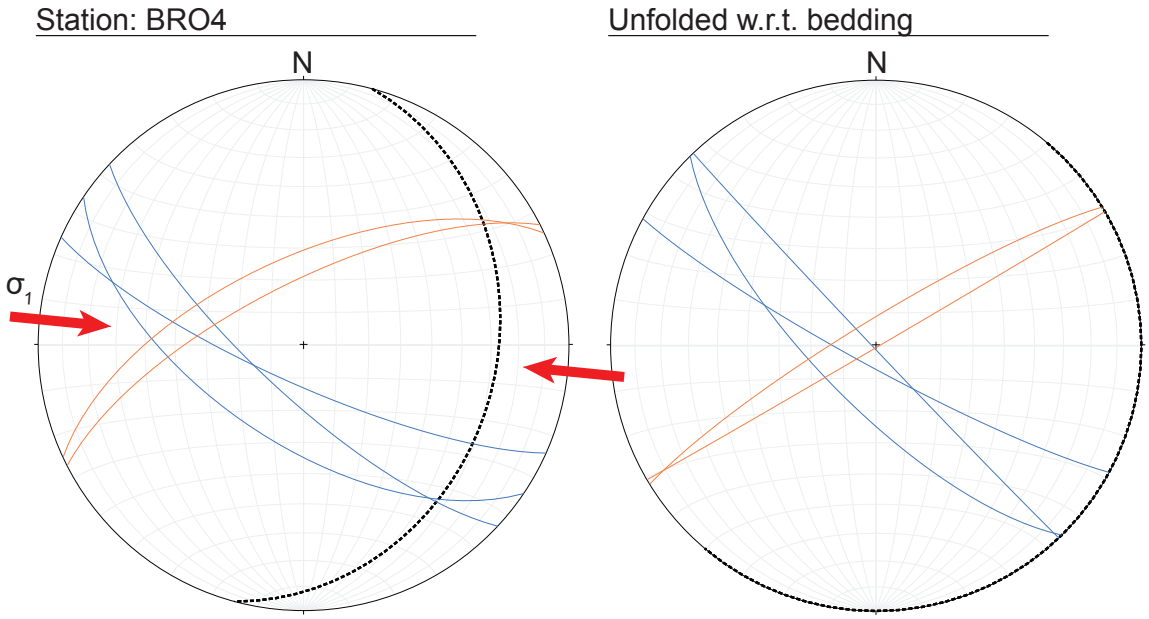

BRO4.1 (S16^{0}25.080 – E135^{0}10.785)
Bedding to the dipping NE and two fracture sets have been identified:
F1(217/88) is a NW-SE trending that has shorter fractures that are often confined by F2 (see sketch)
F2(188/76) is a E-W trending set.

Bedding

Close to the beginning of the N-S ridge (road from Broadmere and just after the N-S junction). Normal position of bedding. Conjugate-looking pattern of fractures and no clear bounding patterns in small pavements. Sigma 1 strike 274 and the set make a angle of 60^{o}.

Angle: Yes	Movement: Yes	Striation: No	Score: 2/3

Figure C.5: Stereonet of BRO4.

Outcrop: BRO5

1/2

Station: BRO5.1

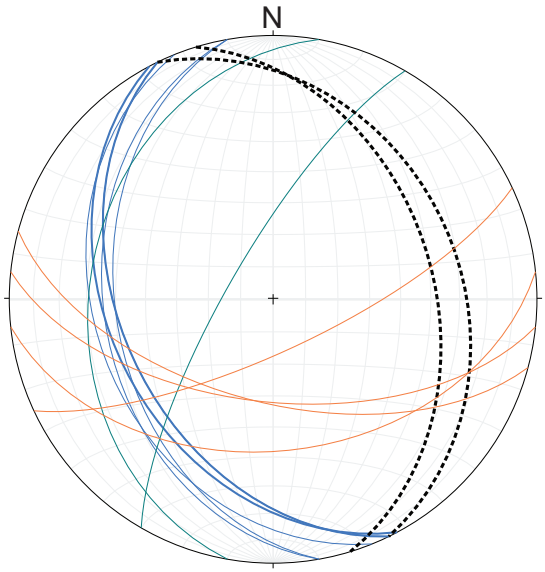

Unfolded w.r.t. bedding

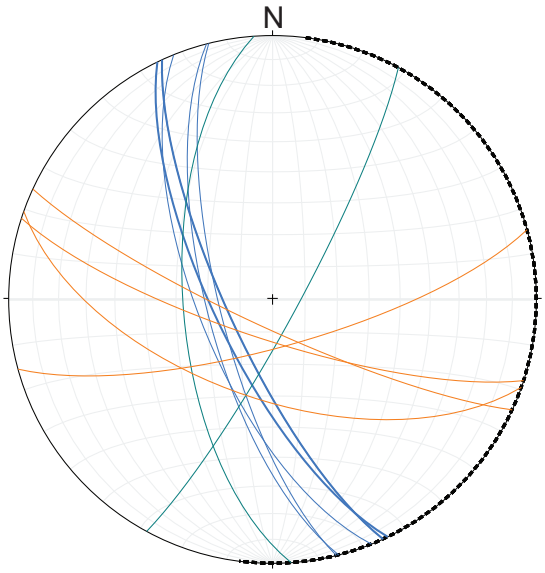

BRO5.1 (S16^{0}18.731 – E135^{0}09.783)

Three fracture sets are observed:

- F1 is a NE-SW trending set.
- F2 is a E-W trending set that seem to form a congjugate system with F1.
- F3 is a set that is perpendicular to the bedding. In a number of cases a 'normal fault' geometry is observed where the upper block is thrown down.

Bedding

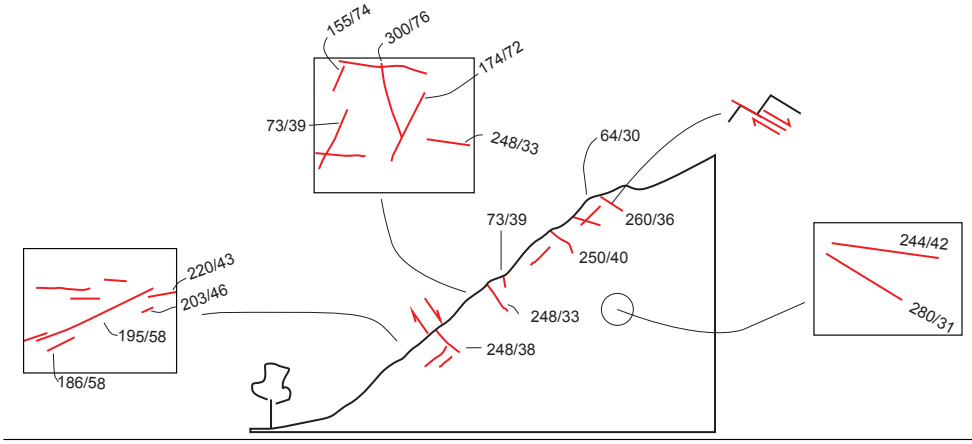

Figure C.6: Stereonet of BRO5.1.

Outcrop: BRO5 2/2

Station: BRO5.2

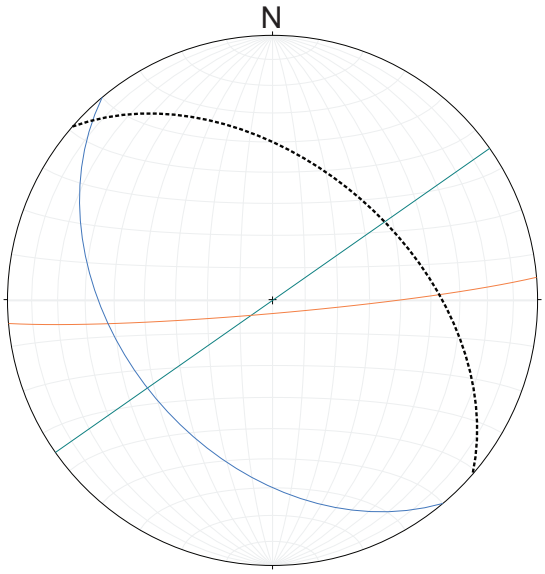

Unfolded w.r.t. bedding

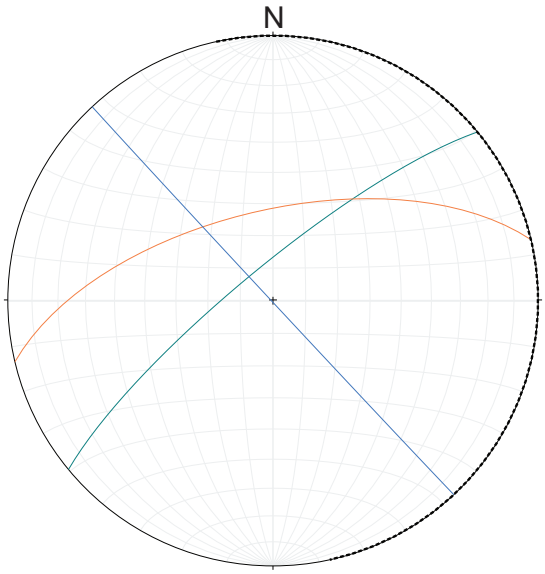

BRO5.2 (S16.31209 – E135.16219)
Three fracture sets are observed:
- F1 is a NE-SW trending set.
- F2 is a E-W trending set that seem to form a congjugate system with F1.
- F3 is a set that is perpendicular to the bedding.

Bedding

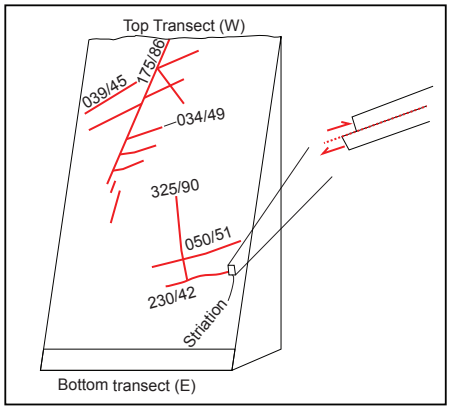

Angle: Yes	Movement: Yes	Striation: No	Score: 2/3

Figure C.7: Stereonet of BRO5.2

Outcrop: BRO6

1/1

Station: BRO6.1

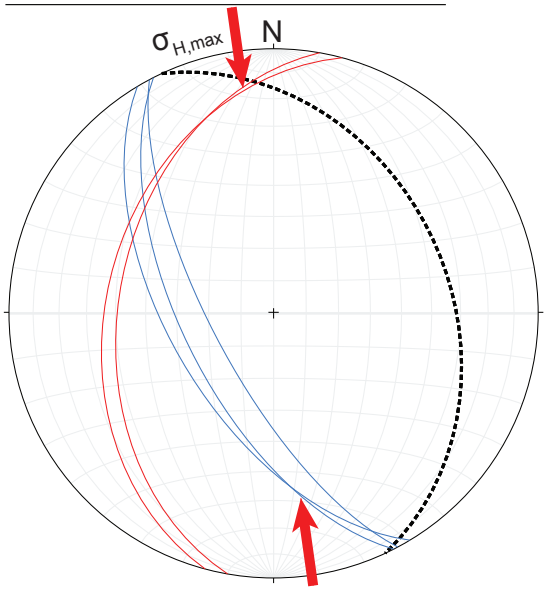

Unfolded w.r.t. bedding

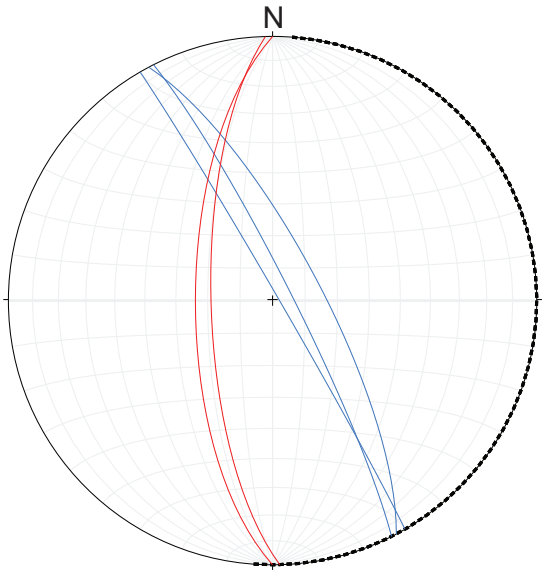

BRO6.1 + BRO 6.2 (S16°24.754 – E135°11.565)

Nice out crop with conjugate-looking faults on NE dipping bed:

- F1(236/58) is a ESE-WNW trending set.
- F2(293/44) is a N-S trending set.

Bedding

F1 and F2 make a conjugate system with interfault angle of 57°, with σ_2 more or less parallel to fold axis. In BRO6.1 the angle is relatively smaller. σ_2 has a strike of 174.

Station: BRO6.2

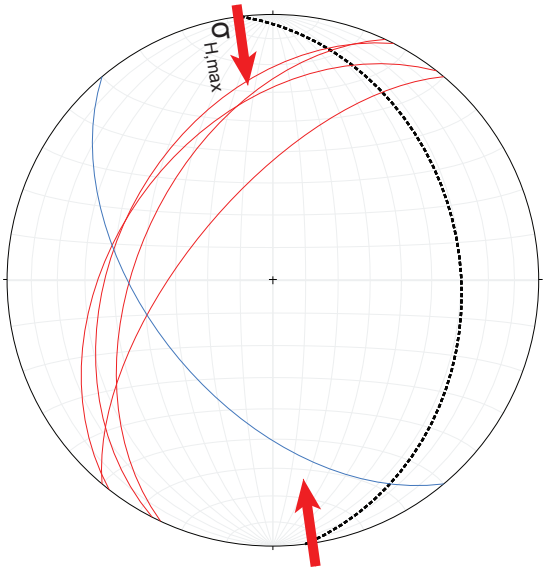

Unfolded w.r.t. bedding

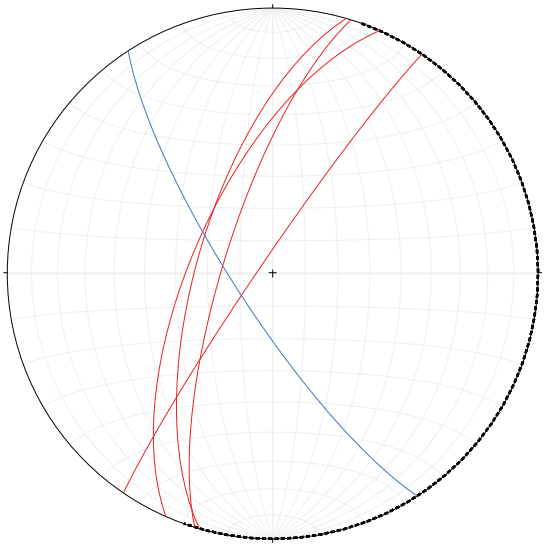

Angle: Yes	Movement: No	Striation: No	Score: 1/3

Figure C.8: Stereonet of BRO6.1.

Outcrop: CAR1

1/2

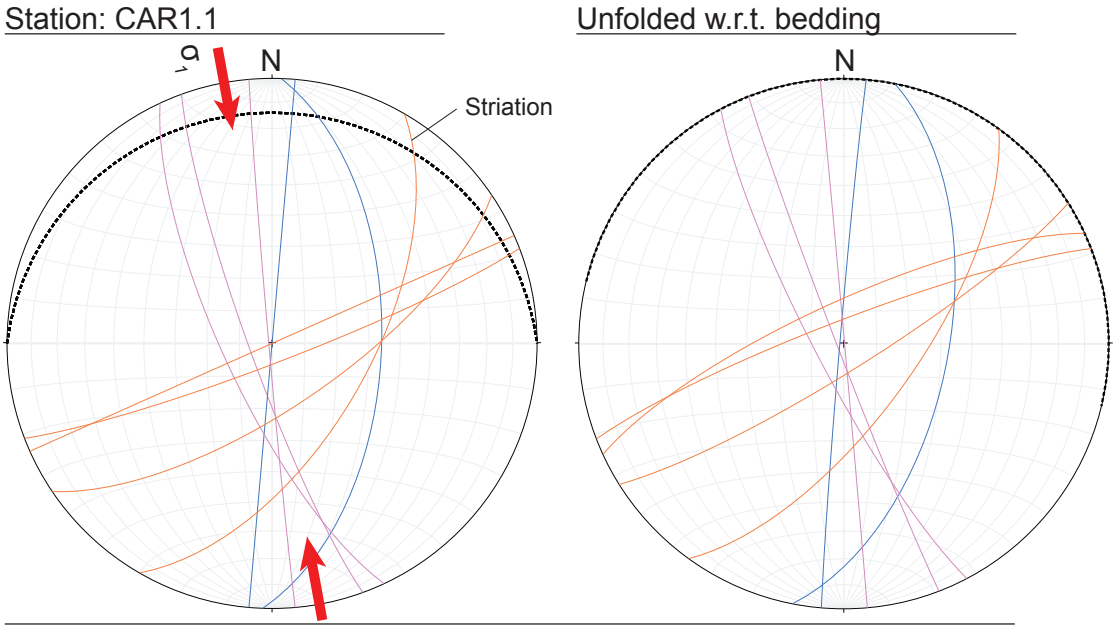

CAR1.1

The following sets were identified:

- F1(004/73) N-S trending set.
- F2(163/82) NW-SE trending set.
- F3(55/76) is a NE-SW trending set.

Striation was observed on a fault N030/60SE, but was of bad quality

Bedding

Central part of the anticline, the bedding is roughly N090/10-15N. Two principal fracture sets are oriented N100-110 and 70-80 low angle congjugate. Angle between sets, based on data from both CAR1.1 and CAR1.2, is 33. The resulting orientation(strike) of σ_1=171.

Figure C.9: Stereonet of CAR1.1.

Outcrop: CAR1

2/2

Station: CAR1.2

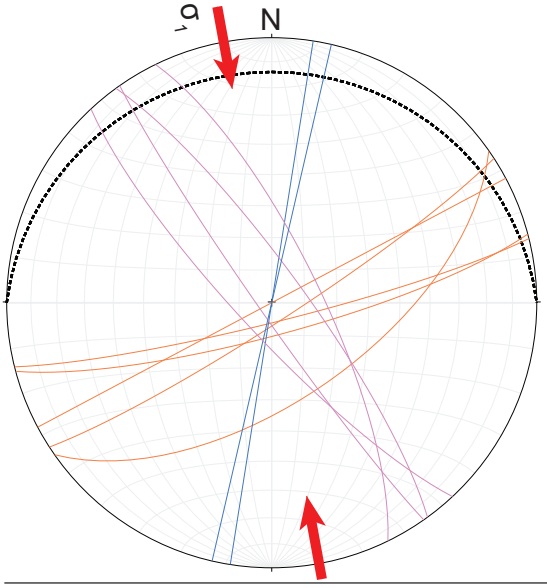

Unfolded w.r.t. bedding

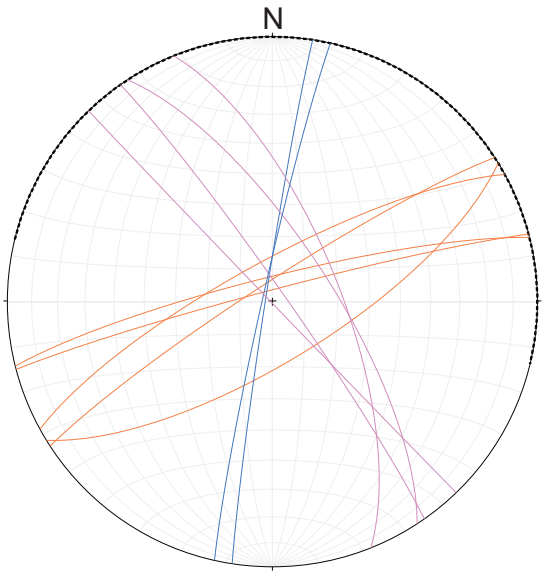

CAR1.1

The following sets were identified:

- F1(189/90) NW-SE trending set.
- F2(145/80) N-S trending set.
- F3(65/80) is a NE-SW trending set.

Beds dipping N (periclinal termination). F3 is fairly long and often dominant F1 and F2 sets are organized as conjugate-looking sets with compression (arrow) perpendicular to bedding strike.

----- Bedding

Walking to the west, bedding seems to change. Angle between sets, based on data from both CAR1.1 and CAR1.2, is 33. The resulting orientation(strike) of σ_1 is 171.

Angle: Yes	Movement: No	Striation: Yes	Score: 2/3

Figure C.10: Stereonet of CAR1.2.

Outcrop: CAR2

1/2

Station: CAR2.1

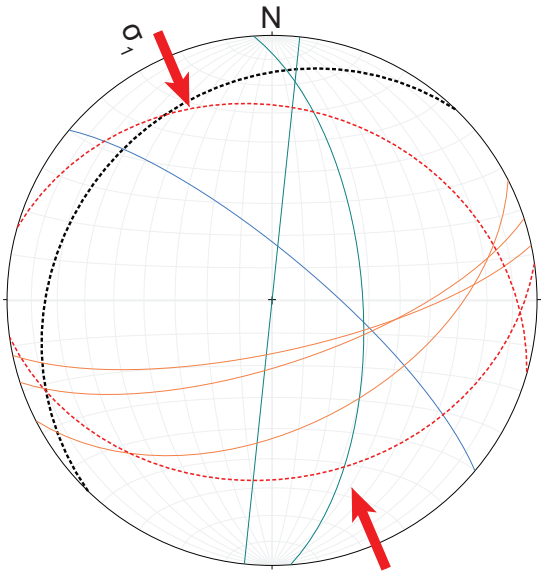

Unfolded w.r.t. bedding

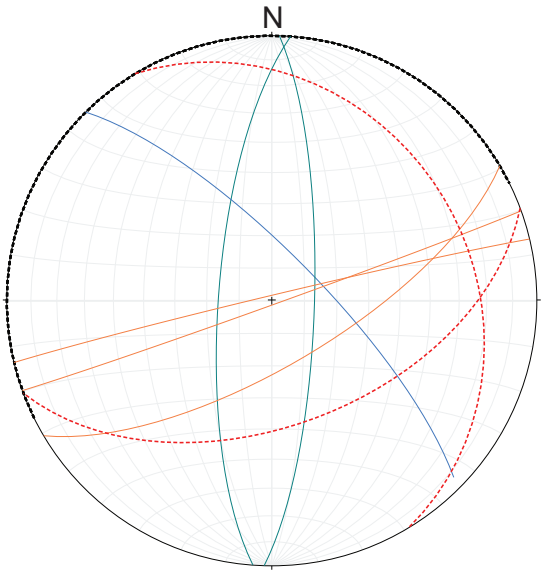

CAR2.1 (S16^{o}31.617 – E135^{o}18.192)

Bedding to NW:

- F1(071/65) is a ENE-WSW striking set and is dominant (same as CAR1).
- F2(271/76) is NW-SE trending set. Together with F3 they are kind of scattered but have a conjugate-like appearance on pavements (also same as CAR1).
- F3(040/76) is a N-S trending set.

Bedding

Fault

Red faults have a sinistral displacement. Reading might have been wrong dipping direction. Based on data from both CAR2.1 and CAR2.2 the conjugate sets make an angle of 68^{o} and σ_1 has a strike orientation of 155.

Figure C.11: Stereonet of CAR2.1.

Outcrop: CAR2

2/2

Station: CAR2.2

Unfolded w.r.t. bedding

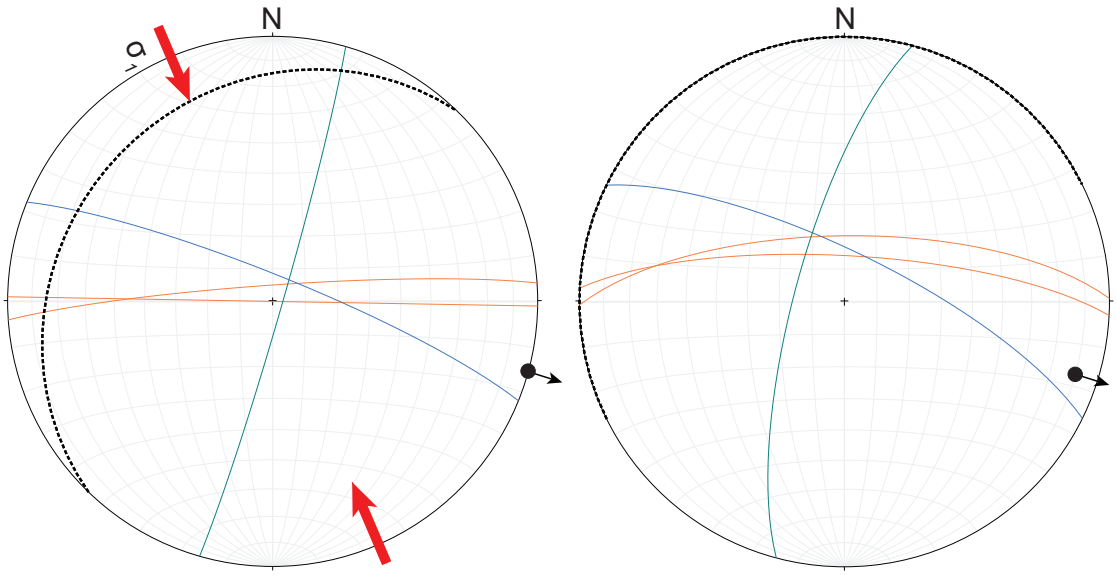

CAR2.2

Bedding to NW:

F1(179/88) is a E-W striking set.

F2(106/87) is a WNW-ESE striking set.

F3(022/82) is ENE-WSW trending set.

Bedding

Fault

Striation measured show horizontal upper block movement towards 105, indicated by the blue arrow. Based on all data from CAR2 the conjugate sets make an angle of 68° and σ_1 has a strike orientation of 155°.

Angle: Yes	Movement: No	Striation: Yes	Score: 2/3

Figure C.12: Stereonet of CAR2.2.

Station: SLC1.1

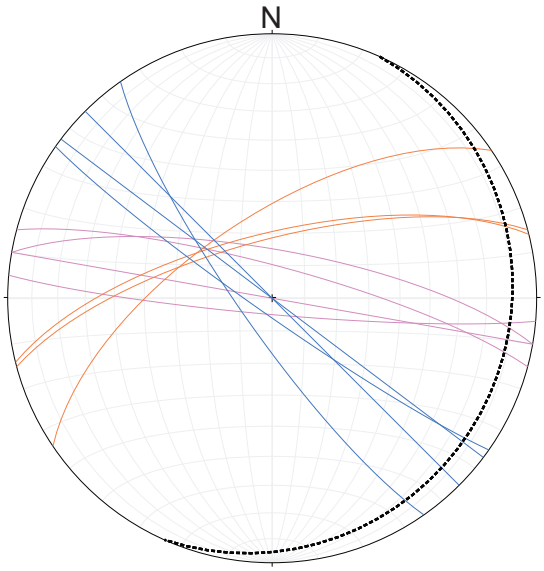

Unfolded w.r.t. bedding

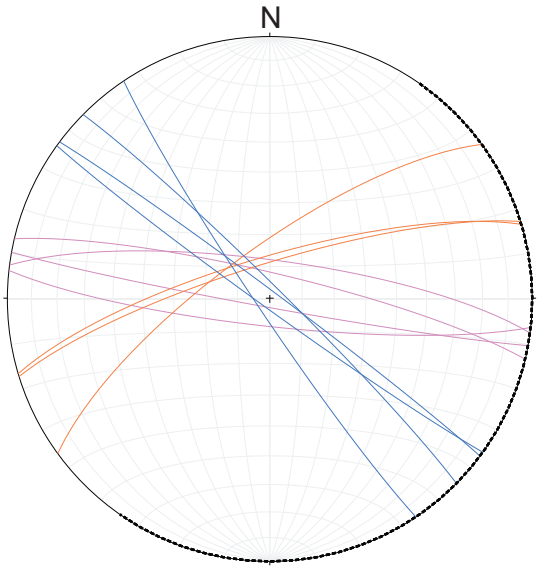

SLC1.1
Station of a vertical section, no indication of shearing:
- F1 is a NW-SE trending.
- F2 is a E-W trending set.
- F3 is a ESE-WNW trending set.

Bedding

Figure C.13: Stereonet of SLC1.1.

Outcrop: SLC1

2/2

Station: SLC1.2

Unfolded w.r.t. bedding

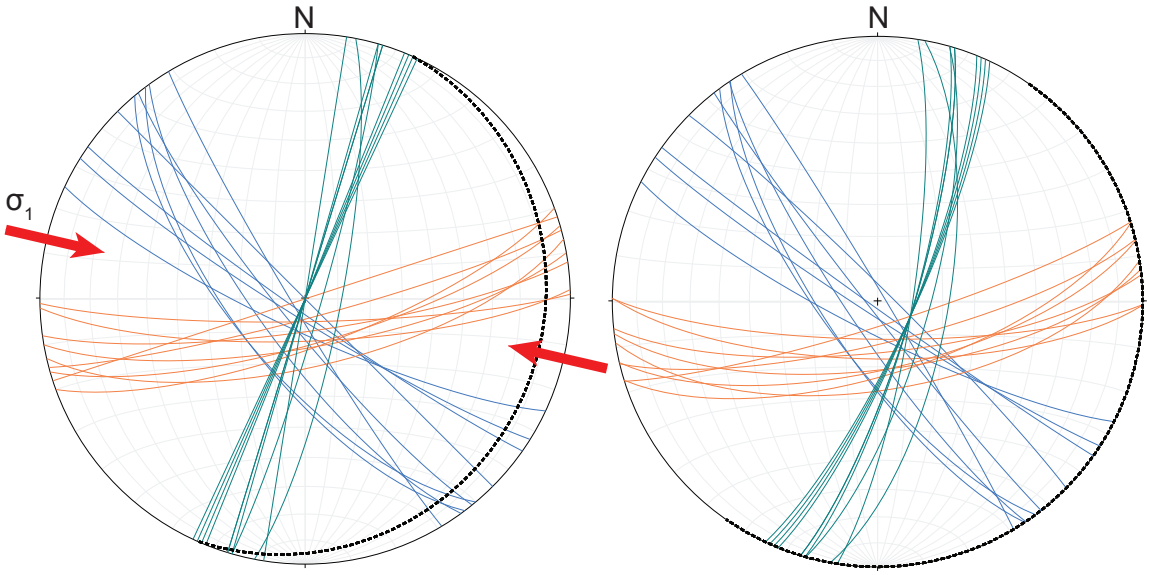

SLC1.2

Three families of fractures:

- F1 (349/79) Very pervasive, horsetail like branches
- F2 (225/80) pervasive
- F3 (288/88) is older and are offset by shear f1 and f2 (observation)

Bedding

Interpretation: In sketch 1 fractures of set 1 and set 3 intersect eachother, between them a sigmoidal connector is present. Sigma 1 is then parallel to this connector. This fits with F1 and F2 being conjugates ofsetting F3 in places.

Sketch 1

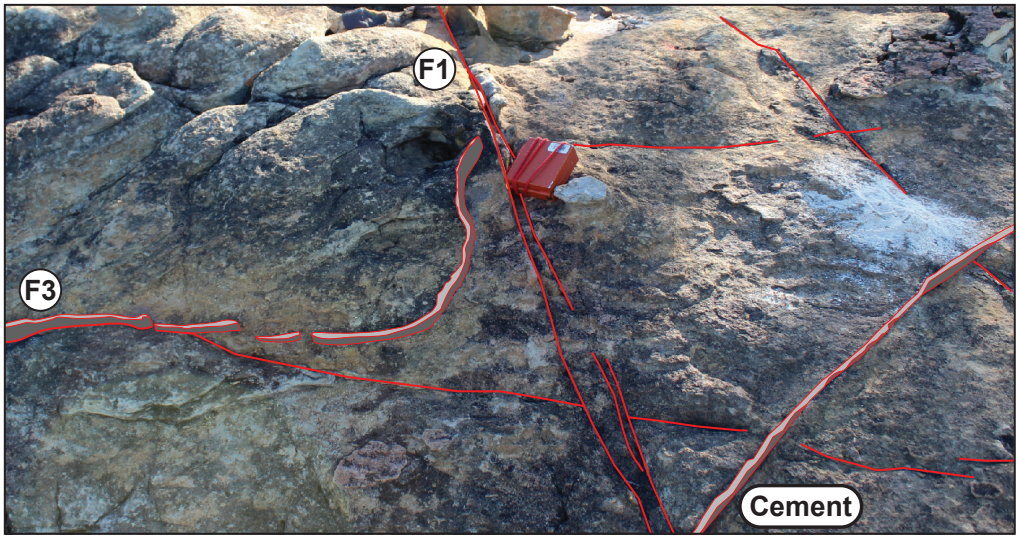

Interpretation of photo 7319

Angle: Yes	Movement: Yes	Striation: No	Score: 2/3

Figure C.14: Stereonet of SLC1.2.

Outcrop: WLC1

1/1

Station: WLC1.1+WLC1.2

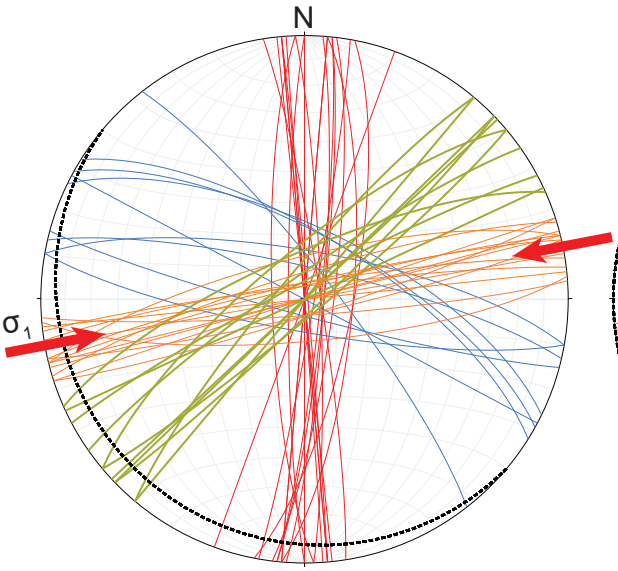

Unfolded w.r.t. bedding

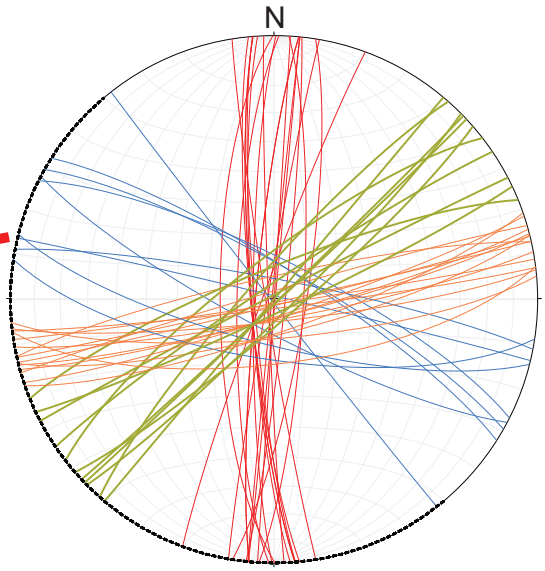

WLC 1.2 (15 46' 23" S – 135 21' 23"E)

Four families of fractures are identified

- F1 (94/85) averages spacing of 2.15m and continuous
- F2 (334/84) very continuous as well
- F3 (027/76) partially continuous, makes sigmoidal connections
- F4 (164/86) not pervasive

---- Bedding

(Sketch 1) En echelon fracturing occurence, this could be an indication of shearing marking sinistral movement. Sigma 1 is then parallel to these fractures, however the orientation is unknown. It was observed that f1 has parallel fractures. If picture is a F1 fracture than this could be a sigma 1 orientation during an other phase.

(Sketch 2) Sigmoidal connection between two fractures. The sketch indicates the orientations of the fractures. According to literature this structures occurs in a shear system in which the sigmoidal connection is parallel to sigma 1. The angle between the sigmoidal connector and the two parallel fracture is about 50 degrees. This set belongs to F3 (027/76).

(**Interpretation**) Sigma 1 is orientated parallel to the sigmoidal connector (348/70), one conjugate set is f3. Assuming that f4, angle is then 43°, is the other conjugate set and f2 is the set parallel to sigma 1.

Sketch 1

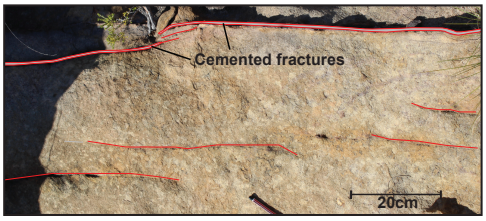

Interpretation of photo 7507

Sketch 2

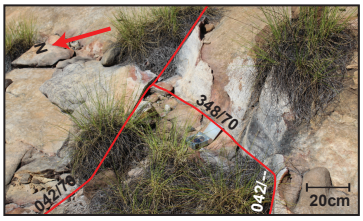

Interpretation of photo 7491

Angle: Yes	Movement: No	Striation: No	Score: 1/3

Figure C.15: Stereonet of WLC1

Wells

Marmbulligan-1

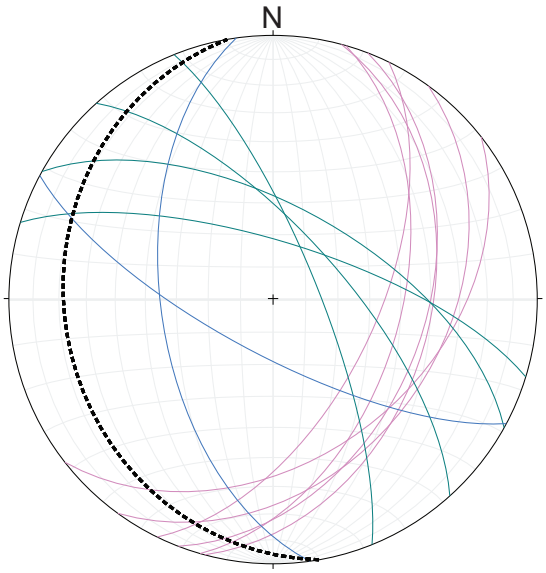

Unfolded w.r.t. bedding

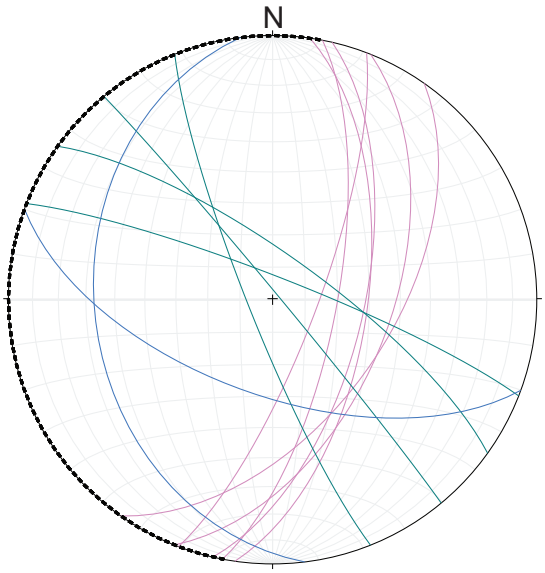

Marmbulligan-1
Three sets are identified:
F1 has a NW-SE orientation.
F2 has also a NW-SE orientation but in opposite dip direction as F1.
F3 has a NE-SW orientation.

Bedding

It is not easy to determine if sets are conjugate from well images. However F1 and F3 of the Marmbulligan well seem to cross eachother at an angle of about 60°. Hinting at a possible conjugate relation between these sets.

Tanumbirini-1

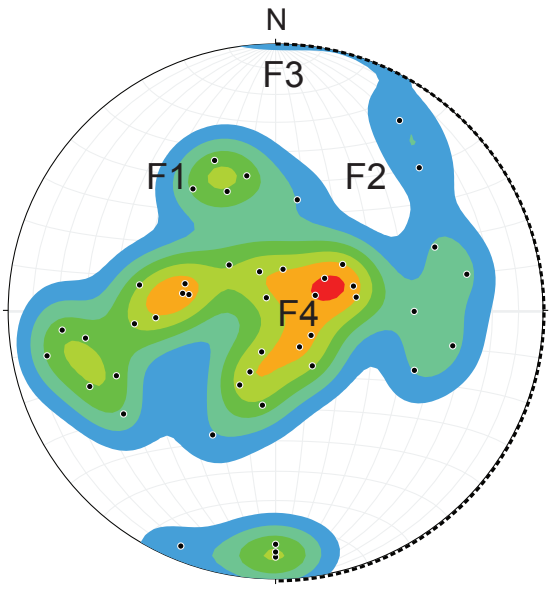

Tanumbirini-1
Five sets are identified:
F1 has a N-S orientation.
F2 has a NW-SE orientation.
F3 has a ENE-WSW orientation.
F4 has NE-SW orientation.

The Tanumbirini well has far more fracture sets and thus make it more ambigious to group sets together. F1 and F2 seem to form a vertical conjugate system, as well as F4 and F5.

Angle: Yes	Movement: No	Striation: No	Score: 1/3

Figure C.16: Stereonet of the Marmbulligan-1 and Tanumbirini-1 wells.

D

Pavements

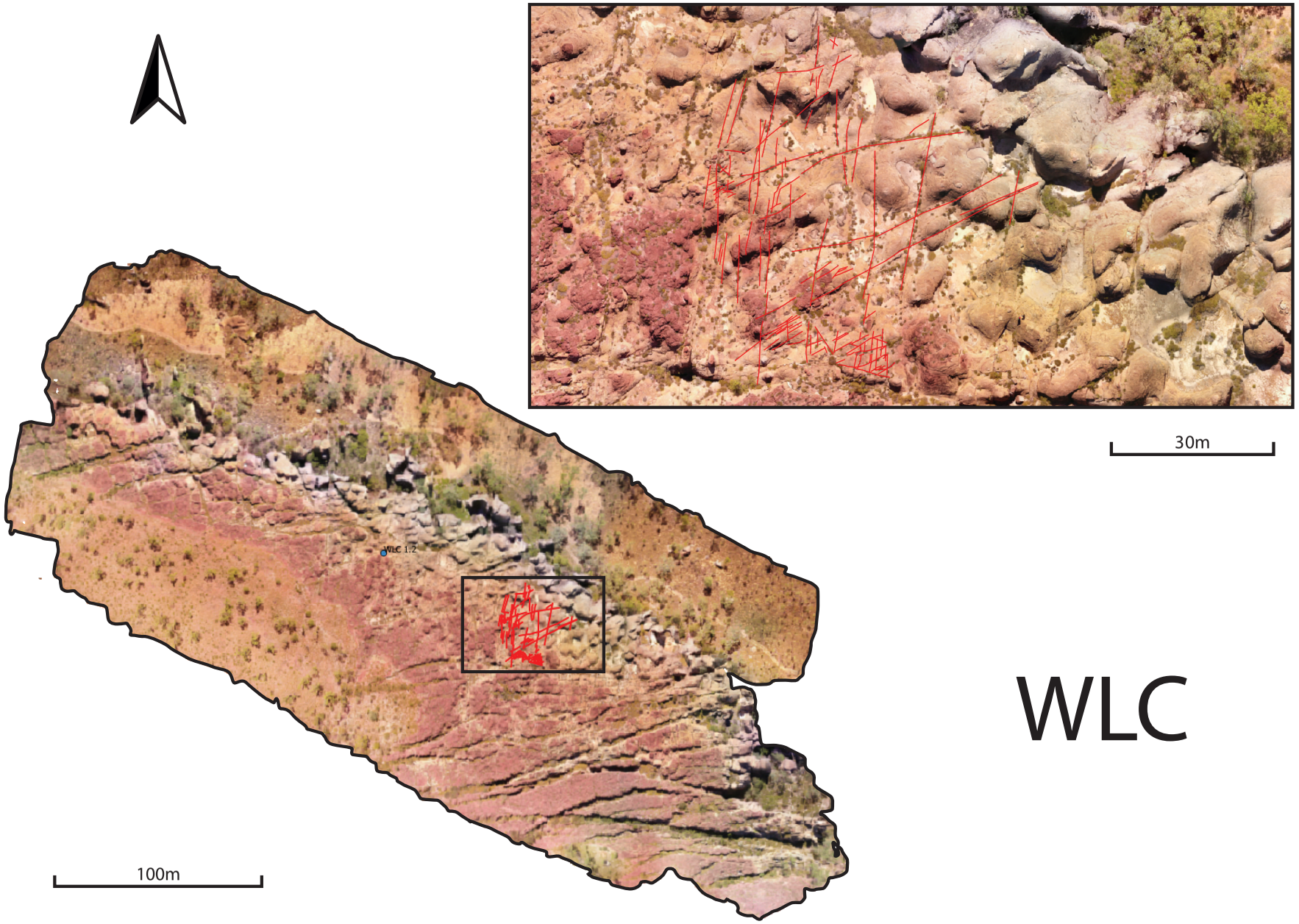

Figure D.1: Pavement of the WLC outcrop and the interpreted section.

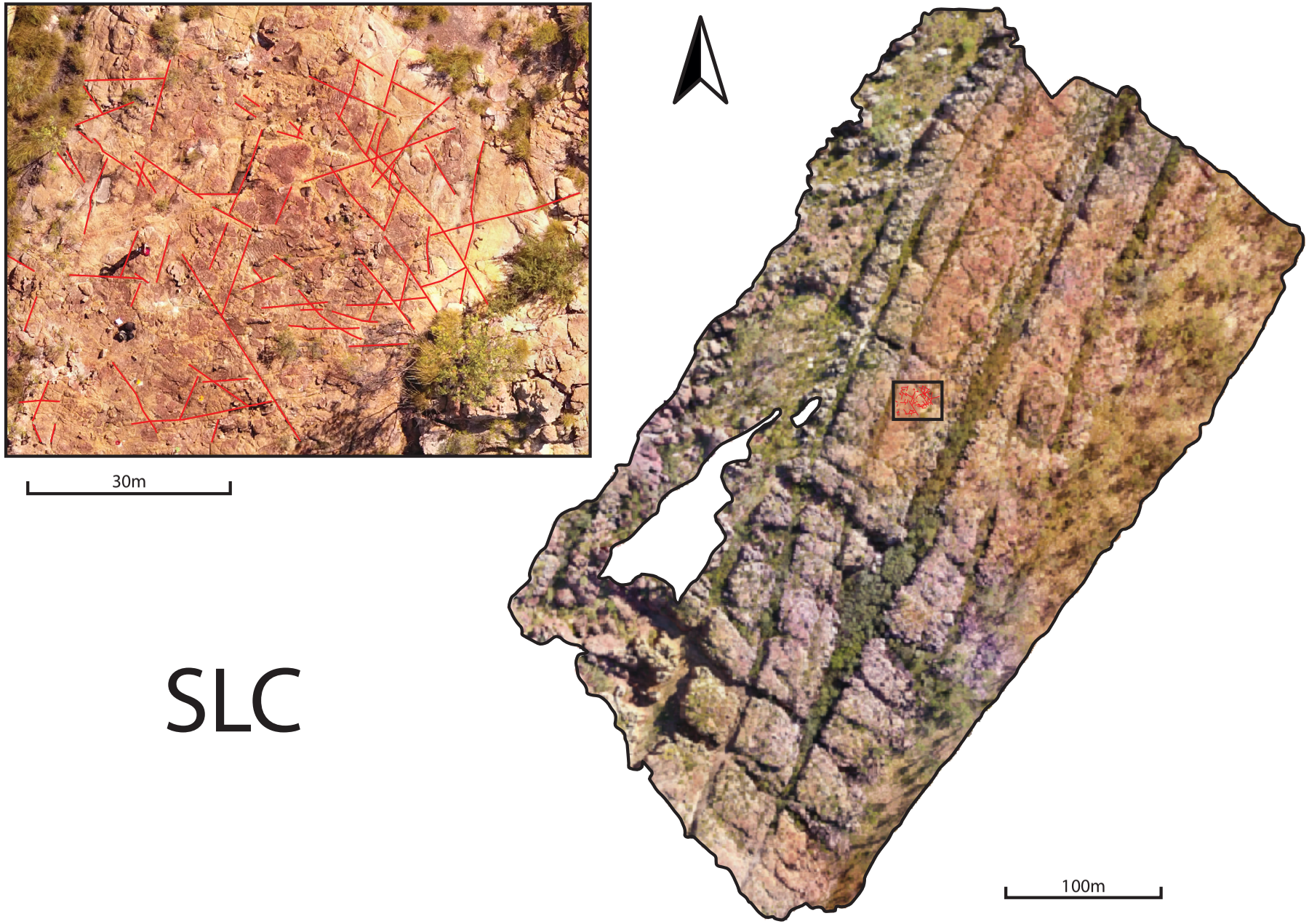

Figure D.2: Pavement of the SLC outcrop and the interpreted section.

E

Techlog tutorial

Techlog 2016.2 was used to do the interpretation of the UBI log. The license is provided by the university which can be installed by launching the 'Schlumberger Licensing Tool'. When starting Techlog and there are no licensing issues it will prompt the user with a menu showing all the modules.

When launching Techlog, the first thing to do is creating a new project (figure E.1). The 'Import' button can be used to add datasets to the project. Importing and viewing normal (GR,DT,RES) logs are straightforward from this point. Borehole images require more steps to be followed. After adding any dataset to the project tree, it can be accessed in the project browser. To plot the datasets, a plot window needs to be added. This can be done by the 'Log View' button under the plot tab. A dataset can be plotted by dragging the set from the browser to the plot window.

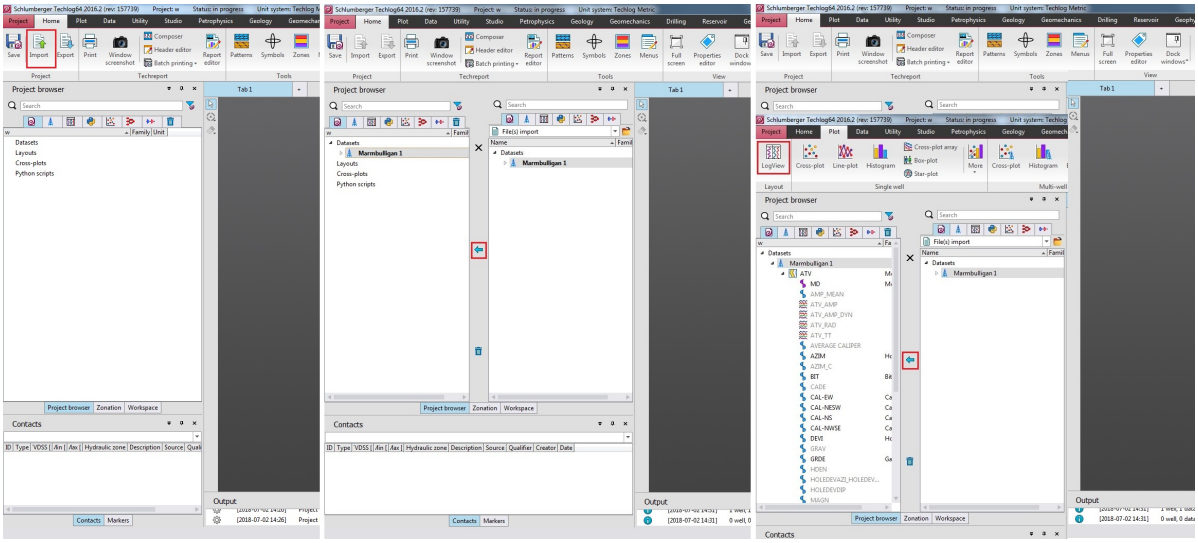

Figure E.1: Screenshot of Techlog highlighting the import process.

An UBI log can similarly be added, however some parameters need to be added first. By pressing F4 while selecting something will launch the properties window of what is selected. After identifying which dataset is the borehole image, press F4 to add the parameters (figure E.2). Set the 'Variable Type' to 'matrix array', this will show another set of parameters to be changed. Additional files like well reports must be studied to get the values. The 'Orientation Type' corresponds to the how the $0°$ of the image relates to its real orientation. For example it could be that the it is relative to the well itself or the North. The 'Orientation' value represents the deviation from the 'datum', e.g. the image is rotated $3°$ from the north.

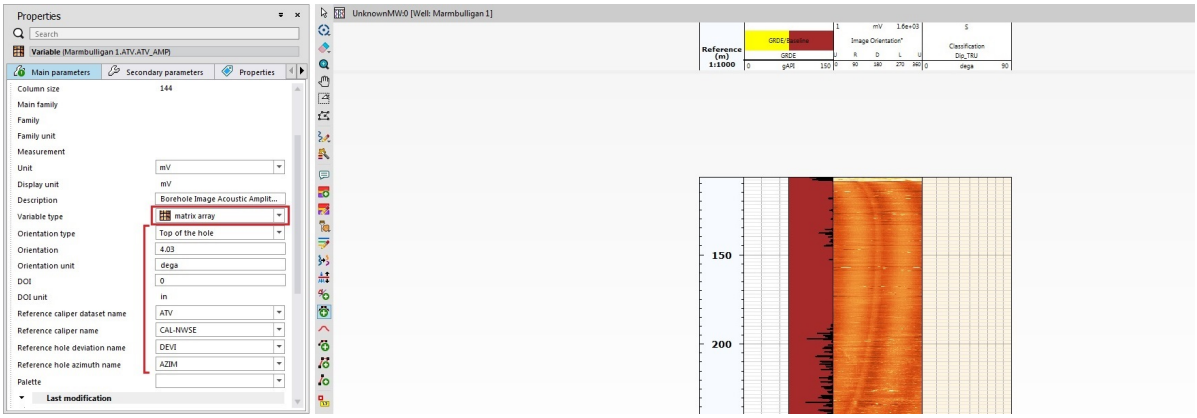

Figure E.2: Screenshot of Techlog showing the parameters for viewing a UBI log.

The depth of investigation is the penetration depth of the tool. For this report this was not mentioned in the available files. This possibly has to do with the radius of the well that is used by the program to do calculations. The references input parameters are datasets themselves for the same well. One must make sure that when there are multiple options to rationalize which one is better or more representable to use. The 'Palette' option does not have to be filled in.

After this process has been finished the image data set can be dragged to the plot window. Select the plotted image by left clicking on it and then right click it to open a drop down menu. Select the 'Create new dip parameter' to be able to mark dips. Another log will show up besides the image. In addition the toolbar on the left has new unlocked buttons, namely 'Dip creation', 'Dip creation sinusoid', 'partial dip creation', 'break out creation' and 'induced fracture creation' (figure E.3). Before starting it is important to know which features need to be interpreted. Under Geology Tab there is a 'Dips handling' button that activates a drop down menu. The 'Dip classification' button will open a window with all types of features like e.g. bedding. Before making an interpretation select what feature it is from this list.

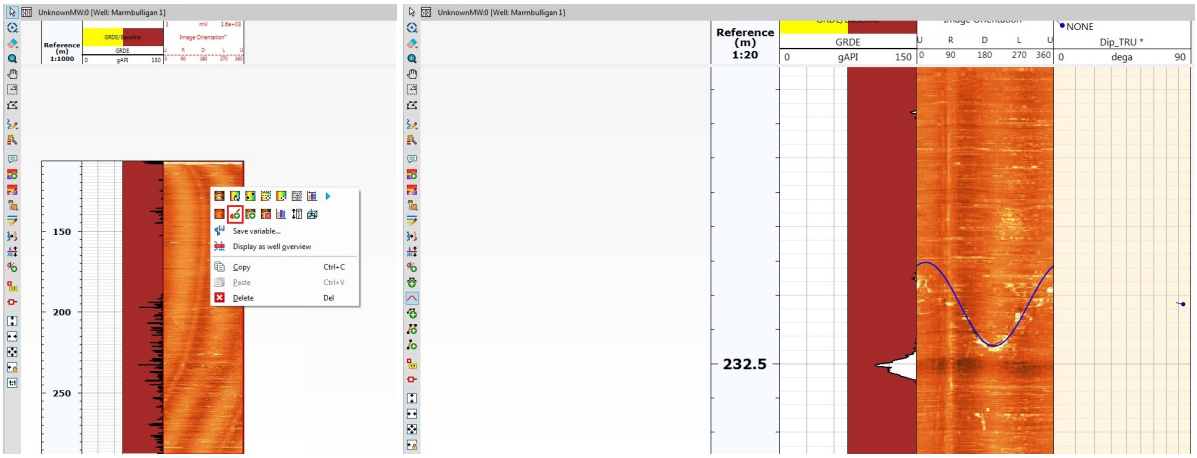

Figure E.3: Screenshot of Techlog showing the dip (log) creation.

Using the middle mouse button one can zoom the image in and out. By scrolling the image is moved up or down. Doing the same while holding the CTRL button will change the resolution. The 'Dip creation sinusoid' button will make a sinusoid appear. The amplitude can be manipulated by holding the left mouse button and moving it up and down. This sinusoid should match the fracture or bedding that is being interpreted. The interpretation can be confirmed by clicking the right mouse button. A tadpole will appear on the neighbouring log. To delete an interpretation use the 'Interactive selection' button to select tadpole. It can then be deleted by pressing the Delete button.

After having interpreted the fractures and bedding, one can save it as a separate dataset. This is done by right clicking the dip log and select save variable. Under the 'Geology Tab' there is the 'Plot' button, here select the Stereonet button. Drag the Dip_TRU to the stereonet, the data will appear in the plot (figure E.4).

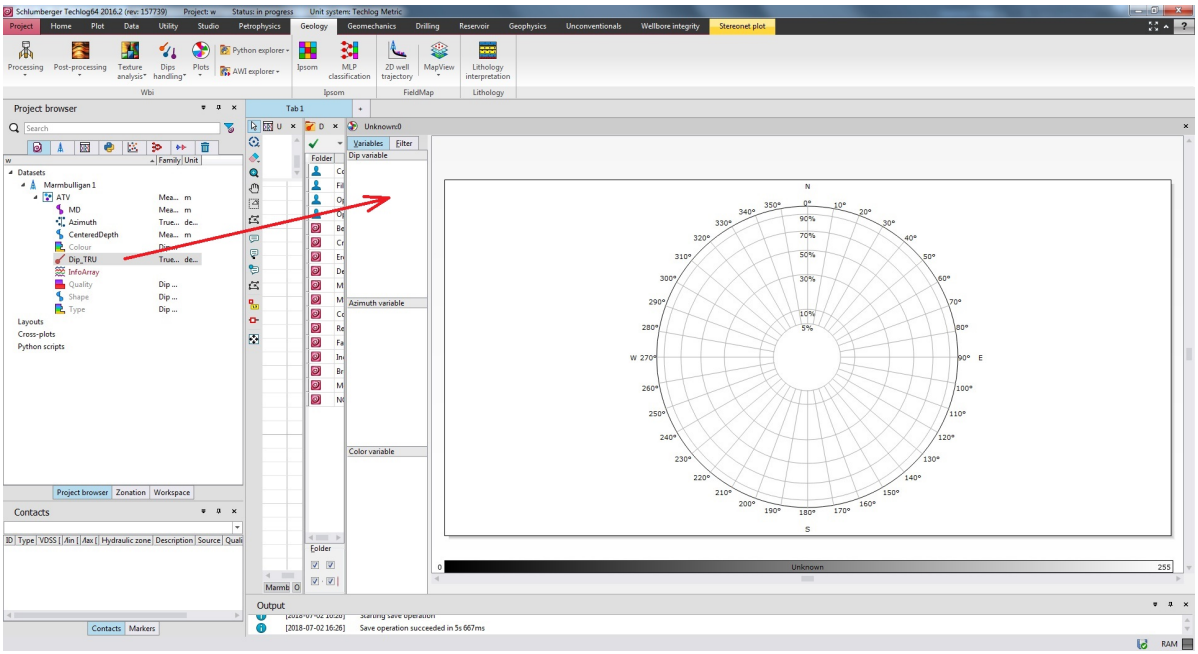

Figure E.4: Screenshot of Techlog showing which parameter needs to be dragged to the indicated box for it to be displayed in the stereonet.

Bibliography

Abbott, S. and Sweet, I. (2000), 'Tectonic control on third-order sequences in a siliciclastic ramp-style basin: An example from the roper superbasin (mesoproterozoic), northern australia', *Australian Journal of Earth Sciences* **47**(3), 637–657.

Abbott, S., Sweet, I., Plumb, K., Young, D., Cutovinos, A., Ferenzi, P., Brakel, A. and Pietsch, B. (2001), 'Roper region: Urapunga and roper river special, northern territory , 1: 250 000 geological map series explanatory notes, sd 53-10 & sd 53-11', *Northern Territory Geological Survey and Geoscience Australia (National Geoscience Mapping Accord)* .

Ahmad, M. c., Munson, T. J. c. and (issuing body.), N. T. G. S. (2013), *Geology and mineral resources of the Northern Territory*, Darwin Northern Territory Geological Survey. Includes bibliographical references and index.

Aitken, A. R. and Betts, P. G. (2009), 'Multi-scale integrated structural and aeromagnetic analysis to guide tectonic models: an example from the eastern musgrave province, central australia', *Tectonophysics* **476**(3-4), 418–435.

Alghalandis, Y. F. (2017), 'Adfne: Open source software for discrete fracture network engineering, two and three dimensional applications', *Computers & Geosciences* **102**, 1–11.

Allmendinger, R. W., Cardozo, N. and Fisher, D. M. (2011), *Structural geology algorithms: Vectors and tensors*, Cambridge University Press.

Anderson, E. M. (1951), *The dynamics of faulting and dyke formation with applications to Britain*, Hafner Pub. Co.

Betts, P., Armit, R. and Ailleres, L. (2014), 'Unravelling the mcarthur basin fault architecture and comparisons with the mount isa terrane'.

Betts, P., Armit, R., Stewart, J., Aitken, A., Ailleres, L., Donchak, P., Hutton, L., Withnall, I. and Giles, D. (2015), 'Australia and nuna', *Geological Society, London, Special Publications* **424**, SP424–2.

Betts, P. G. and Giles, D. (2006), 'The 1800–1100 ma tectonic evolution of australia', *Precambrian Research* **144**(1-2), 92–125.

Blaikie, T., Betts, P., Armit, R. and Ailleres, L. (2017), 'The ca. 1740–1710 ma leichhardt event: Inversion of a continental rift and revision of the tectonic evolution of the north australian craton', *Precambrian Research* **292**, 75–92.

Bruna, P.-O., Dhu, T., Owen, N., Revie, D., Munson, T. and Close, D. F. (2015), 3d architecture of the wilton package throughout the greater mcarthur basin: structural implications for petroleum systems at various investigation scales: in ', *in* 'Annual Geoscience Exploration Seminar (AGES) 2015. Record of abstracts'. Northern Territory Geological Survey, Record', Vol. 2, pp. 26–30.

Darbyshire, F., Bastow, I., Petrescu, L., Gilligan, A. and Thompson, D. (2017), 'A tale of two orogens: Crustal processes in the proterozoic trans-hudson and grenville orogens, eastern canada', *Tectonics* **36**(8), 1633–1659.

Dorrins, P. and Womer, M. (1983), 'Results of 1982 field program, mcarthur river area', *Permits OP* **191**.

Duddy, I. R. (2015), 'Jamison-1 well & zk4001 borehole beetaloo sub-basin, northern territory'.

Duddy, I. R., F., G. P., Gibson, H. J. and Hegarty, K. A. (2004), 'Regional palaeo-thermal episodes in northern australia'.

Etheridge, M., Rutland, R. and Wyborn, L. (1987), 'Orogenesis and tectonic process in the early to middle proterozoic of northern australia', *Proterozic Lithospheric Evolution* pp. 131–147.

Favorskaya, A., Petrov, I. and Grinevskiy, A. (2017), 'Numerical simulation of fracturing in geological medium', *Procedia Computer Science* **112**, 1216–1224.

Fossen, H. (2016), *Structural geology*, Cambridge University Press.

FrogtechGeoscience (2018), 'Seebase® study and gis for greater mcarthur basin'.

Giles, D., Betts, P. and Lister, G. (2002), 'Far-field continental backarc setting for the 1.80–1.67 ga basins of northeastern australia', *Geology* **30**(9), 823.
URL: *https://doi.org/10.1130/0091-7613(2002)030<0823:ffcbsf>2.0.co;2*

Healy, D., Rizzo, R. E., Cornwell, D. G., Farrell, N. J., Watkins, H., Timms, N. E., Gomez-Rivas, E. and Smith, M. (2017), 'Fracpaq: A matlab™ toolbox for the quantification of fracture patterns', *Journal of Structural Geology* **95**, 1–16.

Hibbird, S. A. (1993), 'Well completion report ep18-chanin 1 beetaloo sub-basin of the mcarthur basin'.
URL: *https://geoscience.nt.gov.au/gemis/ntgsjspui/handle/1/79291*

Hoyer, D., Loveless, D., Lavold, G. and Z, F. (2012), 'Well completion report shenandoah-1a (re-entry, completion and stimulation of shenandoah-1a) ep98 beetaloo basin northern territory australia'.
URL: *https://geoscience.nt.gov.au/gemis/ntgsjspui/handle/1/79502*

Jackson, M., Sweet, I., Page, R. and Bradshaw, B. (1999), 'The south nicholson and roper groups: evidence for the early mesoproterozoic roper superbasin', *Integrated Basin Analysis of the Isa Superbasin using Seismic, Well-log, and Geopotential Data: An Evaluation of the Economic Potential of the Northern Lawn Hill Platform: Canberra, Australia, Australian Geological Survey Organisation Record* **19**.

Jackson, M., Sweet, I., Powell, T. et al. (1988), 'Studies on petroleum geology and geochemistry, middle proterozoic, mcarthur basin northern australia i: Petroleum potential', *The APPEA Journal* **28**(1), 283–302.

Kralik, M. (1982), 'Rb□ sb age determinations on precambrian carbonate rocks of the carpentarian mcarthur basin, northern territories, australia', *Precambrian Research* **18**(1-2), 157–170.

Kröner, A. (1981), Chapter 3 precambrian plate tectonics, *in* 'Developments in Precambrian Geology', Elsevier, pp. 57–90.
URL: *https://doi.org/10.1016/s0166-2635(08)70008-2*

Kröner, A. (1984), 'Evolution, growth and stabilization of the precambrian lithosphere', *Physics and Chemistry of the Earth* **15**, 69–106.

Lanigan, K., Hibbird, S., Menpes, S. and Torkington, J. (1994), 'Petroleum exploration in the proterozoic beetaloo sub-basin, northern territory', *The APPEA Journal* **34**(1), 674.

Lindsay, J. (1998), 'The broadmere structure: a window into palaeoproterozoic mineralisation, mcarthur basin, northern australia', *Australian Geological Survey Organisation Record* **98**, 38.

Maerten, L., Maerten, F., Lejri, M. and Gillespie, P. (2016), 'Geomechanical paleostress inversion using fracture data', *Journal of Structural Geology* **89**, 197–213.

Menpes, S. (n.d.), 'Well completion report ep18-ronald 1'.
URL: *https://geoscience.nt.gov.au/gemis/ntgsjspui/handle/1/79423*

Munson, T. (2014), 'Petroleum geology and potential of the onshore northern territory, 2014', p. 242p.

Page, R., Jackson, M. and Krassay, A. (2000), 'Constraining sequence stratigraphy in north australian basins: Shrimp u–pb zircon geochronology between mt isa and mcarthur river', *Australian Journal of Earth Sciences* **47**(3), 431–459.

Page, R. and Sweet, I. (1998), 'Geochronology of basin phases in the western mt isa inlier, and correlation with the mcarthur basin', *Australian Journal of Earth Sciences* **45**(2), 219–232.

Pietsch, B., Rawlings, D., Creaser, P., Kruse, P., Ahmad, P., Ferenczi, P. and Findhammer, T. (1991), 'Bauhinia downs, 1: 250,000 geological map series', *Northern Territory Geological Survey, Explanatory Notes, SE53–3.: Darwin, Northern Territory Geological Survey* .

Plumb, K. and Wellman, P. (1987), 'Mcarthur basin, northern territory: mapping of deep troughs using gravity and magnetic anomalies', *BMR Journal of Australian Geology and Geophysics* **10**(3), 243–251.

Polat, A., Kokfelt, T., Burke, K. C., Kusky, T. M., Bradley, D. C., Dziggel, A. and Kolb, J. (2016), 'Lithological, structural, and geochemical characteristics of the mesoarchean tårtoq greenstone belt, southern west greenland, and the chugach–prince william accretionary complex, southern alaska: evidence for uniformitarian plate-tectonic processes', *Canadian Journal of Earth Sciences* **53**(11), 1336–1371.

Rawlings, D. (1999), 'Stratigraphic resolution of a multiphase intracratonic basin system: the mcarthur basin, northern australia', *Australian Journal of Earth Sciences* **46**(5), 703–723.

Rawlings, D., Korsch, R., Goleby, B., Gibson, G., Johnstone, D. and Barlow, M. (2004), 'The 2002 southern mcarthur basin seismic reflection survey', *Geoscience Australia, Record* **17**, 78.

Revie, D. (2017), 'Unconventional petroleum resources of the roper group, mcarthur basin'.

Rogers, J. (1996), Geology and tectonic setting of the Tawallah Group, southern McArthur basin, Northern Territory, PhD thesis, University of Tasmania,.

RPS Group Plc (2013), 'Evaluation of the hydrocarbon resource potential pertaining to certain acreage interest in the beetaloo basin, onshore australia and mako trough, onshore hungary.'.
URL: *http://www.falconoilandgas.com/uploads/pdf/UCV02226_Falcon_Combined_CPR_release_Main_Body.pdf*

Rutland, R. (1976), 'Orogenic evolution of australia', *Earth-Science Reviews* **12**(2-3), 161–196.

Santos Ltd (2014), 'Tanumbirini 1 basic well completion report'.
URL: *https://geoscience.nt.gov.au/gemis/ntgsjspui/handle/1/83784*

Silverman, M. and Ahlbrandt, T. (2011), 'Mesoproterozoic unconventional plays in the beetaloo basin, australia: The world's oldest petroleum systems', *American Association of Petroleum Geologists (AAPG), Search and Discovery Article* **10295**.

Silverman, M., Landon, S., Leaver, J., Mather, T. and Berg, E. (2008), 'No fuel like an old fuel: Proterozoic oil and gas potential in the beetaloo basin, northern territory, australia', *Proterozoic oil and gas potential in the Beetaloo Basin, Northern Territory* .

Steijn, J. (2018), 'Fracture network characterization in the mcarthur basin, northern territory, australia'.

United States Geological Survey (2015), 'Usgs estimates 53 trillion cubic feet of gas resources in barnett shale'.
URL: *https://www.usgs.gov/news/usgs-estimates-53-trillion-cubic-feet-gas-resources-barnett-shale*

Wade, B., Kelsey, D., Hand, M. and Barovich, K. (2008), 'The musgrave province: stitching north, west and south australia', *Precambrian Research* **166**(1-4), 370–386.

Wal, M., Barrenger, D. and Leitner, B. (2012), 'Centralian mcarthur tas basin analog 2012'.
URL: *http://www.empireenergy.com/pdf/McArthur%20Basin%20Armour%20Co%20Ltd%20Ind.%20Geo's%20Report.pdf*

Warren, J. K., George, S. C., Hamilton, P. J. and Tingate, P. (1998), 'Proterozoic source rocks: sedimentology and organic characteristics of the velkerri formation, northern territory, australia', *AAPG bulletin* **82**(3), 442–463.

Watkins, H., Healy, D., Bond, C. E. and Butler, R. W. (2017), 'Implications of heterogeneous fracture distribution on reservoir quality; an analogue from the torridon group sandstone, moine thrust belt, nw scotland', *Journal of Structural Geology* .

Wilson, T. H., Smith, V. and Brown, A. (2015), 'Developing a model discrete fracture network, drilling, and enhanced oil recovery strategy in an unconventional naturally fractured reservoir using integrated field, image log, and three-dimensional seismic data', *AAPG bulletin* **99**(4), 735–762.

Yang, B., Smith, T. M., Collins, A. S., Munson, T. J., Schoemaker, B., Nicholls, D., Cox, G., Farkas, J. and Glorie, S. (2018), 'Spatial and temporal variation in detrital zircon age provenance of the hydrocarbon-bearing upper roper group, beetaloo sub-basin, northern territory, australia', *Precambrian Research* **304**, 140–155.

Zhao, J. (1995), 'Geochemical and nd isotopic systematics of granites from the arunta inlier, central australia: implications for proterozoic crustal evolution', *Precambrian Research* **71**(1-4), 265–299. **URL:** *https://doi.org/10.1016/0301-9268(94)00065-y*